N72-18285

SUBSONIC AND SUPERSONIC JET FLOW AND
ACOUSTIC CHARACTERISTICS AND SUPERSONIC SUPPRESSORS

BY H.T. NAGAMATSU, R.E. SHEER, JR., AND E.C. BIGELOW

FOREWORD

This report was prepared under contract No. NASW-1784 for NASA
Headquarters, Office of Advanced Research and Technology, Research
Division, under the technical direction of Mr. I.R. Schwartz and
Dr. W.H. Raudebush. The work was conducted at the Mechanical
Engineering Laboratory, General Electric Research and Development
Center in Schenectady, New York.

SUMMARY

Axial surveys were conducted with impact pressure and piezoelectric impact and static pressure probes for a 2 in. diameter convergent nozzle at Mach numbers of 0.6, 1.0, and 1.4. Peak impact pressure fluctuations occurred at approximately 9 diameters for Mach 0.6 and 1.0 jets, and downstream of the peak location the impact pressure fluctuations decreased as $x^{-1.75}$. For the Mach 1.4 jet the peak was located just ahead of sonic point. The peak static pressure fluctuations occurred at approximately 10 diameters for subsonic jets and for supersonic jets the peak occurred in the vicinity of sonic point. The power spectra for subsonic jets were similar and for supersonic jets the peak power occurred at higher frequencies. Sound pressure level spectra for a Mach 1.4 jet indicated a jump in the pressure level at angular positions of 80.4° to 146.4° due to the shock bottles.

Detailed radial and axial surveys were conducted with a piezoelectric static pressure fluctuation probe for a 1 in. diameter convergent nozzle over a Mach number range of 0.6 to 1.4. For subsonic Mach numbers the contours of constant rms static pressure fluctuations were similar with the peak fluctuations occurring close to $r/r_o = 1.0$ near the nozzle exit. For supersonic Mach numbers the contours of constant rms static pressure fluctuations were quite different than the contours for subsonic Mach numbers. The contours of constant piezoelectric impact and static pressure fluctuations were entirely different for both subsonic and supersonic jets. On the axis of the jet the rms static pressure fluctuations in the fully developed subsonic turbulent flow decreased as $x^{-1.95}$, which was close to the analytical prediction.

A suppressor consisting of 191 tubes and 191 shrouds was investigated at jet Mach numbers of 1.4 and 0.7. The multiple tubes and shrouds decreased the primary jet Mach number drastically for both Mach numbers, and the rms impact and static pressure fluctuations on the axis were also reduced from the values existing for an equivalent area single nozzle. For the Mach 1.4 jet the noise level was reduced 15.3 db with the tubes and 20.5 db with the shrouds. And the corresponding reductions for a Mach 0.7 jet were 4.5 db and 7.8 db respectively. A suppressor consisting of a single long shroud and six rods indicated large reduction in the jet velocity at the shroud exit with and without induced flow. For a Mach 1.4 jet the noise level was reduced 14.2 db with induced flow and 4.5 db without induced flow.

TABLE OF CONTENTS

LIST OF FIGURES

LIST OF SYMBOLS

c	velocity of sound
D	nozzle exit diameter
M	Mach number
p_a	ambient pressure
p_o	total pressure
p_o'	impact pressure after normal shock
$\bar{p}$	mean static pressure
$<p'>$	pressure fluctuation caused by turbulence
$\tilde{p}$	pressure fluctuation due to sound field
p_{s_f}	static pressure fluctuation
p_T	total pressure along streamline
p_T'	total pressure fluctuation
q	mean vector velocity
q'	vector turbulent velocity
r	radius from jet centerline
r_o	radius of nozzle exit
U_j	jet exit velocity
$\begin{matrix} u \\ v \\ w \end{matrix} \Bigg\}$	velocity components
$\begin{matrix} u' \\ v' \\ w' \end{matrix} \Bigg\}$	turbulent velocity components in cartesian coordinate system
$\begin{matrix} \bar{U} \\ \bar{V} \\ \bar{W} \end{matrix} \Bigg\}$	mean flow velocities
x	axial distance from jet exit

γ   ratio of specific heats

η   kinematic viscosity, ν/ρ

ρ   density

σ   pressure correlation scale

τ_0 mean viscous shear stress

1.0 INTRODUCTION

For supersonic transports and military aircrafts the exhaust jet
velocities are supersonic so that the jet exhaust noise during
take-offs without a suppressor is quite critical at airports loca-
ted in the metropolitan areas. In order to reduce the noise for
supersonic exhaust velocities, basic information regarding the
noise generation mechanisms and suppression phenomena is required
for supersonic jets. The available information for the actual
location and strength of noise sources for subsonic jets are still
inadequate. For supersonic jets the available flow and acoustic
data is very limited and the relationship between the noise gen-
eration for supersonic jets and the radiation to the far field is
not well understood. To gain fundamental flow and acoustic knowl-
edge for subsonic and supersonic jets a theoretical and experi-
mental investigation was initiated several years ago and some of
the previous results are presented in Refs. 1-8 for both plain
supersonic jets and with suppressors. The supersonic jet noise
suppressor configurations were selected to obtain fundamental in-
formation regarding the necessary flow modifications of supersonic
jets to achieve large noise reductions.

To study the similarities and differences between subsonic and
supersonic jets, velocity and impact pressure fluctuations were
determined along the axis over a jet Mach number range of 0.6 to
1.4 for a 2 in. diameter convergent nozzle in Ref. 4. Also, the
sound pressure level variations with angular position from the
jet exhaust in the far-field and the sound power spectra were
determined for the various subsonic and supersonic jet Mach num-
bers. An investigation was conducted to investigate mean velocity
and piezoelectric impact pressure fluctuation distributions in the
jet flow for both subsonic and supersonic jets with a one in. dia-
meter jet in Ref. 6. Since the acoustic radiation is dependent
upon the fluctuating turbulent stress tensor in the flow field as
postulated by Lighthill in Refs. 9 and 10 for subsonic jets, it is
necessary to determine the mean and fluctuating velocity distri-
butions in subsonic and supersonic jets. The present investigation
was conducted to obtain the static pressure fluctuation distri-
butions due to turbulence and shear in the jet flow for subsonic
and supersonic jets. The acoustic radiation to the far-field from
the subsonic and supersonic jet exhaust velocities must be related
to the static pressure fluctuations within the flow. Also, a study
was made to determine the flow and acoustic characteristics of a
single shroud, and multiple tube and shroud suppressors for super-
sonic and subsonic exhaust velocities. The available literature on
these jet flow phenomena are very limited to resolve the question
of actual noise generation and suppression mechanisms for subsonic
and supersonic jets.

For subsonic jets the variation of the flow velocity along the axis has been determined with impact pressure and hot-wire probes in Refs. 4, 6, 11-14. The uniform core region extended over 4 to 5 diameters from the jet exit in these references, and the core length was dependent upon the initial turbulence level in the reservoir. For convergent nozzles at pressure ratios greater than the critical value to produce supersonic jet velocities downstream of the nozzle exit, the jet flow will always contain shock bottles because of the inertia effects as observed in Refs. 4, 6, 15-18. The flow fields for supersonic jet exhaust velocities from convergent divergent nozzles designed for uniform parallel flow at the nozzle exit operated at the design pressure ratio have been investigated in Refs. 14, 19-21. From these experimental observations for supersonic jets, the supersonic region increased as the square of the jet Mach number and the experimental results are summarized in Refs. 3, 5, 22.

Various investigators[11-13,23-26] have used hot-wires to investigate the turbulent velocity fluctuations in the subsonic jet flow field. In Ref. 11 the mean and fluctuating velocity and temperature distributions were determined for a heated small jet over a velocity range of 65 to 110 ft/sec. Recent investigators[23-26] have used hot-wires for obtaining the turbulent velocity fluctuations in order to investigate the noise generation mechanisms for subsonic jets as well as to evaluate the fluctuating stress tensor distributions in subsonic jet flows. By the use of two hot-wires in a subsonic jet, Davies and colleagues[25] obtained the radial distributions of the turbulence level and the corresponding static pressure fluctuations at several axial distances from the nozzle exit. The results indicated that the maximum static pressure fluctuations in the jet were not located at the maximum turbulent velocity fluctuations. In Ref. 6 the turbulent velocity fluctuation distributions for subsonic jets were determined by means of a piezo-electric impact pressure probe. Also, it was shown in this reference that for low subsonic Mach numbers the output of the piezo-electric impact pressure probe was proportional to the product of the local density, mean velocity, and turbulent velocity fluctuations. At low Mach numbers the output of the piezoelectric impact pressure probe along the jet axis correlated with the hot-wire data obtained by Laurence[12] and Bradshaw[13].

The available literature[27,28] on the turbulence measurements with hot-wires is very limited because maintaining the integrity of the wire in supersonic flows is extremely difficult. At present no hot-wire data is available for supersonic jet velocities because of the difficulties in preserving a small diameter hot-wire with high frequency in the jet stream without failure. To overcome this problem with hot-wire for supersonic jet flows, Fisher and Johnson[29] used an optical "cross-beam" method to measure the turbulence

2

properties of supersonic jets. Pettit[30] has used the laser doppler velocimeter technique for measuring the mean velocity and the turbulence level in a subsonic jet and has obtained good correlation with the hot-wire measurements at a jet Mach number of 0.3. With a more powerful laser light source the mean and fluctuating turbulent velocity have been obtained at a flow Mach number of 0.6 and preliminary measurements have been made for jet Mach numbers of 1.0 and 1.2. At these higher velocities the existing electronic system was inadequate to yield reliable information at locations downstream from the nozzle exit. Thus, an improved electronic system is being constructed to remove the deficiency. With this new system it will be possible to determine the mean and turbulent velocities for high supersonic Mach numbers.

To overcome the limitations of measuring the turbulence level with hot-wire in supersonic flows, in the past several years a few investigators have used microphone and piezoelectric pressure transducers to measure the fluctuating pressures for impact and static pressure probe configurations in subsonic[31-36] and supersonic[2,4,6-8] jet flows. Nakamura and colleagues[32] used a microphone with impact and static pressure probe configurations to measure the turbulence level in a low speed pipe flow. Fuchs[34-37] also conducted investigations with microphones to measure the static pressure fluctuations in a subsonic jet flow. Maestrello and McDaid[38] measured the pressure fluctuations on a plate close to the edge of a subsonic jet for the purpose of attempting to determine the strength and location of noise sources in a high velocity subsonic jet. Nagamatsu and colleagues[2,4,6] have used a piezoelectric impact pressure probe to investigate the turbulence level for subsonic and supersonic jet flows. Along the jet axis the peak impact pressure fluctuations occurred at the axial position of approximately 9 diameters from the exit of the convergent nozzle for subsonic jet Mach numbers of 0.60 to 1.0. But for supersonic Mach numbers of 1.2 and 1.4 the peak impact pressure fluctuations occurred just ahead of the sonic point on the axis. In Ref. 6 both Mach number and impact pressure fluctuation contours were determined for a Mach number range of 0.60 to 1.40. It was observed for subsonic Mach numbers of 0.60 to 1.0 the peak impact pressure fluctuations occurred in a toroidal region located at approximately 5 diameters from the nozzle exit. And for supersonic Mach numbers the peak impact pressure fluctuations occurred along the sonic velocity contour.

Lighthill[9,10], Ribner[39], and others have analyzed the noise generation from subsonic jets and a review of the existing literature on the jet noise phenomena is presented in Ref. 39. Phillips[40] and Williams[41] have analyzed the noise generation phenomenon for supersonic jets by considering the turbulent shear layer. Recently, Plumblee[42], Ollerhead[43], and Nagamatsu and Horvay[3] have considered

the acoustic radiation from supersonic jets. Acoustic radiation from subsonic jets has been investigated by various authors[44-48]. And the acoustic data for supersonic jet exhaust velocities have been published by various investigators[1-8,49-51]. Potter and Jones[21] determined the distribution of the acoustic radiation from a Mach 2.49 jet and found the peak acoustic radiation occurred at 20 diameters from the nozzle exit, near the sonic velocity on the axis. Nagamatsu and colleagues[4,6] also observed from the piezoelectric impact pressure fluctuations and near-field microphone measurements that the maximum acoustic radiation occurred at 12 diameters from the convergent nozzle exit, near the sonic location, for a Mach number of 1.4.

The present investigation was a continuation of the previous studies[4,6] for the purpose of determining the static pressure fluctuation distributions due to turbulence in the flow field for a jet Mach number range of 0.60 to 1.4 from a convergent nozzle. And the second objective of the investigation was to determine the flow and acoustic characteristics of suppressor configurations effective in reducing the acoustic radiation from supersonic and subsonic jet flows. In Ref. 4 the mean velocity and piezoelectric impact pressure fluctuations were determined along the axis for subsonic and supersonic jet velocities. The mean velocity and fluctuating impact pressures in the flow field were determined for a jet Mach number range of 0.60 to 1.4 in Ref. 6. For determining the location and strength of acoustic sources in the turbulent jet flow field, it is necessary to know the static pressure fluctuation distributions due to the turbulence in the subsonic and supersonic jets, and investigations were conducted to determine these distributions in the present study. An analysis was made to show that the piezoelectric static pressure probe fluctuations were related to the local turbulent velocity fluctuations and acoustic field in the flow. Flow and acoustic characteristics of 191 tube and shroud and single shroud supersonic jet noise suppressors were determined for supersonic and subsonic jet exhaust velocities. Mean and fluctuating velocities and static pressure fluctuations in the jet flow field were determined with and without the suppressors. Far-field sound pressure level distributions and power spectra for a convergent nozzle with and without the suppressors were determined over a range of jet Mach numbers.

2.0 EXPERIMENTAL FACILITIES AND PROCEDURES

2.1 Air Supply and Gas Fired Heater

Two compressor systems are available to supply the air to the nominal 2 and 6 in. diameter nozzles for investigating the flow and acoustic characteristics of subsonic and supersonic jets, cf. Fig. 1. One system consists of two 800 hp three-stage compressors and a two-stage 200 hp compressor. For supersonic Mach numbers greater than 1.4 with the 2 in. diameter nozzle, both 800 hp compressors are required. With this system the compressed air can be heated by gas-fired heaters up to 900°F at a mass flow rate of 5 lb/sec. The second system consists of two banks of Fuller compressors with each bank powered with 350 hp motor. It is possible to operate a 6 in. diameter nozzle over a Mach number range of 0.10 to 0.9. And by connecting the two systems of compressors it is possible to supply approximately 20 lbs/sec of air at a pressure of 30 psia. A more detailed description of the compressor facility and method of pressure regulation is presented in Ref. 6.

To obtain the distributions of the mean velocity, piezoelectric impact pressure and static pressure fluctuations over a Mach number range of 0.60 to 1.4, a 1 in. diameter convergent nozzle was utilized in the Fuller compressor room as shown in Fig. 2. The axial and radial surveys were conducted with this nozzle so that the effects of the ambient wind velocity was eliminated, and it was possible to obtain shadowgraph and schlieren photographs as discussed in Ref. 6. Detailed surveys were conducted with impact pressure, piezoelectric impact and static pressure probes over a large distance from the nozzle exit and the results are presented in this report.

2.2 Nozzles and Test Facilities

Convergent nozzles with exit diameters of 2 and 1-9/16 in. were used with the outdoor flow and acoustic facility shown in Fig. 1, and some of the previous flow and acoustic results for subsonic and supersonic exit Mach numbers are presented in Refs. 1 to 8 with and without the various supersonic jet noise suppressor configurations. The 1 in. diameter convergent nozzle has exactly the same geometrical shape as the larger diameter nozzles, and this smaller nozzle was located within the compressor room as shown in Fig. 2. With this nozzle it was possible to conduct detailed impact pressure, piezo-electric impact and static pressure surveys for a jet Mach number range of 0.6 to 1.4. For these axial and radial surveys with different probes, a movable survey rig was used as indicated in Fig. 2. It was possible to obtain the contours of constant Mach number, piezoelectric impact pressure fluctuations and piezoelectric static pressure fluctuations for subsonic and supersonic jet Mach numbers.

5

2.3 Instrumentation

The reservoir pressures in the settling chambers for the different
diameter nozzles were measured with a Heise gage for both the out-
door facility and for the indoor 1 in. diameter nozzle. For the
higher flow velocities the impact pressures were measured with a
Heise gage and for lower velocities the impact pressures were mea-
sured with a mercury manometer. For each test the ambient pressure
and temperature were recorded. All pressure readings were taken
after the jet flow had stabilized. The axial and radial impact
pressure surveys were conducted in the 1 in. nozzle with a 1/16 in.
diameter probe.

A 1/4 in. diameter Kistler quartz piezoelectric pressure transducer
was used as the impact pressure fluctuation probe. The pressure
gage was mounted with the gage face exposed perpendicular to the
free stream. And the output from the pressure transducer was read
with a Ballantine rms meter with the response time of the gage of
approximately 20 μ sec. An analysis of the piezoelectric impact
pressure gage output will be presented in this report indicating
that the rms output is proportional to the turbulent velocity
fluctuations for subsonic flows.

The diameter of the piezoelectric static pressure probe was 0.125
in. with a sharp tip and small orifices were drilled around the
probe as shown in Fig. 3. The static pressure at the orifices was
transmitted through a 0.06 in. diameter hole to the face of the
1/4 in. diameter Kistler gage. An 8 in. diameter calibration shock
tube was used to determine the pressure gage output as a function
of the applied pressure jump produced by the incident shock wave.
By selecting the initial pressure in the shock tube and adjusting
the pressure ratio between the driver and driven tube the pressure
jump across shock wave can be adjusted over a range of values for
the pressure gage calibration.

The total temperature in the plenum chamber was measured with
either a chromel-alumel thermocouple or an Ashcroft dial thermo-
meter. A chromel-alumel thermocouple was used in the total tempera-
ature probe for the axial surveys along the axis, and the outputs
from the total temperature thermocouples in the plenum chamber and
in the jet flow were recorded simultaneously. For both flow and
acoustic investigations at subsonic and supersonic jet velocities,
the outside ambient air temperature and pressure were recorded.

B&K condenser microphones of 1/4 and 1/2 in. diameters were used
to obtain near- and far-field acoustic pressure data with a cathode
follower for a frequency response of 20 Hz to 40 kHz. Before each
test the microphone was calibrated with a B&K piston phone calibrator
which produced an oscillating dynamic pressure of 124 db re 0.0002 μ

6

bar at 250 Hz. Far-field acoustic measurements were made with the microphone placed in the plane of the jet axis at 8 angular positions on a 10-ft. radius for both 1-9/16 and 2 in. diameter nozzles. The output of the microphone was connected to a Ballantine true rms voltmeter, B&K sound level meter, and General Radio tape recorder which had a frequency response of 15 Hz to 16 kHz. A Norelco eight channel tape recorder with a response of 15 Hz to 100 kHz is available for obtaining information at higher frequencies. The Ballantine true rms voltmeter had a flat frequency response to 200 kHz. The tape recordings were analyzed using a B&K 1/3-octave band analyzer coupled to a Hall squaring circuit and a digital integrating voltmeter, and a detailed discussion of the data analysis is presented in Ref. 1.

2.4 Procedure

With both 1-9/16 and 2 in. diameter nozzles located outside the building with various supersonic suppressor configurations, Fig. 1, two separate runs were made at each selected reservoir pressure for jet flow Mach numbers of 0.6 to 1.4 to obtain the acoustic and flow data. After the jet flow had stabilized the nozzle and reservoir pressures and the total temperature in the reservoir were recorded as well as the ambient temperature and pressure. For both 1-9/16 and 2 in. nozzles the total pressure and total temperature surveys were made along the jet axis from the nozzle exit to 40 nozzle diameters. With the 1 in. convergent nozzle, Fig. 2, the total pressure, and the Kistler piezoelectric impact and static pressure fluctuation surveys were conducted at a large number of radial and axial positions for jet Mach numbers of 0.6 to 1.4 in order to obtain the constant Mach number and piezoelectric impact pressure and static pressure fluctuation contours. Mach number and piezoelectric impact pressure fluctuation contours for subsonic and supersonic jets are presented in Ref. 6. These mean and fluctuating quantities in the subsonic and supersonic jets are necessary for understanding the noise generation and suppression mechanisms for subsonic and supersonic jets.

Both near- and far-field acoustic measurements were made with 1-9/16 and 2 in. nozzles located outside the building. The far-field microphone measurements were made on a 10-ft. radius from the jet axis and the output tape recorded. For the near-field microphone positions the output was connected to the Ballantine rms voltmeter to obtain the sound pressure level at each location in db re .0002 microbar as discussed in Ref. 4.

7

3.0 SUBSONIC AND SUPERSONIC JET FLOW AND ACOUSTIC CHARACTERISTICS

3.1 Flow and Acoustic Characteristics of 2 Inch Diameter Convergent Nozzle

3.1.1 Axial Distributions of Mean Velocity, Piezoelectric Impact and Static Pressure Fluctuations

The axial impact pressure surveys for jet Mach numbers of 0.6, 1.0 and 1.4 were conducted from the nozzle exit to 80 in. downstream for the 2 in. convergent nozzle with the trolley system shown in Figure 1. The impact pressure probe tip diameter was 1/16 in. and the results of the axial Mach number distributions are presented in Fig. 4. To determine the Mach number from the impact probe data, the static pressure in the jet was assumed to be equal to the ambient pressure. This assumption is reasonable for subsonic jets and for supersonic jets this assumption is satisfied farther downstream from the nozzle exit. For subsonic jets the local Mach numbers were determined from the equation

$$p_a/p_o = (1 + \frac{\gamma - 1}{2} M^2)^{-\frac{\gamma}{\gamma - 1}} \qquad (1)$$

For supersonic jet velocities the Mach number at the exit of the convergent nozzle is sonic and the static pressure is greater than the ambient pressure. Hence, in the immediate vicinity of the convergent nozzle exit the Mach numbers were determined from the equation

$$p_o'/p_o = (\frac{(\gamma + 1)M^2}{(\gamma - 1)M^2 + 2})^{\frac{\gamma}{\gamma - 1}} (\frac{\gamma + 1}{2\gamma M^2 - (\gamma - 1)})^{\frac{1}{\gamma - 1}} \qquad (2)$$

Farther downstream from the nozzle exit, the Mach numbers were determined from the Rayleigh formula

$$p_a/p_o' = (\frac{2\gamma}{\gamma + 1} M^2 - \frac{\gamma - 1}{\gamma + 1})^{\frac{1}{\gamma - 1}} (\frac{\gamma + 1}{2} M^2)^{-\frac{\gamma}{\gamma - 1}} \qquad (3)$$

In Ref. 4 with a 2 in. convergent nozzle it was shown that the difference in the Mach numbers determined by Eqs. (2) and (3) became smaller as the jet Mach number approached unity.

Because of the large contraction ratio used for 2 in. convergent nozzle, Fig. 1, the Mach number on the axis remained constant over the initial 5 diameters for jet exhaust Mach numbers of 0.6 and 1.0. Normally for subsonic exhaust Mach numbers the uniform region

8

extends over 4 to 5 diameters depending on the turbulence level in the flow. Downstream of the uniform core region the velocity decreases monotonically with distance, and by plotting the Mach number and axial distance on log-log graph paper it was shown in Ref. 6 that the velocity decayed as x^{-1} in a fully developed turbulent subsonic flow region. For the jet Mach number of 1.4 the axial Mach number over the initial portion of the jet is not constant but varies because of the existence of the shock bottles for convergent nozzles shown in Refs. 4 and 6. And the flow decreased to sonic velocity at approximately 14 diameters from the nozzle exit. In the subsonic region downstream of the sonic location on the axis, it was shown in Ref. 6 that the velocity decreased as x^{-1}, similar to that observed for subsonic jets. Thus, the velocity decay in the subsonic region for initial supersonic jets is not affected by the presence of shock waves with a convergent nozzle. In Refs. 4 and 6 more detailed axial Mach number distributions are presented for other subsonic and supersonic jet Mach numbers.

The piezoelectric impact pressure fluctuations along the axis obtained with the 1/4 in. diameter Kistler quartz piezoelectric gage are presented in Fig. 5 for jet Mach numbers of 0.6, 1.0 and 1.4. For the jet Mach number 0.6 the rms impact pressure fluctuation was 0.018 mv at 1 diameter downstream from the nozzle exit and the peak value of 0.38 mv occurred at the 10 diameter location. Beyond the peak value the rms impact pressure fluctuations decreased as $x^{-1.75}$ as observed previously in Ref. 6. At sonic jet velocity the impact pressure fluctuation was 0.056 mv at the 1 diameter location and the peak value was 1.16 mv at 10 diameters. At a nominal jet Mach number of 1.4, the piezoelectric impact pressure fluctuation was 0.20 mv at a location of 1 diameter from the nozzle exit. This value is influenced by the presence of the detached shock wave for the impact probe in the supersonic region of the flow. Further investigations are being conducted to determine the relationship between the fluctuating turbulent velocity ahead of the probe detached shock wave and the probe output. A laser doppler velocimeter is being developed to determine the mean velocity and the fluctuating turbulent velocity in the subsonic and supersonic flows without disturbing the flow. By comparing the piezoelectric impact pressure probe output with laser doppler velocimeter results, it is anticipated that a calibration can be developed for the piezoelectric impact pressure output in supersonic flows. The peak impact pressure fluctuation of 2.6 mv occurred 12.5 diameters from the nozzle exit, which is just ahead of the sonic location on the axis, Fig. 5. Downstream of this peak fluctuation the impact pressure fluctuation output decreased as $x^{-1.75}$, similar to that observed for subsonic jet Mach numbers. Thus, both the velocity and impact pressure fluctuations in a fully developed turbulent flow decayed like subsonic jets over the subsonic portion of an initial supersonic jet.

With the trolley system, Fig. 1, axial surveys were also conducted
to determine the static pressure fluctuations due to turbulence for
subsonic and supersonic exhaust velocities. A sharp tip was used
for the static pressure probe, Fig. 3, with a piezoelectric pres-
sure transducer to measure the fluctuating static pressure fluctua-
tions caused by the turbulent flow and acoustic waves present in
the jet. The convergent nozzle with an exit diameter of 2 in. was
used for the investigation and the pressure ratio across the nozzle
was selected to produce flow Mach numbers of 0.6, 1.0, and 1.4, cor-
responding to the flow conditions used to determine the impact
pressure fluctuations with a piezoelectric impact probe. For jet
Mach numbers of 0.6 and 1.0 the static pressure fluctuations over
the initial 4 diameters from the nozzle exit were nearly constant
as indicated in Fig. 6. The axial velocity distributions for these
subsonic Mach numbers, Fig. 4, indicated the uniform core region
extended over the initial 5 diameters. For a jet Mach number of
0.6 the peak static pressure fluctuations occurred at approximately
9 diameters from the nozzle exit, and the peak pressure fluctuations
was approximately twice the value observed over the initial 4 dia-
meters. The peak impact pressure probe fluctuations along the axis
also occurred at approximately 9 diameters from the nozzle exit.
Downstream of the peak location the static pressure decreased con-
tinuously up to the 20 diameter location, and further downstream
the static pressure fluctuations decreased more rapidly as shown in
Fig. 6. Additional investigations will be conducted at other sub-
sonic Mach numbers to determine the variation of the static pres-
sure fluctuations with axial distance.

For sonic jet flow the peak static pressure fluctuations occurred
at approximately 11 diameters from the nozzle exit as shown in Fig.
6, which is located slightly farther downstream than for the Mach
0.6 jet flow. The peak impact pressure fluctuations occurred also
at approximately 11 diameters as indicated in Fig. 5. The peak
static pressure fluctuation was approximately twice the value ob-
served over the initial 4 diameters. Beyond the peak value the
static pressure fluctuations decreased continuously up to a loca-
tion of 40 diameters from the nozzle exit. Additional static pres-
sure fluctuation measurements will be made over greater axial dis-
tances and other subsonic jet Mach numbers to determine the varia-
tion of the static pressure fluctuation with distance more
accurately.

The axial static pressure fluctuations were determined with a sharp
static probe at a jet Mach number of 1.4 and the results are pre-
sented in Fig. 6. For this convergent nozzle there were seven
visible shock bottles at a nominal Mach number of 1.4 with the
sonic velocity occurring at a distance of 14.4 diameters from the
nozzle exit in Fig. 4. The rms values of the static pressure
fluctuations have scatter in the supersonic region of the jet

10

because of the presence of the shock bottles. The peak static pressure fluctuation occurred at approximately nine diameters and the peak value was nearly twice as large as that observed near the jet exit. The location of the peak piezoelectric impact pressure fluctuation was at approximately 12.5 diameters, Fig. 5, which is farther downstream than for the location of the peak static pressure fluctuation. Downstream of the sonic location on the axis, the static pressure fluctuations in the subsonic region decreased with the slope similar to that observed for the sonic jet as shown in Fig. 6.

3.1.2 Sound Pressure Level Distributions and Power Spectra for Subsonic and Supersonic Jets

The acoustic characteristics of the convergent nozzle with an exit diameter of 2 in. were determined by tape recording the microphone output at eight angular positions from 19.1 to 146.4° on a 10-ft. radius from the nozzle exit. The overall sound pressure levels determined from the microphone are presented as a function of the angular position from the jet axis in Fig. 7.

For subsonic Mach numbers of 0.6 to 1.0 the peak sound pressure level occurred at the 19.1° position from the jet axis, and the sound pressure level decreased monotonically over the angular positions for both Mach numbers. This is the typical angular variation of the sound pressure level for subsonic jets as observed in Refs. 2, 4, 6, 44-48. But for a supersonic jet Mach number of 1.4 the maximum overall sound pressure level occurred at the 19.1° location and the sound pressure level decreased to the 44.1° position. For larger angular positions the overall sound pressure level did not decrease but remained nearly constant because of the presence of the seven shock bottles. In Ref. 2 it was observed that the overall sound pressure level decreased continuously from the peak near the jet exit for a contoured nozzle operated at a design Mach number of 1.5.

The microphone data was analyzed and the third-octave band sound power were determined as a function of the frequency for the jet Mach numbers, of 0.6, 1.0, and 1.4. These microphone data were obtained on a 10-ft. radius from the jet exit so that the power spectra at frequencies less than 100 Hz is in the near-field causing the scatter as indicated in Fig. 8. And with the General Radio tape recorder the upper limit of the frequency response was 16 kHz for recording the microphone data. For subsonic Mach numbers of 0.6 and 1.0 the power spectra were quite similar with peak sound power levels occurring at 1.6 kHz and 5.0 kHz at about the same power levels at these peak. Between these peak frequencies there is a slight dip in the sound power levels for this particular nozzle. At a supersonic jet Mach number of 1.4 the dip in the power

spectra disappeared and the peak sound power level occurred at approximately 5 kHz. For higher frequencies the sound power level decreased to 16 kHz as indicated in Fig. 8.

The peak sound power level for the Mach 1.4 jet was 145 db and the overall sound power level was 152.5 db re 10^{-13} watts as indicated in Fig. 8. For the sonic jet Mach number the peak power level was approximately 127 db with an overall sound power level of 136.2 db. The differences in the overall sound power levels for jet Mach numbers of 1.4 and 1.0 is 16.3 db. And the difference in the overall sound power levels between the jet Mach numbers of 1.4 and 0.6 is 32.9 db. These results indicate that it is possible to achieve large noise reduction from a supersonic jet by shielding the acoustic radiation from the supersonic region and decreasing the jet velocity by inducing the flow through the shrouds as observed in Refs. 1, 2, 7, and 8.

To confirm the accuracy of the power spectra determined by the spectrum analyzer described in Section 2, the recorded tape data was also analyzed with a General Radio Multichannel third-octave band analyzer. The microphone data was obtained for a jet Mach number of 1.4 and at the angular position of 19.1° from the jet axis on a 10-ft. radius from the nozzle exit. The comparison of the sound pressure spectra determined by the two analyzer systems is presented in Fig. 9, and the agreement between the two analyzer systems is excellent over the frequency range of 40 Hz to 16 kHz.

The sound pressure level variations with frequency were determined at the eight angular positions for a Mach 1.4 condition, and the results are presented in Fig. 10. Again in this figure the sound pressure levels for frequencies less than 100 Hz are not reliable because the microphone data were obtained on a 10-ft. radius. At the 19.1° location from the jet axis the sound pressure level increased to a peak value at approximately 2.7 kHz before decreasing, and over the frequency range of 100 Hz to 2.7 kHz the sound pressure levels were the highest compared to the other angular positions. For the 33.6° position the sound pressure levels were lower than that observed for the 19.1° position over the frequency range of 100 Hz to 2.5 kHz, where the peak sound pressure level occurred. And at higher frequencies the sound pressure levels were greater than for the 19.1 position. For the 43.8° position the sound pressure level increased from 100 Hz to 2.5 kHz, and over the frequency range of 2.5 to 16 kHz the sound pressure level remained nearly constant. For the 60° angular position the sound pressure level increased continuously from 100 Hz to 11 kHz before decreasing.

At an angular position of 80.4° the sound pressure level increased from 100 Hz to 6.4 kHz before decreasing at higher frequencies. The sound pressure level increased from 100 Hz to 3 kHz for the

12

99.6° location and the sound pressure level increased rapidly from 105 db at 3 kHz to a peak of 117 db at 4.5 kHz. This rapid increase in the sound pressure level over the frequency range of 3 to 4.5 kHz could be caused mainly by acoustic radiation from the shock bottles. For the 120° location the rapid increase in the sound pressure level occurred over the frequency range of 2 to 4 kHz, and for the 146.4° location the sound pressure level increased rapidly over the frequency range of 1.5 to 3.3 kHz. It would be interesting to compare the sound pressure variation with frequency for different angular positions for convergent and contoured nozzles at supersonic jet Mach numbers. The differences in the sound pressure levels at the different angular positions would indicate the acoustic radiation due to the shock bottles for convergent nozzles.

3.2 Mean and Fluctuating Velocities and Static Pressure Fluctuations Distributions for Subsonic and Supersonic Jets

3.2.1 Contours of Mach Number and Static Pressure Fluctuations

Impact and static pressure probes were used to survey at various axial and radial locations from the exit of the one inch diameter convergent nozzle, Fig. 2, over a jet Mach number range of 0.6 to 1.4. The impact pressure probe opening was 1/16 in. diameter at the tip. The 1/8 in. diameter static pressure probe had a sharp tip with a 1/4 in. diameter quartz pressure transducer to measure the rms value of the static pressure fluctuations as shown in Fig. 3. As discussed previously the Mach numbers were determined from the impact pressure measurements and with the assumption that the static pressure in the jet was equal to the ambient pressure. The subsonic Mach numbers were determined from Eq. (1) and for the supersonic region the Mach number was determined from Eq. (3). The Mach number distributions for jet Mach numbers of 0.6 to 1.4 are presented in Figs. 11a to 16a. In Ref. 6 the Mach number and piezo-electric impact pressure fluctuation contours were obtained for these jet Mach numbers.

For a jet Mach number of 0.6 the Mach number and rms value of the piezoelectric static pressure fluctuation contours are presented in Fig. 11a. With this convergent nozzle the core region extends to approximately 4 diameters from the nozzle exit. And downstream of the core region the velocity on the axis decays rather rapidly. Also, the jet boundary increases nearly linearly over the initial portion of the jet plume and the jet diameter is approximately twice the nozzle exit diameter at an axial location of 4 diameters. The jet plume expands rapidly to 3.5 diameters at an axial location of 9 diameters from the nozzle exit. Farther downstream the jet plume does not expand as rapidly.

The corresponding static pressure fluctuation contours for the Mach

13

0.6 jet are presented in Fig. 11a and are plotted as a function of the radial distance for constant axial locations in Fig. 11b. The peak rms value for the static pressure fluctuations are located near the nozzle exit at a radial location equal to the nozzle radius. These static pressure fluctuation contours are entirely different than the contours for the constant impact pressure fluctuations observed in Ref. 6. It is also interesting that the static pressure probe detects pressure fluctuations outside the jet plume as indicated in Fig. 11a. This would indicate that the static pressure probe is measuring the acoustic pressure outside the jet boundary, and within the jet plume the probe is measuring the static pressure fluctuations due to the turbulence and the acoustic waves. For a given axial location the maximum static pressure fluctuations do not occur on the axis but occur at radial locations slightly greater than the nozzle radius.

The variations of the piezoelectric static pressure fluctuations across the jet plume for various axial locations are presented in Fig. 11b for a jet Mach number of 0.6. For an axial distance of 2 diameters from the nozzle exit the peak pressure fluctuation occurred at $r/r_O = 1.2$ and the static pressure fluctuation decreased for greater radial positions toward the jet boundary which occurred at $r/r_O = 1.5$. The static pressure fluctuation was appreciable at this boundary location and it decreased rather rapidly outside the jet plume. For an axial position of 4 diameters the peak static pressure fluctuations occurred at a radial location of $r/r_O = 1.25$, and the peak value was much less than for the $x/D = 2$ location. Even at the jet boundary, $r/r_O = 2.05$, the static pressure fluctuation is appreciable and the decrease was more gradual outside the jet plume than at the location closer to the nozzle exit. As the axial distance from the nozzle exit increased, the change in the radial static pressure fluctuation distributions became more gradual with lower peak values which were located at larger r/r_O values in the jet plume. And at axial locations of 14 and 18 diameters the magnitude of the static pressure fluctuations across the jet plume were nearly constant and the pressure outside the jet decreased rather slowly with radial distance.

The mean Mach number and static pressure fluctuation contours for jet Mach numbers of 0.7 and 0.85 are presented in Figs. 12a and 13a. For these Mach numbers the spreading of the jet plume with distance from the nozzle exit is quite similar, and the jet core region on the axis extends to a region slightly less than 4 diameters. The contours of constant Mach numbers at these two exit Mach numbers are also quite similar. The contours for the constant static pressure fluctuations for the Mach 0.7 jet is quite similar to that observed for the Mach 0.6 jet in Fig. 11a with the peak static pressure fluctuations located at $r/r_O = 1.25$ at an axial location of 2 diameters in Fig. 12a. And farther downstream the

14

peak static pressure locations are at greater radial distances
from the jet axis. The static pressure fluctuation contours for a
jet Mach number of 0.85, Fig. 13a, are slightly different than
those observed for the lower Mach numbers of 0.6 and 0.7 near the
nozzle exit. The peak static pressure fluctuations occurred at
r/r_o = 1.25 and x/D = 2, and the radial location of the peak
fluctuations were located farther away from the jet axis with
axial distance than that observed for the lower jet Mach numbers.

Piezoelectric static pressure fluctuations profiles across the jet
plume for various axial distances from the nozzle exit are pre-
sented in Figs. 12b and 13b for jet Mach numbers of 0.7 and 0.85
respectively. At the axial location of 2 diameters the peak static
pressure fluctuations were located at r/r_o = 1.25 for both jet Mach
numbers with the peak value for M_j = 0.85 being approximately 30
percent higher than for M_j = 0.7. The radial variations of the
static pressure fluctuations were quite similar for these Mach num-
bers with the jet plume boundary being located at approximately
r/r_o = 1.6 and 1.75. For both Mach numbers the static pressure
fluctuations decrease rather rapidly outside the jet plume as in-
dicated in Figs. 12b and 13b. The location of the peak static
pressure fluctuations moved farther away from the jet axis as the
plume spread out with distance for both Mach numbers. At the
farthest distance downstream from the jet exit, x/D = 18, the
radial distributions of the static pressure fluctuations were not
as uniform as observed for the jet Mach number of 0.6.

In Fig. 14a the constant Mach number and static pressure fluctua-
tion contours are presented for a jet Mach number of unity. The
spreading of the jet plume is similar to that observed for the
lower Mach numbers and the velocity contours are also similar. In
the vicinity of the jet exit the sonic region is very small com-
pared to the subsonic mixing region. The peak static pressure
fluctuation region occurred at r/r_o = 1.25 and x/D = 2.25 as in-
dicated in Fig. 14a, which was similar to the type of peak static
pressure fluctuations observed for the Mach 0.85 jet, Fig. 13a.
The peak static pressure fluctuations as a function of the axial
distance from the nozzle exit moved radially farther out from the
jet axis. For this sonic exhaust velocity the static pressure
fluctuations throughout the jet plume were greater than that ob-
served at lower subsonic Mach numbers.

The radial piezoelectric static pressure fluctuation profiles across
the jet plume for various axial locations are presented in Fig. 14b
for sonic exhaust velocity. At x/D = 2 location the static pressure
fluctuations were low in the vicinity of the axis and increased to
a peak value at r/r_o = 1.25 before decreasing rapidly. Even at the
jet boundary, r/r_o = 1.75, the static pressure fluctuation is
appreciable and it decreases rather rapidly outside the jet plume.

The location of the peak static pressure fluctuations moved farther out from the jet axis as the jet plume increased in diameter. And at the farthest location downstream of $x/D = 18$, the static pressure fluctuations were quite large throughout the jet plume compared to the lower jet Mach numbers.

Contours for mean velocity and static pressure fluctuations for supersonic jet Mach numbers of 1.2 and 1.4 from a convergent nozzle are presented in Figs. 15a and 16a respectively. For a Mach number of 1.2 the supersonic region extends to approximately $x/D = 7.4$ from the nozzle exit as shown in Fig. 15a. The jet plume expands very similar to that observed for the sonic jet Mach number condition. Even at the axial location of 2 diameters the subsonic mixing region is nearly as large as the supersonic region, and the increase in the thickness of the subsonic mixing region around the supersonic region increased very rapidly with axial distance. The corresponding static pressure fluctuation contours for this jet Mach number are presented in Fig. 15a. Since the nozzle is convergent, there were six shock bottles at Mach 1.2 as discussed in the previous Ref. 6. Over the supersonic region of the jet the static pressure fluctuation contours are not regular like the sonic and subsonic jet Mach numbers, Figs. 11a-14a, because of the presence of the shock waves in the jet. The peak static pressure fluctuations occurred near the jet axis at $x/D = 3.0$ in the shock bottle region, while for subsonic jet Mach numbers the peak static pressure fluctuations occurred at a radial location of approximately $r/r_O = 1.25$ near the nozzle exit. For this supersonic jet Mach number the static pressure fluctuations outside the jet plume were much greater than observed for sonic and subsonic Mach numbers. Downstream of the supersonic region, $x/D \geq 7.4$, the contours of the static pressure fluctuations in the subsonic jet plume region were similar to those observed with the sonic and subsonic jets, but the pressure levels were much higher than for the subsonic jets.

The radial profiles of the static pressure fluctuations as a function of the distance from the nozzle exit for a Mach 1.2 jet are presented in Fig. 15b. At an axial location of $x/D = 2$ the static pressure fluctuations increase from the jet axis to a peak value at $r/r_O = 1.3$. For this axial location the sonic velocity was at $r/r_O = 0.9$ and the outer edge of the jet plume was at $r/r_O = 1.75$. Thus, the peak static pressure fluctuations occurred in the subsonic mixing region of the jet instead of being in the supersonic region. And outside the jet plume for $r/r_O > 1.75$ the static pressure decreased rapidly at a rate similar to that observed for a sonic jet at this axial location as indicated in Fig. 14b. For an axial location of $x/D = 4$ the peak static pressure fluctuations occurred at $r/r_O = 0.5$ which is in the supersonic region since the sonic velocity is at $r/r_O = 0.65$. The outer edge of the jet plume at this axial location was at $r/r_O = 2.25$. Over the subsonic mixing

16

region, $0.65 \leq r/r_o \leq 2.25$, the peak pressure fluctuations occurred at $r/r_o = 1.75$. The static pressure fluctuations outside the jet plume, $r/r_o \geq 2.25$ decreased rather rapidly as indicated in Fig. 15b.

For an axial location of $x/D = 6$ the sonic velocity occurred at $r/r_o = 0.35$ and the outer edge of the jet plume was at $r/r_o = 2.75$. Thus, the subsonic mixing region at this distance from the nozzle exit is very large. The peak pressure fluctuations occurred at $r/r_o = 1.75$ and the pressure decreased towards the outer edge of the jet. For axial locations of 8 to 18 diameters from the nozzle exit, the flow at these locations was subsonic since sonic velocity on the axis occurred at $x/D = 7.4$. Over these axial locations the static pressure fluctuation profiles were similar to those observed for the sonic and subsonic jets, Figs. 11b-14b, with the location of the peak static pressure fluctuations moving farther away from the jet axis with increasing distance from the nozzle exit. At the axial location $x/D = 18$ the static pressure fluctuations increased from the jet axis to a peak at $r/r_o = 2.5$ before decreasing towards the jet boundary.

In Fig. 16a the contours of constant Mach number and static pressure fluctuations are presented for a jet Mach number of 1.4. The supersonic region extends to $x/D = 10.7$ from the nozzle exit while the sonic location was $x/D = 7.4$ for the Mach 1.2 jet. Because of the convergent nozzle operated at supersonic velocity, at this Mach number there were seven bottles as discussed in Ref. 6. Even for this supersonic Mach number the subsonic mixing region grows rapidly with distance from the nozzle exit so that the supersonic flow region is surrounded with an appreciable subsonic flow. The rate of decrease of the radius of the supersonic region with distance from the nozzle exit was smaller than for the Mach 1.2 jet, Fig. 15a, but the increase in the radius of the jet plume was similar to that observed for the Mach 1.0 and 1.2 jets.

The contours of the static pressure fluctuations for the Mach 1.4 jet, Fig. 16a, were similar to those observed for the Mach 1.2 jet over the supersonic region of the jet. And the peak pressure fluctuations occurred at $x/D = 6.7$ and near the jet axis. The static pressure fluctuation contours are quite irregular over the supersonic region of the jet because of the presence of shock bottles. Over the initial portion of the supersonic jet the static pressure fluctuations outside the jet plume was quite appreciable compared to the subsonic jets. The static pressure contours for the subsonic region of the jet plume, $x/D > 10.7$, were similar to those observed for sonic and subsonic jets, Figs. 11a-14a, but the magnitude of the static pressure fluctuations were much larger than for subsonic jets.

The static pressure fluctuation profiles across the jet as a
function of the distance from the nozzle exit are presented in
Fig. 16b for a jet Mach number of 1.4. At an axial location of
$x/D = 2$ the sonic location is at $r/r_0 = 1.05$ and the outer edge of
the jet plume is at $r/r_0 = 1.7$. The highest peak static pressure
occurred in the supersonic region at $r/r_0 = 0.25$ and a second peak
pressure fluctuation occurred at $r/r_0 = 1.5$, which is in the sub-
sonic mixing region. Outside the jet plume the static pressure
fluctuations did not decrease as rapidly as for the sonic and sub-
sonic jets. For an axial location of 4 diameters the sonic velo-
city occurred at $r/r_0 = 0.95$ and the outer edge of the jet plume
was located at $r/r_0 = 2.1$. The peak static pressure fluctuations
occurred in the supersonic region at $r/r_0 = 0.3$ and the second peak
occurred in the subsonic mixing region at $r/r_0 = 1.75$, and outside
the jet plume the static pressure fluctuations decreased rather
slowly.

At an axial location of $x/D = 6$ the sonic velocity occurred at
$r/r_0 = 0.8$ and the outer edge of the jet boundary was located at
$r/r_0 = 2.6$. Again the peak static pressure fluctuations occurred
in the supersonic region on the axis and the second lower peak
occurred in subsonic mixing region at $r/r_0 = 1.75$ as shown in Fig.
16b. Outside the jet plume the static pressure fluctuations de-
creased rather slowly. For $x/D = 8$ location the sonic velocity was
located at $r/r_0 = 0.55$ and the edge of the jet boundary was at r/r_0
$= 3.1$. The peak static pressure fluctuation occurred in the super-
sonic region at $r/r_0 = 0.25$ and the static pressure fluctuation de-
creased with the radial distance from the jet axis. The sonic velo-
city was located at $r/r_0 = 0.25$ for an axial location of $x/D = 10$
and the outer edge of the jet plume was at $r/r_0 = 3.5$. For this
axial location the peak static pressure occurred close to the jet
axis, Fig. 16b, and the second lower peak pressure occurred in the
subsonic mixing region at $r/r_0 = 2.0$. Outside the jet plume the
static pressure fluctuations decreased rather gradually. Over the
subsonic region of the jet, $x/D = 14$ and 18, the static pressure
fluctuation profiles were similar to those observed for sonic and
subsonic jets. The peak pressure fluctuations occurred at $r/r_0 =$
2.5 for an axial location of $x/D = 14$, and at $r/r_0 = 3.0$ for $x/D =$
18.

The contours for mean velocity and static pressure fluctuation were
quite similar for subsonic jet Mach numbers of 0.6 to 1.0. But the
contours for the supersonic jet Mach numbers of 1.2 and 1.4 were
quite different from those observed for sonic and subsonic jets.
With a convergent nozzle operated at supersonic Mach numbers the
presence of the shock bottles changed the static pressure fluctua-
tion contours compared to subsonic jets. For both subsonic and
supersonic jets the static pressure fluctuations varied continuously
across the jet plume and to the region outside the plume so that the

18

piezoelectric pressure probe was measuring the static pressure fluctuations due to turbulence and the pressure fluctuation associated with the acoustic waves.

In Figs. 17a and 17b the contours for constant impact and static pressure fluctuations are presented for jet Mach numbers of 1.0 and 1.4 respectively. It was shown in Ref. 6 by comparing the hot-wire and laser doppler velocimeter with the piezoelectric impact pressure probe data that the rms output of the impact probe was proportional to the local turbulent velocity fluctuations for subsonic flow. Thus, the contours of the impact pressure fluctuations are proportional to the local turbulent velocity fluctuations. For sonic jet velocity the peak turbulent velocity fluctuations occurred in a toroidal region located at $r/r_0 = 0.5$ and over axial distances of $x/D = 4$ to 6.5 as indicated in Fig. 17a. On the axis of the jet the peak velocity fluctuations occurred at approximately 7 diameters from the nozzle exit and farther downstream the impact pressure fluctuations decreased as $x^{-1.75}$, Refs. 4 and 6. The corresponding static pressure fluctuation contours are quite different than the piezoelectric impact pressure fluctuation contours as shown in this figure. The peak static pressure fluctuations occurred at approximately $r/r_0 = 1.25$ and $x/D = 2.1$ from the nozzle exit. Thus, the peak turbulent velocity fluctuations and static pressure fluctuations are located at entirely different locations within the jet plane. Kraichnan[52] in the analysis of subsonic turbulent flow showed that the static pressure fluctuations due to turbulence were dependent upon the local turbulent velocity and the mean velocity gradient for shear flows. Thus, for sonic and subsonic jet flows the shear gradient existing in the turbulent mixing region plays an important part in the static pressure fluctuations caused by turbulent flow.

The contours for the constant piezoelectric impact pressure fluctuations for a jet Mach number of 1.4, Fig. 17b, are quite different than the contours observed for the sonic jet, Fig. 17a. The peak pressure fluctuations are located over a toroidal region near the axis but farther downstream than that observed for the sonic Mach number. Over the supersonic portion of the jet, $0 < x/D < 10.7$ the peak pressure fluctuations occurred close to the radial sonic location for a given axial distance from the nozzle exit. Downstream of the supersonic region the impact pressure fluctuations contours were similar to those observed for the fully developed turbulent subsonic jet in Ref. 6. The corresponding static pressure fluctuation contours were again different than the impact pressure fluctuation contours at this supersonic Mach number of 1.4. And the locations of the peak impact and static pressures were closer for this jet Mach number than for the sonic jet, Fig. 17a. The static pressure fluctuations outside the jet plume were quite appreciable for this supersonic Mach number. Downstream of

the supersonic region the radial location of the peak static pressure fluctuations moved farther away from the jet axis, similar to that observed for the sonic and subsonic jets.

3.2.2 Axial Distributions of Piezoelectric Static Pressure Fluctuations for Jet Mach Numbers of 0.6 to 1.4.

With a 1/8 in. diameter piezoelectric static pressure probe, Fig. 3, the variations of the static pressure fluctuations were determined for the 1 in. diameter convergent nozzle, Fig. 2, over a jet Mach number range of 0.6 to 1.4 and the results are presented in Fig. 18. Because of the probe length the static pressure fluctuations were determined over axial distances of 1 to 26 diameters with the upper limit being imposed by the travel of the probe holder, Fig. 2. For jet Mach numbers of 0.6 and 0.7 and static pressure fluctuations over the initial 3 diameters from the jet exit were about the same with the peak fluctuations occurring at $x/D = 2$. For both Mach numbers the core region extended to $x/D = 4$ and the end of the transition region occurred at approximately 8 diameters from the nozzle exit. The static pressure fluctuations for the Mach 0.6 jet decreased rather slowly over the region $4 < x/D < 10$ and more rapidly at greater distances. The static pressure fluctuations for the Mach 0.7 jet also decreased slowly over the region $4 < x/D < 10$, but the static pressures fluctuations were higher than that observed for the Mach 0.6 jet at distances greater than $x/D = 3$. For the Mach 0.85 jet the static pressure fluctuations were much greater than that observed for the lower Mach numbers near the nozzle exit. And over the range of $4 < x/D < 10$ the static pressure fluctuations are nearly constant before decreasing more rapidly with distance. Over the range of $17 < x/D < 26$ the static pressure fluctuations decreased approximately as $x^{-1.95}$, which is a slightly faster decrease than for the piezoelectric impact pressure variation with distance of $x^{-1.75}$ as discussed in Refs. 4 and 6.

For sonic jet exhaust velocity the static pressure fluctuations at $x/D = 1$ was very close to the values observed at this location for jet Mach numbers of 0.6 and 0.7 as shown in Fig. 18. The peak static pressure fluctuation, occurred at $x/D = 4$ and the pressure fluctuations remained nearly constant over the range $6 < x/D < 10$ before decreasing rapidly with distance. The rate of decrease of the static pressure fluctuations with distance for $x/D > 17$ was close to that observed for the Mach 0.85 jet. Because of the presence of the shock bottles for supersonic Mach numbers of 1.2 and 1.4 the static pressure fluctuations over the supersonic region varied more randomly than for sonic and subsonic jets as indicated in Fig. 18. For a supersonic jet Mach number of 1.2 the peak pressure fluctuations occurred in the supersonic region at $x/D = 3$, and the pressure decreased rather rapidly up to the sonic location,

20

x/D = 7.4. Over the range of 10 $\leq$ x/D $\leq$ 15 the static pressure
fluctuations decreased rather slowly and then decreased rapidly
with distance for x/D > 15. The peak static pressure fluctuations
occurred at x/D = 6.5 location for the Mach 1.4 jet. From this
location to the sonic location x/D = 10.7 the static pressure
fluctuations decreased very rapidly as shown in Fig. 18. Over the
initial subsonic region the static pressure fluctuations decreased
rather slowly similar to that observed for Mach 1.2 jet. For axial
distance greater than x/D > 15 the static pressure fluctuations de-
creased rapidly with distance as observed for sonic and subsonic
jets.

4.0 ANALYSIS OF PIEZOELECTRIC IMPACT AND STATIC PRESSURE FLUCTUATIONS AND TURBULENT VELOCITY FLUCTUATIONS

4.1 Hot-Wire, Piezoelectric Impact Pressure Fluctuations, Laser Doppler Velocimeter

For subsonic jets the noise of the flow exhausting to the ambient air is produced primarily by the turbulence in the highly sheared mixing region as shown by Lighthill[9,10]. To solve the Lighthill equation for the acoustic propagation from subsonic jets, it is necessary to know the strength and distributions of the stress tensor in the jet plume. At the present this information is not available for subsonic jets and investigations are being conducted to determine the acoustic source distributions for both subsonic and supersonic jets. The acoustic phenomena for supersonic jets are more complicated than the subsonic jets because of the presence of shock waves and supersonic mixing regions. In this section the piezoelectric impact pressure probe results will be correlated with the hot-wire and laser doppler velocimeter measurements. And an analysis will be presented to show the relationship between the piezoelectric impact and static pressure fluctuations and the local turbulent velocity fluctuations.

In Fig. 19 the hot-wire data along the axis for a Mach number of 0.3 are presented, which were obtained by Laurence[12], Bradshaw[13], and Pettit[30]. All of these data were normalized with respect to the peak value of the turbulent velocity fluctuations on the axis. The nozzle diameters used by these investigators were 3.5, 2.0, and 0.5 in. respectively. Pettit[30] determined the turbulent velocity fluctuations along the jet axis with both hot-wire and laser doppler velocimeter technique with excellent agreement between the two entirely different methods at a jet Mach number of 0.3. It is interesting to note that the turbulent velocity fluctuations along the axis determined by these authors agreed within the experimental accuracy for different nozzle diameters.

The piezoelectric impact pressure fluctuations along the axis for a convergent nozzle with an exit diameter of 2 in. were determined over a jet Mach number range of 0.6 to 1.4 in Ref. 4. For this nozzle at a Mach number of 0.6 the peak impact pressure fluctuations occurred at approximately 9 diameters from the nozzle exit, and the results are presented in Fig. 19. There is an excellent agreement between the hot-wire data for the turbulent velocity fluctuations and the piezoelectric impact pressure data from the nozzle exit to the peak velocity fluctuation location. Downstream of the peak the impact pressure fluctuations are less than the normalized hot-wire results because the velocity on the axis decreased as x^{-1} as shown in Ref. 6.

22

4.2 Analysis of Piezoelectric Impact and Static Pressure Fluctuations

Goldstein in Ref. 53 analyzed the measurements of the total and static pressures in an incompressible turbulent flow with pitot and static pressure probes. Fage[54] conducted experiments to determine the effects of fully developed turbulence on the reading of static pressure probes in subsonic flows. Siddon[31] and Bradshaw and Goodman[55] investigated the effects of turbulent flow in subsonic jets on the static pressure measurements, and they found that the correction to the root-mean-square pressure level was small in fully turbulent flow. Fuchs and associates[34-37] and Nakamura and associates[32,33] conducted investigations with total and static pressure probe geometries with microphones as the sensing elements to measure the impact and static pressure fluctuations in fully developed subsonic turbulent pipe flow and in the mixing region of a subsonic jet.

For a fully developed turbulent flow at low subsonic velocities with no appreciable shear gradient, the turbulence can be considered roughly isotropic, so that if (u',v',w') are the turbulent velocity components, then

$$\overline{u'^2} = \overline{v'^2} = \overline{w'^2} = \frac{1}{3} \overline{q'^2}. \tag{4}$$

For a flow with uniform mean velocity in the x-direction of a cartesian coordinate system, the velocity components can be expressed as

$$u = \overline{U} + u'$$

$$v = v' \tag{5}$$

$$w = w',$$

since $\overline{V}$ and $\overline{W}$ vanish in the assumed axial symmetric turbulent flow. For this assumed uniform low speed homogeneous isotropic turbulent flow there will be a mean static pressure, $\overline{p}$, and the uniform flow with no mean flow shear gradient implies

$$\frac{\partial \overline{U}}{\partial y} = \frac{\partial \overline{U}}{\partial z} = 0. \tag{6}$$

Under these conditions the turbulence can be considered to be isotropic. Kraichnan[52] derived the expression for the mean-square pressure fluctuation associated with the isotropic subsonic turbulence flow as

$$<p'^2> = \overline{p^2}\ u'^4\ c^{-4} \tag{7}$$

where c is the velocity of sound. And the ratio of the turbulence velocity in the flow direction to the local velocity of sound can be expressed as the local turbulence Mach number

$$M' = \frac{u'}{c}. \tag{8}$$

At low Mach number, $\overline{U}/c << 1$, the turbulent velocity u' is usually much less than the mean flow $\overline{U}$; hence, the magnitude of pressure fluctuations associated with the turbulent flow itself is small as given by Eq. (7). Only at higher subsonic velocities does the turbulent pressure fluctuations become appreciable to produce audible acoustic radiation.

In the actual subsonic jet flow there is always a mean velocity gradient in the turbulent mixing region, and for these conditions the isotropic turbulence would quickly evolve into nonisotropic state. Kraichnan[52] approximated this subsonic turbulent shear flow by considering the interaction of the isotropic turbulence with the uniform mean velocity gradient, which is characterized by uniform shear. Under these assumptions for the turbulent flow the mean-square pressure fluctuation is given by

$$<p'^2> = (4/15)\ \tau_0^2\ u'^2\ \eta^{-2}\ \sigma^{-2}, \tag{9}$$

where τ_0 is the mean viscous shear stress, $\eta = \nu/\rho$ is the kinematic viscosity, and σ is related to the area scale of the pressure correlation, as defined in Ref. 52. Thus, the mean-square pressure fluctuation due to turbulence depends upon the mean shear present in the turbulent flow. On the axis of the subsonic jet, $\partial \overline{U}/\partial r = 0$, because of axial symmetric flow, so that Eq. (7) may be used to estimate the static pressure fluctuation due to turbulence and off the axis with radial mean velocity gradient, $\partial \overline{U}/\partial r \neq 0$, Eq. (9) can be used to estimate the static pressure fluctuation.

Besides the turbulent static pressure fluctuations there will be a pressure fluctuation in low speed flows due to a sound field being superimposed from the outside jet flow or generated aerodynamically in the flow. This acoustic pressure fluctuation will be denoted by $\tilde{p}$. Thus, in a low speed turbulent jet flow there will be a static pressure in the flow given by

$$p = \overline{p} + <p'> + \tilde{p} \tag{10}$$

and $<p'>$ is the static pressure fluctuation caused by turbulence, Eq. (7) or Eq. (9), depending upon the mean shear in the turbulent flow. The pressure fluctuations caused by turbulence will be assumed to propagate close to the velocity of the airflow, while the

24

pressure fluctuation due to the acoustic field will propagate with the velocity of sound for low speed flows. And the rms output of the static pressure probe in the jet plume is a function of the static pressure given by Eq. (10) for subsonic flows.

At the stagnation point of the piezoelectric impact pressure probe, the turbulent flow is brought to rest through large gradients of the flow properties. In a low subsonic flow the density can be considered as being constant and at the stagnation region there will be large velocity and pressure gradients as the flow is decelerated to zero velocity at the stagnation point. Thus, in this region the spatial changes will exceed any temporal ones. For these conditions the total pressure along a streamline in turbulent flow from Bernoulli's equation is given by

$$P_T = p + \frac{1}{2} \rho q^2 \tag{11}$$

where q is the vector velocity consisting of a mean vector velocity, and a vector turbulent velocity. By substituting Eqs. (5) and (10) into Eq. (11) and neglecting higher order terms of the turbulent velocity fluctuations, Eq. (11) can be split into mean and fluctuating parts:

$$\overline{P_T} = \overline{p} + \frac{1}{2} \overline{\rho} \ \overline{U}^2 \tag{12}$$

$$P_T' = <p'> + \tilde{p} + \overline{\rho} \ \overline{U} \ u' \tag{13}$$

In this linearization it is implied that the following velocity conditions are satisfied

$$u', \ v', \ w' \ll \overline{U}$$
$$u'^2, \ v'^2, \ w'^2 \ll u' \ \overline{U} \tag{14}$$

and the flow velocity is low so that turbulent flow can be considered as being incompressible with constant density. The contribution to the impact pressure fluctuation by the static pressure fluctuations due to turbulence <p'> given by Eqs. (7) and (9) for low speed turbulent flow should be small. Nakamura et al[32,33] have obtained experimental data in low speed turbulent pipe flow with microphone impact and static pressure probes and confirmed the low level of static pressure fluctuations due to turbulence. Fuchs[33] in his analysis of the pressure fluctuations at the stagnation point for low speed turbulent flow showed that the static pressure fluctuations was an order of magnitude smaller than the total head fluctuations as observed by Nakamura[32,33] and in the present investigation.

When the acoustic field from outside the flow field and the aerodynamic noise produced by the turbulence in subsonic flow is negligible, the acoustic pressure fluctuation $\tilde{p}$ in Eq. (13) can also be neglected. Under these conditions the piezoelectric impact pressure fluctuation with a total head probe configuration in a low speed turbulent flow with negligible acoustic field is given by

$$p_T' \cong \bar{\rho}\, \bar{U}\, u' \tag{15}$$

which is dependent on the local axial velocity fluctuations, mean velocity, and mean density. Therefore, a piezoelectric impact pressure probe can be used in place of hot-wire to investigate the fluctuations in unsteady flows as discussed by Siddon[31], Fuchs[33], and Nagamatsu and associates[6]. And the correlation of the hot-wire and piezoelectric impact pressure probe data in Fig. 19 confirms this hypothesis for low speed turbulent flow encountered along the axis of subsonic jets.

The application of Eq. (15) to determine the turbulent velocity fluctuations for higher subsonic and supersonic turbulent flows must be used with caution because the flow can no longer be considered as being incompressible and the presence of shock waves for supersonic jets. In deriving this equation it was assumed that the static pressure fluctuation due to turbulence and the sound field generated aerodynamically are negligible, which are satisfied for low speed flows. At higher velocities where compressibility effects and static pressure fluctuations due to turbulence and aerodynamically generated sound fields are not negligible in Eq. (10), they must be considered in the piezoelectric impact pressure fluctuations. For supersonic flows there will be a detached shock ahead of the impact pressure probe so that the pressure fluctuations associated with the shock waves must be considered. Laser doppler velocimeter method[30] is being developed to determine the mean and fluctuating velocities in turbulent supersonic flows. With this technique it is possible to determine the local turbulent velocities without disturbing the subsonic and supersonic flows. The piezoelectric impact and static pressure probe results will be correlated with the laser measurements to determine the probe calibration factors for high subsonic and supersonic turbulent flows.

For low speed flows the piezoelectric impact pressure fluctuations can be normalized with respect to the jet exit velocity $\bar{U}_j$ to obtain

$$\frac{p_T'}{\bar{\rho}\, \bar{U}_j^2} = \frac{\bar{U}}{\bar{U}_j}\, \frac{u'}{\bar{U}_j} \tag{16}$$

And the axial velocity fluctuations can be expressed as

$$\frac{u'}{\overline{U}_j} = \frac{p'_T}{\overline{\rho}\ \overline{U}_j^2} \cdot \frac{1}{\overline{U}/\overline{U}_j} \tag{17}$$

It was observed in Refs. 4 and 6 for both 1 and 2 in. convergent nozzles that the velocity decay in the fully developed subsonic turbulent jet, even for original supersonic jet velocities, was given by

$$\frac{\overline{U}}{\overline{U}_j} \propto (x/D)^{-1} \tag{18}$$

And the variation of the piezoelectric impact pressure fluctuations with distance in the fully developed subsonic turbulent flow was expressed as

$$p'_T \propto (x/D)^{-1.75}, \tag{19}$$

also as shown in Fig. 5.

The piezoelectric static pressure fluctuations on the axis for 2 in. and 1 in. convergent nozzles are presented in Figs. 6 and 18 respectively. For the 2 in. diameter nozzle the piezoelectric static pressure fluctuations along the axis were determined for jet Mach numbers of 0.6, 1.0 and 1.4 in Fig. 6. Additional static pressure fluctuations on the axis will be determined at other subsonic and supersonic jet Mach numbers over greater distances to determine the variation of the static pressure fluctuations with distance. With the 1 in. nozzle the piezoelectric static pressure fluctuations along the nozzle were determined over the Mach number range of 0.6 to 1.4 in Fig. 18. For jet Mach numbers of 0.6 to 1.0 the piezoelectric static pressure fluctuations decrease approximately as

$$p_{s_f} \propto (x/D)^{-1.95} \tag{20}$$

in the fully developed subsonic turbulent flow region. On the axis of the jet the radial velocity gradient $\partial\overline{U}/\partial r = 0$ because of symmetry so that the mean static pressure fluctuation due to turbulence can be expressed from Eq. (7) as

$$<p'> \propto \overline{\rho}\ u'^2 \tag{7a}$$

By assuming that the turbulence in the fully developed subsonic turbulent jet is approximately constant and using the experimental velocity decay along the jet axis, Eq. (18), the mean static pressure fluctuation associated with the turbulence Eq. (7a) becomes

$$\langle p' \rangle \propto (x/D)^{-2} \tag{21}$$

Thus, the experimental variation of the piezoelectric static pressure fluctuations along the jet axis, Eq. (20), is close to that calculated from the Kraichnan theory for isotropic subsonic turbulent flow with no mean shear, Eq. (21).

5.0 FLOW AND ACOUSTIC CHARACTERISTICS OF SUPERSONIC JET NOISE SUPPRESSORS

5.1 Multiple Tubes and Shrouds Suppressor

5.1.1 Flow and Acoustic Characteristics of Suppressor for Mach 1.4 Jet.

The available fundamental information regarding the suppression of supersonic jet exhaust noise is very limited, and consequently an investigation was initiated to determine the flow and acoustic characteristics of various suppressor configurations for reducing the noise level of supersonic jets. The initial suppressor configuration consisted of six small rods to produce shock waves in the primary jet flow and a long single shroud for shielding the acoustic radiation from the supersonic region and inducing ambient air to reduce the velocity of the primary jet flow by momentum exchange as discussed in Refs. 1 and 2. Since the length of the single shroud was very long for effective noise reduction of a supersonic jet, it was decided to investigate the multiple tubes and shrouds suppressor configurations presented in Ref. 7. In these references only limited flow information were obtained to show the change in the flow characteristics associated with large jet noise reduction. Thus, additional flow characteristics were obtained with piezoelectric impact and static pressure probe surveys along the axis in the present study. To obtain further insight regarding the jet noise suppression phenomena, power spectra at various angular positions from 19.1 to 146.4° were obtained for the single shroud configuration.

A sketch of the multiple tubes and shrouds suppressor configuration is presented in Fig. 20. The tube bundle consists of 191 tubes with an outside diameter of 0.125 in., inside diameter of 0.115 in., and length of 2 in. The ratio of the base area of the tube bundle to the internal area of the tube is 4.72, and the internal area of the tubes is equal to a 1-9/16 in. diameter convergent nozzle. The 191 multishrouds are made of hexagonal aluminum honeycomb material that provides a separate shroud for each tube of the 191 tube bundle as shown in Fig. 20. In the present investigation the shrouds were 6 in. long and other lengths have been investigated in Ref. 7. Each side of the hexagonal element was 0.155 in.

The axial variation of the flow Mach number for the convergent nozzle operated at a pressure ratio across the nozzle of 3.2, which corresponds to an isentropic expansion Mach number of 1.4, was determined from the impact pressure probe measurements and the results are presented in Fig. 21a. Because of the presence of the shock bottles[4,6] for a convergent nozzle operated above the critical pressure, the Mach number in the shock bottle region varies,

depending on the location of the impact pressure probe. On the axis the sonic velocity is attained at a distance of 19 in. from the nozzle exit, which corresponds to $x/D = 12.1$. With the 191 tubes operated at a pressure ratio of 3.2 the sonic velocity is located very close to the tube exit and the flow attains a nearly constant Mach number of approximately 0.73 at 1.5 in. from the tube exit. The supersonic region is a function of the nozzle exit diameter and the jet Mach number as discussed in Ref. 3, and hence, the supersonic region was drastically decreased from the plain convergent nozzle with an exit diameter of 1-9/16 in. to the case with the tubes with exit diameter of 0.115 in. Downstream of the multiple tubes the merged Mach number remains nearly constant over a distance of approximately 16 in. before decreasing with distance. This 16 in. distance corresponds to approximately 4 diameters of the merged jet flow region. With the addition of the 191 shrouds to the 191 tubes with the shroud entrance located 3/16 in. upstream of the tube exits, the axial Mach number downstream of the multiple shrouds was decreased even further to approximately 0.57 as indicated in Fig. 21a. The Mach number was approximately constant for approximately 12 in. before decreasing with distance. Because of the large wetted area in the 6 in. long shrouds, the viscous effects are very pronounced with a more rapid decay in the velocity than for the convergent nozzle and for the 191 tubes.

The axial piezoelectric impact pressure measurements were obtained with a 1/4 in. diameter quartz piezoelectric pressure gage and the rms impact pressure fluctuations for the plain nozzle, multiple tubes and shrouds are presented in Fig. 21b. It was shown in the previous section that the piezoelectric impact pressure fluctuation for subsonic flow is a function of the local density, mean velocity, and turbulent velocity fluctuation, Eq. (15). For the plain nozzle at a Mach number of 1.4, the peak impact pressure fluctuations occurred just ahead of the sonic location as observed previously in Refs. 2, 4, and 6, and the decay of the rms impact pressure fluctuations was approximately $x^{-1.75}$ over the subsonic turbulent flow region. With the 191 tubes the rms peak impact pressure fluctuation was approximately 1.02 mv located at 30 in. from the tube exits. This peak rms value is approximately 1/4 of the peak value observed for the plain nozzle. Downstream of the peak impact pressure fluctuation location the pressure fluctuations decayed close to $x^{-1.75}$, which was also observed for the plain nozzle in the subsonic turbulent region. The rms peak impact pressure fluctuation with the multiple shrouds was approximately 0.58 mv located at 21 in. from the shroud exit as shown in Fig. 21b.

The overall sound pressure levels as a function of the angular position from the jet axis for the plain jet, multitubes, and multishrouds are presented in Fig. 22 for a jet Mach number of 1.4. These sound pressures were obtained on a radius 10 ft. from the

30

exit of the nozzle, multitubes, and multishrouds. For the convergent nozzle the highest sound pressure level was closest to the jet axis and decreased to the 80° position before increasing because of the shock bottles. At the 19.1° position the sound pressure level with the 191 tubes was approximately 17 db less than that observed with the convergent nozzle. For this configuration the peak sound pressure level occurred at the 43.4° position and at higher angular positions the sound pressure level decreased continuously as observed for subsonic jets. With the addition of the multiple shrouds to the multiple tubes, the sound pressure level at the 19.1° position was approximately 26 db less than that observed for the plain nozzle. The peak sound pressure level occurred at approximately the 50° location, and the sound pressure level decreased for larger angular positions as shown in Fig. 22.

From the eight microphone measurements at 19.1° to 146.4° angular positions on a 10-ft. radius, the microphone data was analyzed to obtain the third-octave band sound power spectra for the various configurations, and the results are presented in Fig. 23 for a Mach number of 1.4. In this figure the power spectra below 100 Hz cannot be too reliable because the microphone is in the near-field for frequencies lower than this value. For the convergent nozzle the peak sound power level of approximately 144.5 db is at 5 kHz and the power decreased for higher frequencies. The overall sound power level for the plain nozzle with a pressure ratio of 3.2 to produce a nominal Mach number of 1.4 was 150.8 db. With the 191 tubes the sound power spectra was less than for the plain nozzle with approximately 24 db lower power at a frequency of 5 kHz. Over the frequency range of 1 kHz to 8 kHz the sound power level was close to 120 db, and it increased slightly from 8 kHz to 16 kHz. The overall sound power level with the multiple tubes was 135.3 db which is 15.3 db less than that observed for the convergent nozzle. By adding multiple shrouds to the multiple tubes the sound power spectra was decreased from that of the multiple tubes over the frequency range of 80 Hz to 3.2 kHz as shown in Fig. 23. The sound power level increased rather sharply for frequency range of 3.2 to 5 kHz and for higher frequencies the sound power level was approximately 120 db. And the overall sound power level for this configuration was 130.3 db which is 20.5 db less than that for the convergent nozzle. Thus, the multiple tubes and shrouds are very effective suppressor configurations for a supersonic Mach 1.4 jet. The multiple shroud suppressor is not too practical because of the size and large wetted area with a corresponding large thrust loss as discussed in Ref. 7. Concepts are being developed to replace the multiple shrouds with other devices to achieve the same noise level reduction of supersonic jets without the complexity and large thrust loss.

In the previous investigations of the multiple tubes and shrouds

suppressor configurations in Ref. 7 the acoustic characteristics of these suppressors at a jet Mach number 0.7 were determined but no flow characteristics were obtained. To obtain additional information regarding these suppressors at subsonic jet Mach numbers, axial surveys were conducted with an impact probe and piezoelectric impact and static pressure probes to determine the mean and fluctuating velocities and fluctuating static pressures. The 1-9/16 in. diameter convergent nozzle was operated at a pressure ratio across the nozzle of 1.4 to produce a jet Mach number of 0.7, and the axial Mach number distribution for this condition is presented in Fig. 24a. Over the initial 8 in. the flow Mach number is nearly constant, and the velocity decreases rapidly in the fully developed turbulent flow region. With the multiple tubes the Mach number decreased from 0.4 at the tube exit to approximately a Mach number of 0.31 at the 2 in. location. And the Mach number along the axis was nearly constant from this location to 20 in. downstream. For distances farther downstream the Mach number approached that for the plain nozzle as indicated in this figure. By adding the multiple shrouds to the multiple tubes the Mach number at the shroud exit was approximately 0.28 and it decreased to 0.25 at the 2 in. location. The Mach number remained nearly constant to the location 12 in. from the tube exit before decreasing rapidly with distance.

In Fig. 24b the rms impact pressure fluctuations distributions along the jet axis are presented for the convergent nozzle, multiple tubes, and multiple shrouds at a jet Mach number of 0.7. The peak rms impact pressure fluctuation of 0.6 mv occurred for the plain nozzle at a distance 14 in. from the nozzle exit. Downstream of this location the impact pressure fluctuation decreased close to $x^{-1.75}$, which is the case for a fully developed subsonic turbulent jet flow. With the multiple tubes the peak impact pressure fluctuation of 0.14 mv occurred at 30 in. from the tube exit before decreasing rapidly with distance. This peak rms impact pressure fluctuation is approximately 1/4 of the peak value observed for the plain nozzle. For the multiple tubes and shrouds the peak impact pressure fluctuation of 0.078 mv occurred at a location 18 in. from the shroud exit. Downstream of the peak location the rms impact pressure fluctuation decreased similar to that observed for the plain nozzle and multiple tubes.

The axial piezoelectric static pressure fluctuations for the various configurations at a jet Mach number of 0.7 were obtained with a sharp tip static pressure probe and a quartz piezoelectric pressure transducer, and the results are presented in Fig. 24c. For the convergent nozzle the rms static pressure fluctuations increased from 2 in. downstream of the nozzle to a peak value of 0.066 mv at 16 in., which is located 2 in. farther downstream than the location of the peak impact pressure fluctuation, Fig. 24b. Downstream of this peak location the static pressure fluctuations decreased slowly

32

to the 50 in. location, and beyond this point the static pressure fluctuations decreased more rapidly with distance. For the 191 tube configuration the rms static pressure fluctuation values are 0.016 mv at 25 and 35 in. from the tube exit. And this peak value is approximately 1/4 of the peak rms static pressure fluctuation for the convergent nozzle. With the addition of the multiple shrouds to the tubes the peak rms static pressure fluctuation of 0.015 mv occurred at 40 in. from the shroud exit. This peak value is close to the peak value for the multiple tubes even though the Mach number for the multiple shrouds is lower than for the multiple tubes as indicated in Fig. 24a. Evidently the large wetted surface in the multiple shrouds increased the viscous effects in the jet plume.

The overall sound pressure levels as a function of the angular position from the jet axis for the various configurations at a jet Mach number of 0.7 are presented in Fig. 25. For the convergent nozzle the peak sound pressure level occurred at the 19.1° location and it decreased monotonically with angular position as observed previously in Refs. 4 and 6 for a 2 in. diameter convergent nozzle at subsonic Mach numbers. With 191 tubes the peak sound pressure level increased from the 19.1° location to a peak at 46.4° before decreasing at larger angular positions from the jet axis. At the 19.1° location the sound pressure level was approximately 9 db less than that observed for the plain nozzle. For the multiple tubes with the multiple shrouds the overall sound pressure level at the 19.1° location was 13 db lower than for the plain nozzle at this location. The sound pressure level increased to a peak value of 83.2 db at approximately 45°, and then decreased to the 80° position after which it was nearly constant.

In Fig. 26 the sound power spectra for the convergent nozzle, multiple tubes, and multiple shrouds configurations are presented for a jet Mach number of 0.7. For the plain nozzle the peak power of 112.8 db occurred at 4 kHz, and the power spectra increased from 100 Hz to 2.5 kHz before dipping at 3.2 kHz and increasing to 4 kHz. At higher frequencies the sound power level decreased continuously to 16 kHz, and the overall sound power level was 120.5 db. With the 191 tubes the sound power level was less than that for the plain nozzle over the frequency range of 160 Hz to 16 kHz. with the greatest difference of approximately 15 db from 1 kHz to 4 kHz. The sound power level increased from 5 kHz to 16 kHz and it approached the plain nozzle condition at the highest frequency. With these tubes the overall sound power level was 116 db which was 4.5 db less than for the convergent nozzle. By adding the multiple shrouds to the tubes the sound power level was decreased over the frequency range of 100 Hz to 1 kHz from that of the multiple tube configuration. And over the frequency range of 1 kHz to 6.5 kHz the sound power level was slightly higher than for

the tubes. Over the frequency range 6.5 to 16 kHz the sound power
level was nearly constant and lower than for the multiple tubes.
The overall sound power level was 112.7 db which was 7.8 db lower
than that observed for the convergent nozzle. Thus, the addition
of the multiple shrouds to the tubes increased the suppression by
3.3 db.

5.2 Single Shroud with Six Rods Suppressor

5.2.1 Flow and Acoustic Characteristics of Suppressor for Mach 1.4 Jet.

An initial supersonic jet noise suppressor configuration was
selected in Ref. 2 to achieve large induced flow with shielding
of the acoustic radiation from the supersonic region of the jet.
This was accomplished by the use of a long 4 in. diameter pipe
with a length of 58 in. as shown in Fig. 27. The primary nozzle
was a convergent nozzle with an exit diameter of 2 in., and six
1/4 in. diameter rods were inserted at the outer periphery of the
nozzle to produce shock waves which interacted with the shock bot-
tles in the primary supersonic jet flow. The leading edge of the
shroud was located 3-1/4 in. upstream of the convergent nozzle
exit. By placing a barrier at the shroud entrance the induced flow
from the ambient air was prevented from entering the shroud.

The convergent nozzle was operated at pressure ratios of 3.2 and
3.7 to achieve nominal jet Mach numbers of 1.4 and 1.5. In Ref. 2
the axial impact Mach number distributions were determined for the
various configurations of the nozzle, rods, and shroud at a jet
Mach number of 1.5 and the results are presented in Fig. 28. Be-
·cause of the shock bottles in the jet plume, the Mach numbers
determined from the impact pressure measurements varied over the
initial portion of the supersonic jet. The flow became sonic at a
location 31 in. from the convergent nozzle exit. And over the
subsonic portion of the jet plume the axial Mach number decreased
monotonically as observed for a Mach 1.4 jet in Ref. 4. With the
long shroud and with six 1/4 in. rods inserted 1/4 in. into the
jet flow, cf. Fig. 27, the axial Mach number at the shroud exit
was 0.78 and it remained nearly constant for 16 in., which cor-
responds to 4 diameters, before decreasing slowly with distance.
With the entrance of the shroud sealed so there is no induced flow,
the Mach number at the shroud exit was approximately 0.56 and the
Mach number remained nearly constant over a distance of 18 in.
before the velocity decayed with distance.

To obtain the overall sound pressure level distribution and the
power spectra over angular positions of 19.1° to 146.4°, the con-
vergent nozzle was operated at a jet Mach number of 1.4 with and
without the single shroud and six rods. For these conditions the

overall sound pressure level distributions with angular position
from the jet axis are presented in Fig. 29. For the plain nozzle
the overall sound pressure level was the highest at the 19.1°
position and decreased to approximately 50° and remained nearly
constant for larger angular positions. The single shroud with six
rods configuration decreased the overall sound pressure level 19.1
db at the 19.1° position from the value observed for the plain noz-
zle. And the sound pressure level increased to a peak value at the
60° location before decreasing at larger angular positions. At
this position the sound pressure level was 8.4 db less than the
value observed with the convergent nozzle. With no induced flow
through the shroud the sound pressure level at the 19.1° location
was decreased 13.7 db from that observed with the plain nozzle.
And the sound pressure level increased to a peak at the 60° posi-
tion before decreasing at larger angular positions. At this angu-
lar position the overall sound pressure level was slightly higher
than the value existing with the plain nozzle. Similar results
were observed in Ref. 2 for a primary jet Mach number of 1.5.

From the microphone measurements the data was analyzed to obtain
the third-octave band sound power level spectra for the convergent
nozzle, shroud, and six rods configuration for a jet Mach number of
1.4 and the results are presented in Fig. 30. For the convergent
nozzle the sound power level increased from 80 Hz to 4 kHz before
decreasing at higher frequencies. With the long shroud and six
rods inserted 1/4 in. into the jet plume, the sound power spectra
was lower than for the plain nozzle with largest reduction of 22
db at 3.2 kHz. At 16 kHz the reduction from the convergent nozzle
was 11 db, and the overall sound power level reduction with this
configuration was 14.2 db from the convergent nozzle at Mach 1.4.
By sealing the entrance to the single shroud, no induced flow, the
primary supersonic jet flow became subsonic in the shroud within a
few diameters from the nozzle exit as observed in Ref. 2 from the
static pressure measurements along the shroud. There was also a
noticeable organ pipe effect present as indicated by the power
spectra at 150 Hz. For the frequency range of 250 Hz to 8 kHz the
power spectra increased before reaching a peak and decreasing to
16 kHz. At 8 kHz the sound power level was approximately 3 db
lower than the value for the convergent nozzle. The Mach number
at the exit of the shroud for this condition was only 0.56, Fig.
28, and the power spectra observed for a Mach number 0.6 in Ref. 4
was much lower than that observed for the long shroud with no in-
duced flow. The overall sound power level was 147.5 db which is
only 4.5 db lower than the value observed for the convergent noz-
zle. Without the shock waves in the shroud and for a jet Mach
number of 0.56 the overall sound power level reduction from a Mach
1.4 jet should be approximately 28 db as discussed in Ref. 2.
Thus, the noise produced by shock waves in a long shroud propagates
to the outside through a subsonic flow without appreciable
attenuation.

35

The sound pressure level versus frequency at the angular positions of 19.1° to 146.4° were determined for the convergent nozzle with and without the shroud for a jet Mach number of 1.4, and the results are presented in Figs. 31a-31h. This investigation was conducted to obtain information regarding the suppression phenomena for a supersonic jet with a long shroud with and without induced flow. Again for frequencies less than 100 Hz the sound pressure levels are not too accurate because the microphone on a 10-ft. radius from the jet exit is in the near-field for lower frequencies.

At 19.1° angular position the sound pressure level at 1.6 kHz for the shroud with induced flow is 23 db lower than that for the convergent nozzle, and the peak pressure level for this condition occurred at 640 Hz as indicated in Fig. 31a. With the long shroud and no induced flow the sound pressure level increased continuously from 320 Hz to 8 kHz before decreasing. And over the frequency range of 10 to 16 kHz the sound pressure level was close to the values for the plain nozzle. For the angular position of 33.6°, Fig. 31b, the sound pressure level increased continuously from 100 Hz to 1 kHz for the shroud with induced flow, and remained nearly constant over the frequency range of 1 to 8 kHz before increasing at higher frequencies. At 2 kHz the sound pressure level was 22 db lower than the value for the plain nozzle. With the shroud and no induced flow the sound pressure level increased from 250 to 8 kHz and remained nearly constant from 10 to 16 kHz, similar to that observed for the plain nozzle. The sound pressure level with the shroud and induced flow increased continuously from 80 Hz to 13 kHz at the 43.8° location Fig. 31c, and the pressure level was 16 db less than that observed for the plain nozzle at a frequency of 2.5 kHz. Again for the shroud without induced flow the sound pressure level increased from 250 Hz to 8 kHz, and it remained nearly constant for higher frequencies. Above 5 kHz the pressure levels were higher for this configuration than for the plain nozzle. The sound pressure levels as a function of the frequency for the 60° position with and without the shroud are presented in Fig. 31d. With the shroud, rods, and induced flow the sound pressure level increased continuously from 340 Hz to 13 kHz before decreasing at 16 kHz. And at all frequencies the sound pressure level was less than that observed for the convergent nozzle. For the case of the long shroud without induced flow the sound pressure level increased from 340 Hz to 8 kHz, and over the frequency range of 3.2 kHz to 6.4 kHz the sound pressure level was close to the values for the plain jet.

At the 80.4° location from the jet axis the sound pressure level for the convergent nozzle increased rather rapidly over the frequency range of 4 kHz to 6.4 kHz before decreasing at higher frequencies as indicated in Fig. 31e. With the shroud, rods, and induced flow configuration, the sound pressure level increased

continuously over the frequency range of 340 Hz to 13 kHz before decreasing at 16 kHz. And at a frequency of 6.4 kHz the sound pressure level was 21 db less than the level for the plain jet. Without the induced flow through the shroud the sound pressure level was close to the values for the plain jet up to 4 kHz and again over the frequency range of 10 kHz to 16 kHz.

The acoustic radiation from the shock bottles for the convergent nozzle at a Mach number of 1.4 is more evident at the angular position of 99.6° in Fig. 31f. There is a very rapid increase in the sound pressure level over the frequency range of 2.5 kHz to 5 kHz. For higher frequencies the sound pressure level decreased rather rapidly. With the shroud and induced flow the sound pressure level increased continuously. And at a frequency of 5 kHz the sound pressure level was 26 db less than that existing for the plain jet. The shroud with induced flow attenuated the shock bottle radiation from emitting to the outside. With the shroud and no induced flow the sound pressure levels over the frequency range up to 2.5 kHz were slightly lower than for the plain jet levels, and the pressure level was nearly constant over the frequency range of 4 kHz to 16 kHz.

The shock noise due to the shock bottles are even more pronounced at the 120° angular location for the convergent nozzle as shown in Fig. 31g. There is a rapid increase in the sound pressure level over the frequency range of 2 kHz to 4 kHz, and at higher frequencies the pressure level decreased to 16 kHz. With the shroud and induced flow the sound pressure level increased from 80 to 10 kHz, and there was a large increase between 10 kHz and 13 kHz before decreasing. At a frequency of 4 kHz the sound pressure level was 29 db less than the value for the plain nozzle. For the case of the shroud with no induced flow the sound pressure levels were lower than for the plain nozzle at all frequencies with the greatest difference of 19 db occurring at a frequency of 4 kHz. Even at the angular position of 146.4° the shock noise is still very noticeable for the convergent nozzle as indicated in Fig. 31h. There is an increase in the sound pressure level of 16 db over the frequency range of 2 kHz to 3.2 kHz. The sound pressure level increased nearly monotonically over the frequency range of 80 Hz to 10 kHz with the shroud and induced flow, and there was a rapid increase in the pressure level from 10 kHz to 16 kHz. This increase in the sound pressure level at this angular position for the microphone is due to the high frequency mixing and shock noise propagating forward through the entrance of the long shroud, cf. Fig. 27. And at a frequency of 3.2 kHz the sound pressure level was 31 db lower than the value observed with the plain jet. With the shroud and no induced flow the sound pressure levels were lower than for the values observed with the plain nozzle with the greatest reduction of 23 db occurring at 3.2 kHz. Over the frequency range of 4 kHz to 16 kHz

the sound pressure level was approximately constant.

These detailed sound pressure level spectra for the convergent noz-
zle with shroud, rods, and induced flow at various angular positions
from the jet axis have indicated the effects of shock bottle noise
and the shielding and attenuation characteristics of the long shroud
with and without induced flow. Without the induced flow through the
shroud the transition shock waves through which the primary super-
sonic jet flow becomes subsonic in a few diameters from the nozzle
exit produce appreciable acoustic radiation. The long shroud with
induced flow shields the shock bottle noise from the primary jet
and the induced flow decreases the jet flow so that the acoustic
radiation from the subsonic flow from the shroud exit is drasti-
cally reduced from that of the plain supersonic jet.

6.0 CONCLUSIONS

Axial surveys were conducted with impact pressure and piezoelectric impact and static pressure probes for a 2 in. diameter convergent nozzle at Mach numbers of 0.6, 1.0, and 1.4. The axial distributions of the velocity for jet Mach numbers of 0.6 and 1.0 were similar with core length of 5 diameters. For a Mach 1.4 jet the sonic location was approximately 14 diameters from the nozzle exit.

The peak piezoelectric impact pressure fluctuations occurred at approximately 9 diameters for both Mach 0.6 and 1.0 jets. Downstream of the peak location in the fully developed subsonic turbulent jet the impact pressure fluctuations decreased as $x^{-1.75}$. For the Mach 1.4 jet the peak impact pressure fluctuations occurred just ahead of the sonic location, and downstream of this location the pressure decreased approximately as $x^{-1.75}$.

The peak static pressure fluctuations occurred at approximately 10 diameters for subsonic jet Mach numbers. Downstream of the peak location the static pressure fluctuations decreased with distance. For the Mach 1.4 jet the peak static pressure fluctuations occurred just ahead of the sonic location on the axis. In the subsonic region the static pressure fluctuations varied similar to that existing for a Mach 1.0 jet.

For jet Mach numbers of 0.6, 1.0, and 1.4 the highest overall sound pressure levels occurred at an angular position of 19.1° from the jet axis. For subsonic jet Mach numbers the sound pressure level decreased continuously with the increase in the angular position. And for the Mach 1.4 jet the sound pressure level decreased over the angular positions of 19.1° to 43.8° and remained nearly constant for larger angles. The power spectra for subsonic jet Mach numbers were quite similar with the peak power occurring at approximately 4 kHz. For the jet Mach number of 1.4 the peak power occurred at approximately 5 kHz due to the presence of shock bottles for the convergent nozzle.

Overall sound pressure level spectra were determined for a Mach 1.4 jet with the convergent nozzle over angular positions of 19.1° to 146.4° from the jet axis. At angular positions of 80.4° to 146.4° the sound pressure level spectra indicated a jump in the pressure level at a frequency of approximately 2.5 kHz. This jump in the pressure spectra is caused mainly by the seven shock bottles existing in the supersonic jet plume.

Detailed radial and axial surveys were conducted with a piezoelectric static pressure probe for a 1 in. diameter convergent nozzle at a Mach number range of 0.6 to 1.4. Contours of constant piezoelectric static pressure fluctuations for subsonic jet Mach numbers of 0.6

to 1.0 were similar with the peak fluctuations occurring close to $r/r_0 = 1.0$ for axial locations near the nozzle exit. At distances farther downstream the peak location moved farther out radially.

For supersonic jet Mach numbers of 1.2 and 1.4 the contours of the constant piezoelectric static pressure fluctuations were quite different than the contours for subsonic jet Mach numbers. The peak static pressure fluctuations occurred close to the jet axis ahead of the sonic location for these supersonic Mach numbers. In the radial direction at a fixed axial location from the nozzle exit there were two peaks in the static pressure fluctuations, one in the supersonic flow region and the second in the subsonic mixing region.

The contours of constant piezoelectric impact and static pressure fluctuations were entirely different for both subsonic and supersonic jet Mach numbers. The location of the peak piezoelectric impact pressure fluctuations, which is related to the turbulent velocity fluctuations, was in a toroidal region downstream of the nozzle for subsonic jet exhaust velocities. But the peak piezoelectric static pressure fluctuations were located radially at approximately one nozzle radius from the axis and close to the nozzle exit. Similar differences were observed for the supersonic jet Mach numbers.

On the axis of the 1 in. convergent nozzle the piezoelectric static pressure fluctuations for subsonic jets increased from close to the jet exit to a peak value and then decreased rapidly in the fully developed turbulent region approximately as $x^{-1.95}$. For supersonic jet Mach numbers the peak piezoelectric static pressure fluctuations occurred ahead of the sonic location on the jet axis, and in the subsonic region the pressure fluctuations decreased similar to subsonic jets.

An analysis was made to show that the output of a piezoelectric impact pressure probe is related to the local turbulent velocity fluctuations for subsonic flows. And the output of the piezoelectric static pressure probe was the sum of the static pressure fluctuations due to turbulence and the acoustic pressure wave present in the flow. The magnitude of the static pressure fluctuation caused by turbulence depends upon the intensity of the turbulence and the mean velocity gradient.

A supersonic jet noise suppressor consisting of 191 tubes and 191 hexagonal shrouds was investigated at pressure ratios of 3.2 and 1.4, which corresponds to jet Mach numbers of 1.4 and 0.7 respectively. The multiple tubes and shrouds decreased the primary jet Mach number drastically for both jet Mach numbers. Axial surveys with piezoelectric impact and static pressure probes indicated

40

large reductions in the impact and static pressure fluctuations from the values existing for the convergent nozzle at supersonic and subsonic Mach numbers.

With the multiple tubes the Mach 1.4 jet noise level was reduced 15.3 db and for the Mach 0.7 jet the reduction was 4.5 db. By adding the multiple shrouds to the tubes the noise level reduction for the Mach 1.4 jet was increased to 20.5 db, while the reduction for the Mach 0.7 jet was 7.8 db.

A supersonic jet noise suppressor consisting of single long shroud, six small rods, and induced flow indicated the large reduction in the jet velocity at the exit of the shroud with and without the induced flow. The Mach 1.4 jet noise level was decreased 14.2 db with the shroud, rods, and induced flow, and without the induced flow the reduction was only 4.5 db. This smaller reduction was due mainly to the large acoustic radiation from the shock waves in the long shroud.

The sound pressure level spectra were determined for the Mach 1.4 jet with the long shroud suppressor and the results indicated that the shroud with rods and induced flow is effective in shielding the acoustic radiation from the supersonic region of the primary jet flow. The noise generated by the strong shock waves within the shroud for the case of no induced flow is propagated to the outside through the subsonic flow with little attenuation.

REFERENCES

1. Nagamatsu, H.T., Sheer, R.E., Jr., and Wells, R.J., "Supersonic Jet Exhaust Noise Reduction With Rods, Shroud, and Induced Flow," Proc. AFOSR-UTIAS Symposium on Aerodynamic Noise, Toronto, May 1968.

2. Nagamatsu, H.T., Pettit, W.T., and Sheer, R.E., Jr., "Flow and Acoustic Measurements on a Convergent Nozzle Supersonic Jet Ejector," General Electric Research and Development Center, Report No. 69-C-156, April 1969.

3. Nagamatsu, H.T. and Horvay, G., "Supersonic Jet Noise," AIAA Paper No. 70-237 (1970).

4. Nagamatsu, H.T., Sheer, R.E., Jr., and Gill, M.S., "Flow and Acoustic Characteristics of Subsonic and Supersonic Jets From Convergent Nozzle," AIAA Paper, No. 70-802 (1969).

5. Nagamatsu, H.T., Sheer, R.E., Jr., and Horvay, G., "Supersonic Jet Noise Theory and Experiments," Basic Aerodynamic Noise Research Conf., NASA SP-207 (1969).

6. Nagamatsu, H.T., Sheer, R.E., Jr. and Bigelow, E.C., "Mean and Fluctuating Velocity Contours and Acoustic Characteristics of Subsonic and Supersonic Jets," General Electric Research and Development Center, Report No. 70-C-391 (1970). AIAA Paper (in press).

7. Nagamatsu, H.T., Sheer, R.E., Jr., and Gill, M.S., "Flow and Acoustic Characteristics of 191 Tubes and 191 Shrouds Supersonic Jet Noise Suppressor," AIAA Paper No. 71-153 (1971).

8. Nagamatsu, H.T. and Sheer, R.E., Jr., "Flow, Thrust, and Acoustic Characteristics of 50 Tubes With 50 Shrouds Supersonic Jet Noise Suppressor," General Electric Research and Development Center, Report No. 71-C-258 (1971).

9. Lighthill, M.J., "On Sound Generated Aerodynamically," Proc. Roy. Soc. A211, 564-587 (1952).

10. Lighthill, M.J., "Jet Noise," AIAA Journal, Vol. 1, No. 7, 1507-1517 (1963).

11. Corrsin, S. and Uberoi, M., "Further Experiments on the Flow and Heat Transfer in a Heated Turbulent Air Jet," NACA, Rept. 998 (1948).

42

12. Laurence, S.C., "Intensity, Scale, and Spectra of Turbulence in Mixing Region of Free Subsonic Jet," NACA, Rept. 1292 (1956).

13. Bradshaw, P., Ferriss, D.H., and Johnson, R.E., "Turbulence in the Noise Producing Region of a Circular Jet," J. Fluid Mech., Vol. 19, Part 4, 591-624 (1964).

14. Warren, W.R., "An Analytical and Experimental Study of Compressible Free Jets," Doctoral Dissertation, Princeton Univ. (1957).

15. Love, E.S., Grigsby, C.E., Lee, L.P., and Woodling, M., "Experimental and Theoretical Studies of Axisymmetric Free Jets," J.A. Sci., 25, p. 791-799 (1958).

16. Powell, A., "The Noise of Choked Jets," JASA, Vol. 25, p. 385-389 (1953).

17. Gibbings, J.C., Inghan, J., and Johnson, D., "Flow in a Supersonic Jet Expanding From a Convergent Nozzle," Aero. Res. Council, ARC. FM. 3968 (1968).

18. Dosanjh, D.S. and Montegani, F.J., "Underexpanded Jet Noise Reduction Using Radial Flow Impingement," AIAA J., Vol. 7, No. 3, p. 458-464 (1969).

19. Johannesen, N.H., "Further Results on the Mixing of Free Axially-Symmetrical Jets of Mach Number 1.40," Aero. Res. Council, ARC. R&M No. 3292 (1959).

20. Eggers, S.M., "Velocity Profiles and Eddy Viscosity Distribution Downstream of a Mach 2.22 Nozzle Exhausting to Quiescent Air," NASA TN D-3601 (1966).

21. Potter, R.C. and Jones, J.H., "An Experiment to Locate the Acoustic Sources in a High Speed Jet Exhaust Stream," Wyle Lab. Rept. (1967).

22. Ollerhead, J.B., "On the Prediction of the Near Field Noise of Supersonic Jets," NASA CR-857 (1967).

23. Davies, P.O.A.L., Fisher, M.J., and Barratt, M.J., "The Characteristics of the Turbine in the Mixing Region of a Round Jet," J. Fluid Mech., Vol. 15, Part 2, 337-366 (1963).

24. Chu, W.T., "Turbulence Measurements Relevant to Jet Noise," Univ. of Toronto, UTIA Rept. 119 (1966).

25. Davies, P.O.A.L., Ko, N.W.M., and Bose, B., "The Local Pressure Field of Turbulent Jets," ARC. C.P. 989 (1967).

26. Nayer, B.M., Siddon, T.E., and Chu, W.T., "Properties of the Turbulence in the Transition Region of a Round Jet," Univ. of Toronto, UTIA Rept. 131 (1969).

27. Kovasznay, L.S.G., "Turbulence in Supersonic Flows," J. Aero. Sci., Vol. 25, No. 10, 657-682 (1953).

28. Laufer, J., "Aerodynamic Noise in Supersonic Wind Tunnels," J. Aero. Sci., Vol. 28, No. 9, 685-692 (1961).

29. Fisher, M.J., "Turbulence Measurements in Supersonic Shock-Free Jets by the Optical Cross Beam Method," NASA TN D-5206 (1970).

30. Pettit, W.T., III, "The Laser Doppler Velocimeter for Measuring Turbulence in Gas Flows," Polytechnic Inst. of Brooklyn, M.S. Thesis (1970).

31. Siddon, T.E., "On the Response of Pressure Measuring Instrumentation in Unsteady Flow," Univ. of Toronto, UTIAS Rept. 136 (1969).

32. Nakamura, A., Matsumoto, R., Sugiyama, A., and Tanaka, T., "Some Investigations on Output Level of Microphones in Air Streams," JASA, Vol. 46, No. 6, 1391-1396 (1969).

33. Nakamura, A., Sugiyama, A., Tanaka, T., and Matsumoto, R., "Experimental Investigation for Detection of Sound-Pressure Level by a Microphone in an Airstream," JASA, Vol. 50, No. 1, 40-46 (1971).

34. Fuchs, H.V., "Fluctuations in a Uniform Moving Medium Originating From Convected Sources," Univ. of Southampton, Inst. of Sound and Vib., Memo. 280 (1969).

35. Fuchs, H.V., "Energy-Balance for Small Fluctuations in a Moving Medium," Univ. of Southampton, Inst. of Sound and Vib., Rept. 18 (1969).

36. Fuchs, H.V., "Measurements of Pressure Fluctuations With Microphones in an Air Stream," Univ. of Southampton, Inst. of Sound and Vib., Memo. 281 (1969).

37. Lau, J.C., Fuchs, H.V., and Fisher, M.J., "A Study of Pressure and Velocity Fluctuations Associated With Jet Flows," Univ. of Southampton, Inst. of Sound and Vib., Rept. 28 (1970).

38. Maestrello, L. and McDaid, E., "Acoustic Characteristics of a High Subsonic Jet," AIAA Paper No. 70-238 (1970).

44

39. Ribner, H.S., "The Generation of Sound by Turbulent Jets," Adv. Appl. Mech., Vol. 8, Academic Press, Inc., N.Y. (1964).

40. Phillips, O.M., "On the Generation of Sound by Supersonic Turbulent Shear Layers," J. Fluid Mech., Vol. 9, Part I, 1-28 (1960).

41. Williams, J.E.F., "The Noise From Turbulence Convected at High Speed," Phil. Trans. Roy. Soc. London, Series A225, 479-503 (1963).

42. Plumblee, H.E., Jr., "The Effect of Exhaust Temperature on the Noise Generation," Lockheed-Georgia Co. Rept. (1967).

43. Ollerhead, J.B., "On the Prediction of the Near Field Noise of Supersonic Jets," Wyle Laboratories, NASA CR-857 (1967).

44. Lassiter, L.W. and Hubbard, H.H., "Experimental Studies of Noise From Subsonic Jets in Still Air," NACA TN 2757 (1952).

45. Lassiter, L.W. and Hubbard, H.H., "The Near Field Noise of Static Jets and Some Model Studies of Devices for Noise Reduction," NACA Rept. 1261 (1954).

46. Mollo-Christensen, E. and Narasimha, R., "Sound Emission From Jets at High Subsonic Velocity," J. Fluid Mech., Vol. 8, 49-60 (1960).

47. Mollo-Christensen, E., "Jet Noise and Shear Flow Instability Seen From an Experimenter's Viewpoint," Trans. of ASME, Paper No. 67, APM-C (1966).

48. Gerrard, J.H., "An Investigation of the Noise Produced by Subsonic Air Jet," J. Aero. Sci., Vol. 23, 855-866 (1956).

49. Mayes, W.H., Lanford, W.E., and Hubbard, H.H., "Near Field and Far Field Noise Surveys of Solid Fuel Rocket Engines for a Range of Nozzle Exit Pressures," NASA TN D-21 (1959).

50. Tatge, R.B. and Wells, R.J., "Model Jet Noise Study at Alplaus Facility," General Electric Engineering Laboratory, Rept. 61GL25 (1961).

51. Smith, E.B. and Brown, W.L., "Acoustic Scale-Model Tests of High-Speed Flows," Martin-Marietta Corp. Rept. CR-66-75 (1966).

52. Kraichnan, R.H., "Pressure Field Within Homogeneous Anisotropic Turbulence," JASA, Vol. 28, 64-72 (1956).

53. Goldstein, S., "A Note on the Measurement of Total Head and Static Pressure in a Turbulent Stream," Proc. Roy. Soc. A155, 570-575 (1936).

54. Fage, A., "On the Static Pressure in Fully Developed Turbulent Flow," Proc. Roy. Soc. A155, 576-596 (1936).

55. Bradshaw, P. and Goodman, D.G., "The Effect of Turbulence on Static-Pressure Tubes," Aeronautical Research Council, R&M No. 3527 (1968).
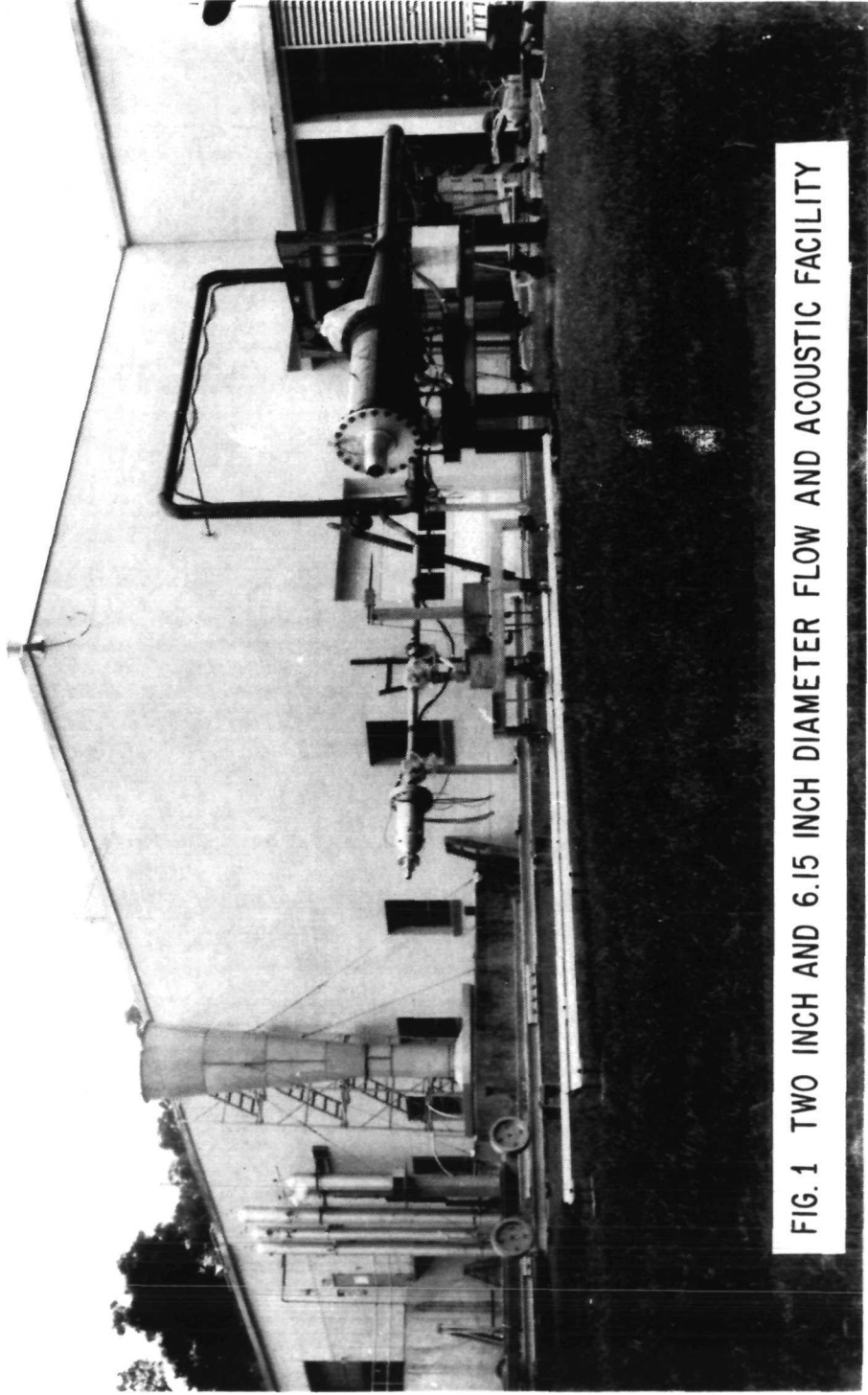
FIG. 1 TWO INCH AND 6.15 INCH DIAMETER FLOW AND ACOUSTIC FACILITY
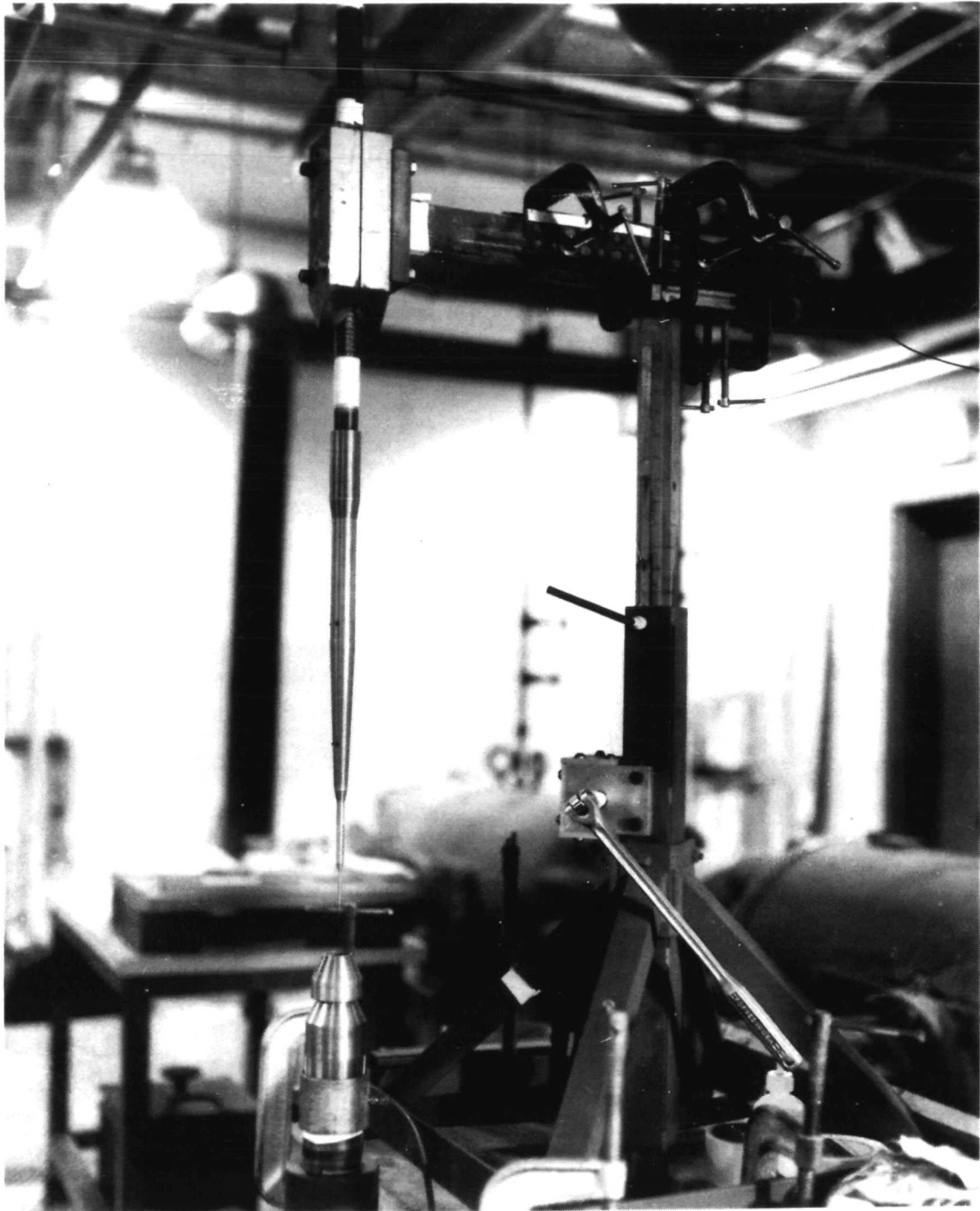
FIG. 2 ONE INCH CONVERGENT NOZZLE AND FLOW FIELD SURVEY EQUIPMENT
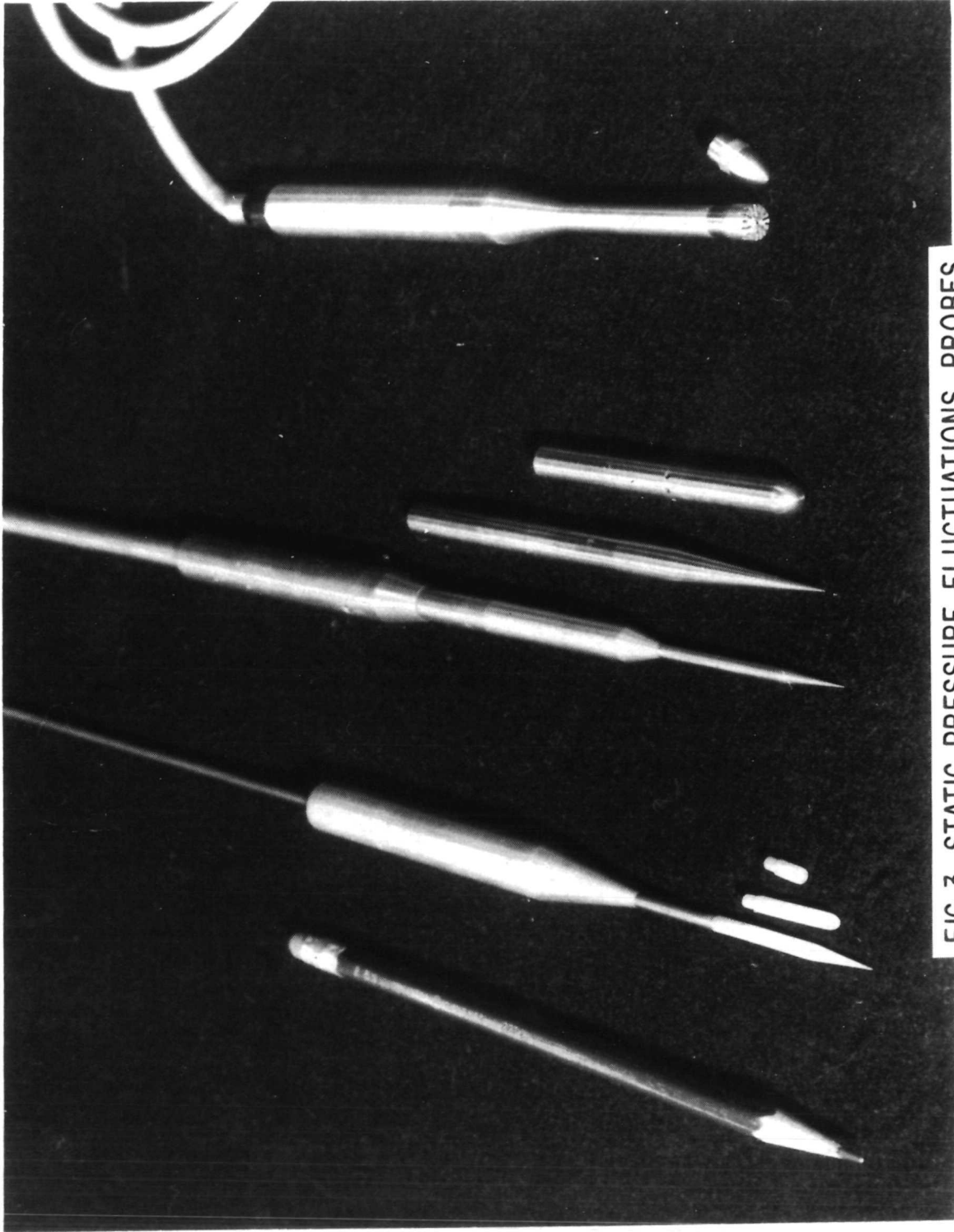
FIG. 3 STATIC PRESSURE FLUCTUATIONS PROBES
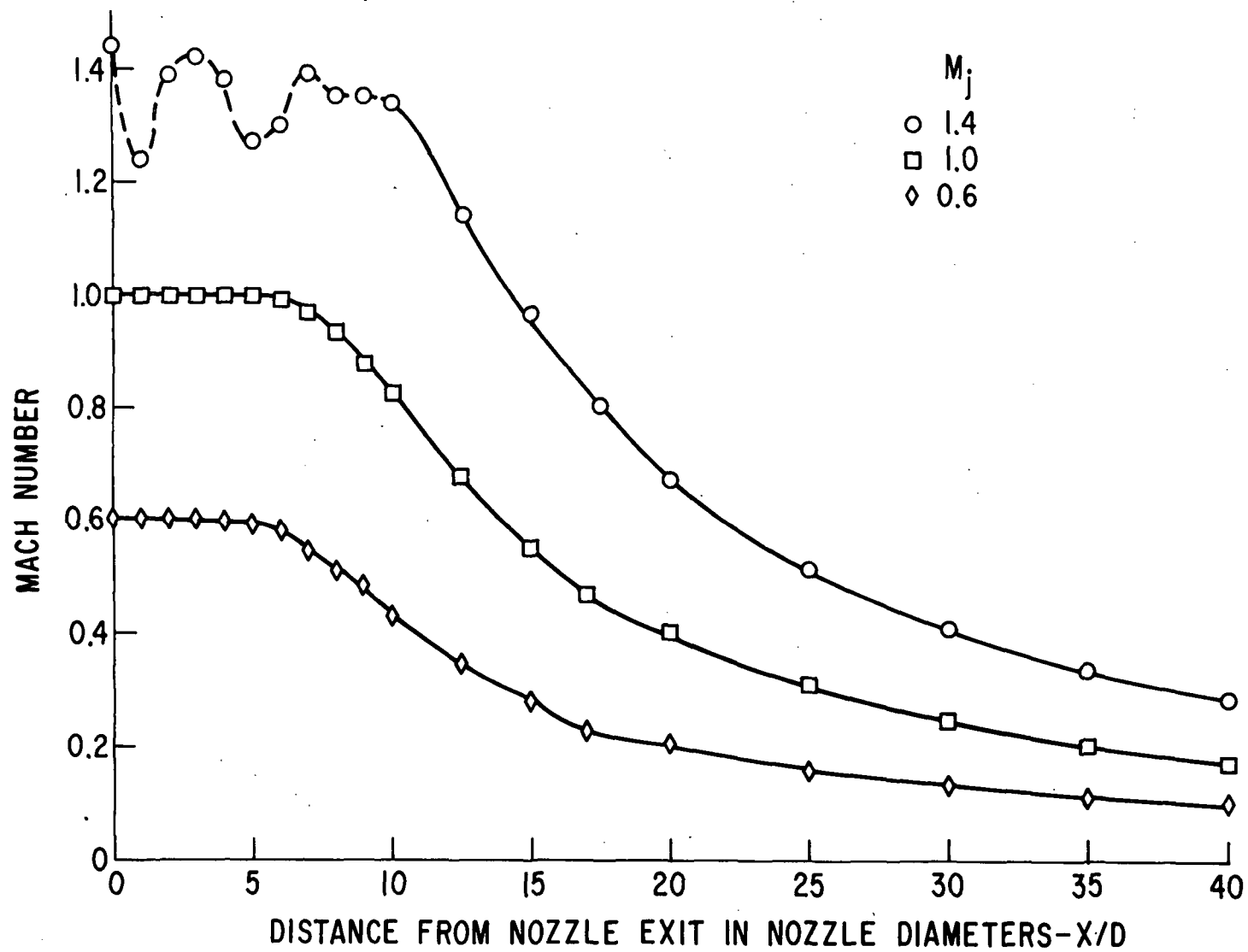
FIG. 4   AXIAL MACH NUMBER DISTRIBUTION FOR 2 INCH CONVERGENT NOZZLE
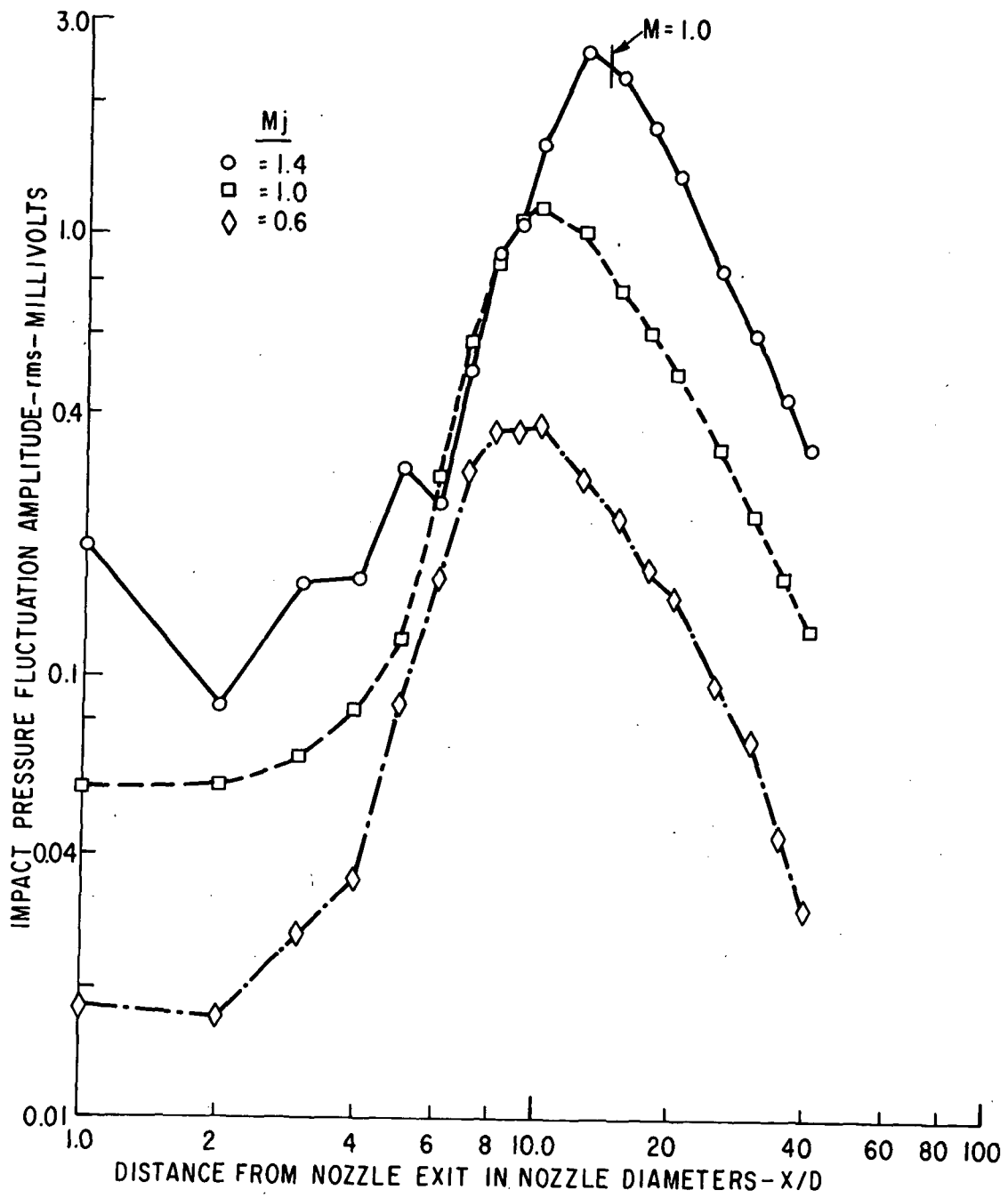
FIG.5 AXIAL IMPACT PRESSURE FLUCTUATIONS FOR 2 INCH CONVERGENT NOZZLE
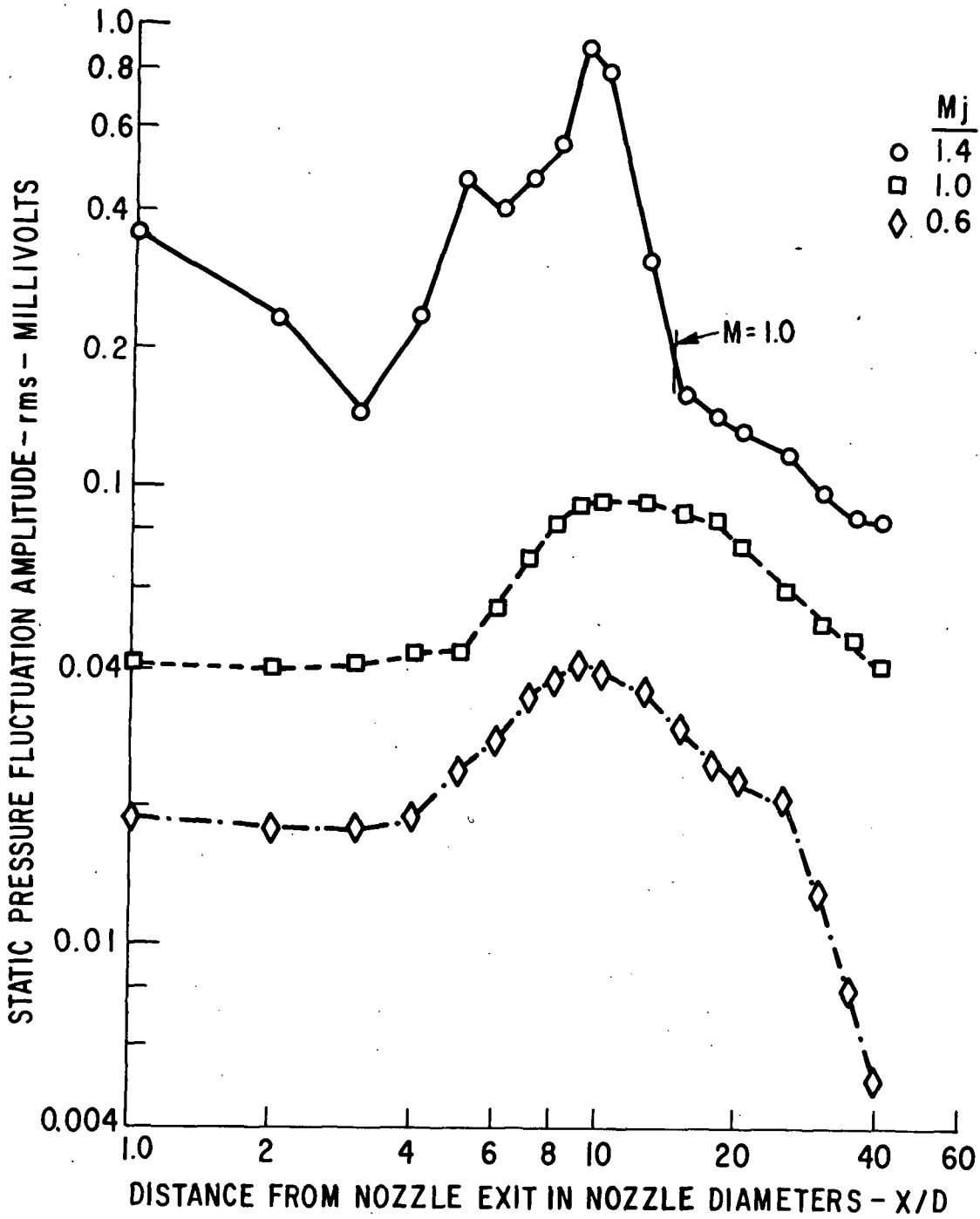
FIG. 6 AXIAL STATIC PRESSURE FLUCTUATIONS FOR 2 INCH CONVERGENT NOZZLE
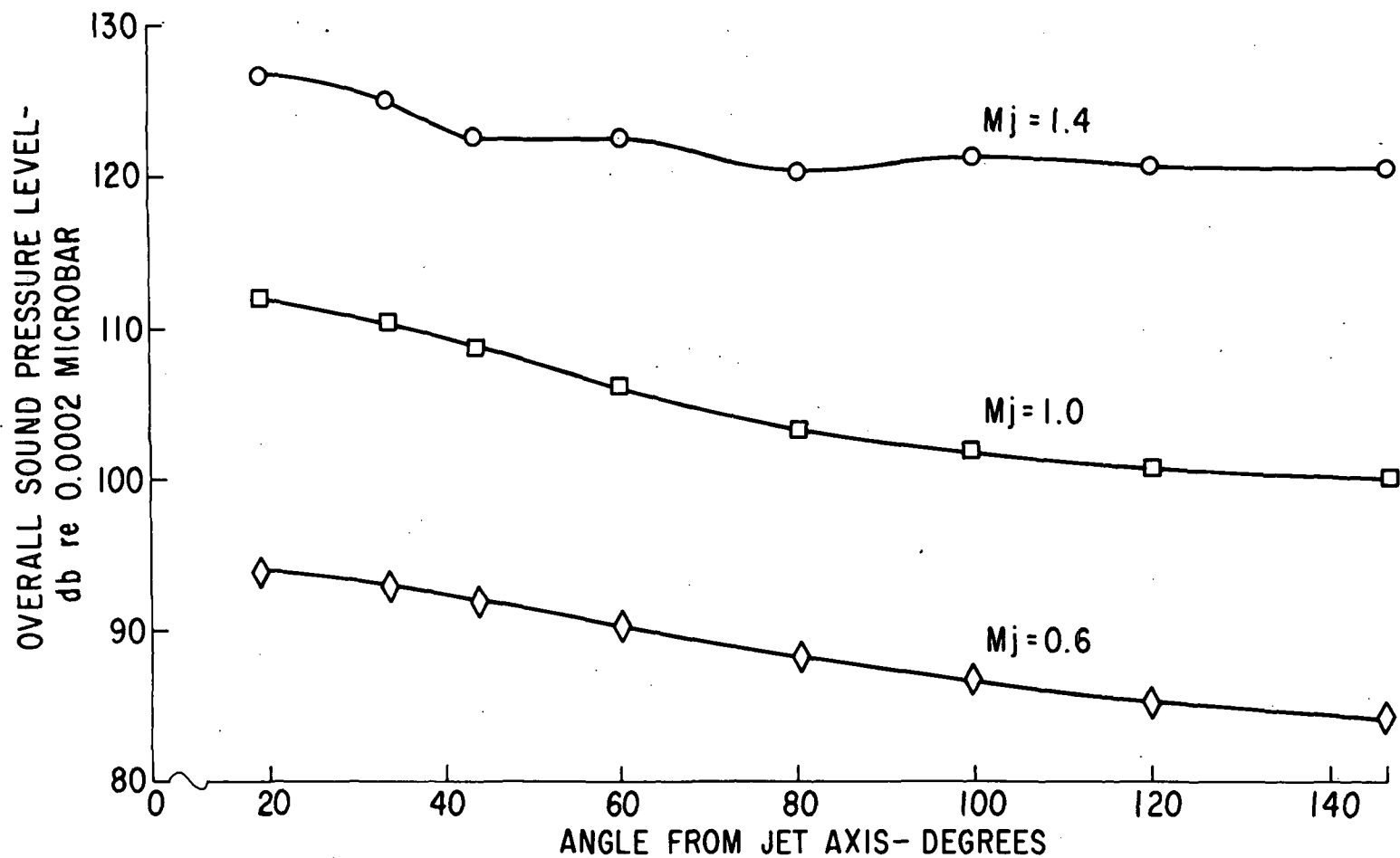
FIG.7   OVERALL SOUND PRESSURE LEVEL AS A FUNCTION OF ANGULAR POSITION FROM AXIS FOR 2 INCH DIAMETER CONVERGENT NOZZLE AT DIFFERENT MACH NUMBERS
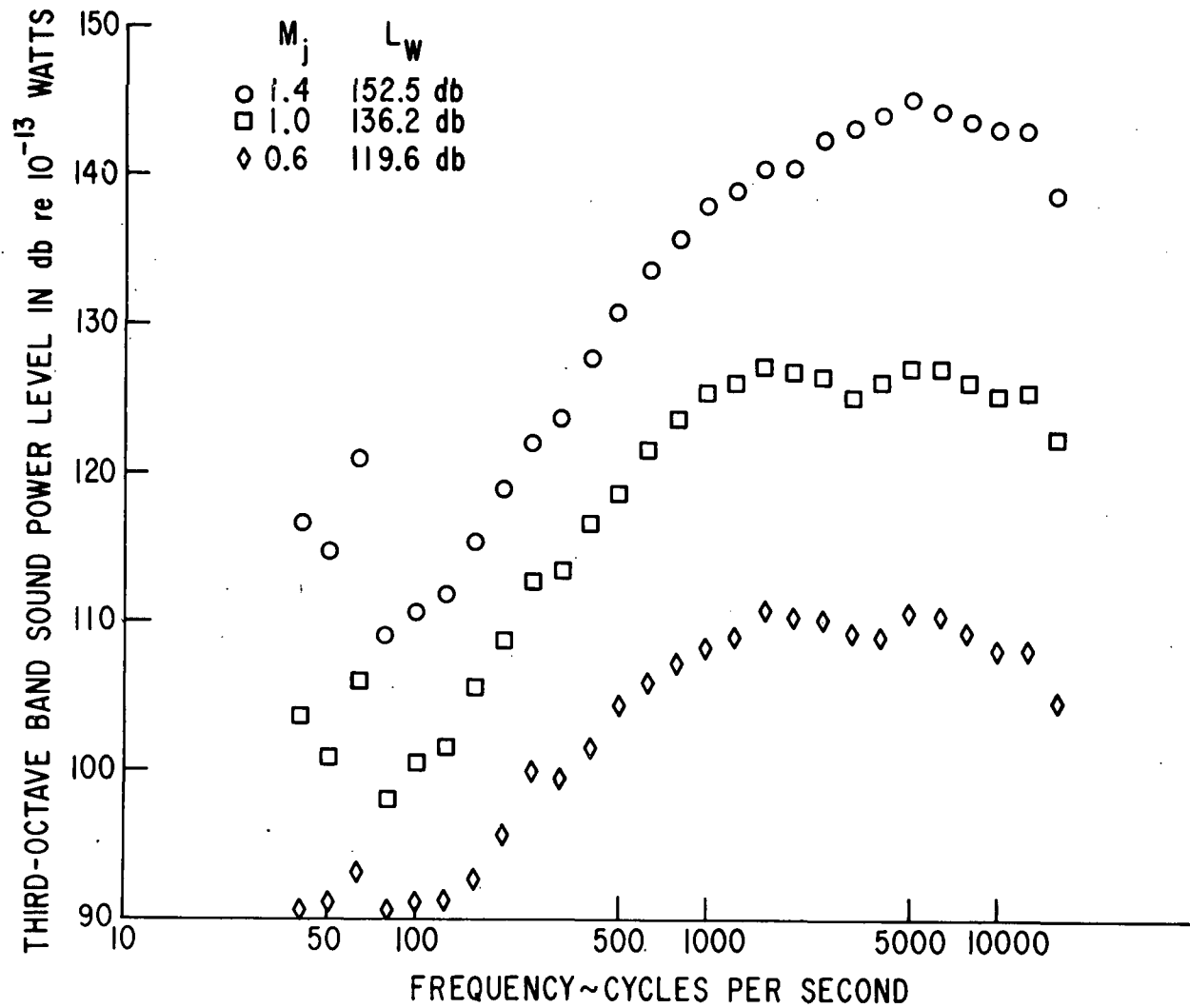
FIG. 8 COMPARISON OF SOUND POWER SPECTRA FOR 2 INCH DIAMETER CONVERGENT NOZZLE AT DIFFERENT MACH NUMBERS
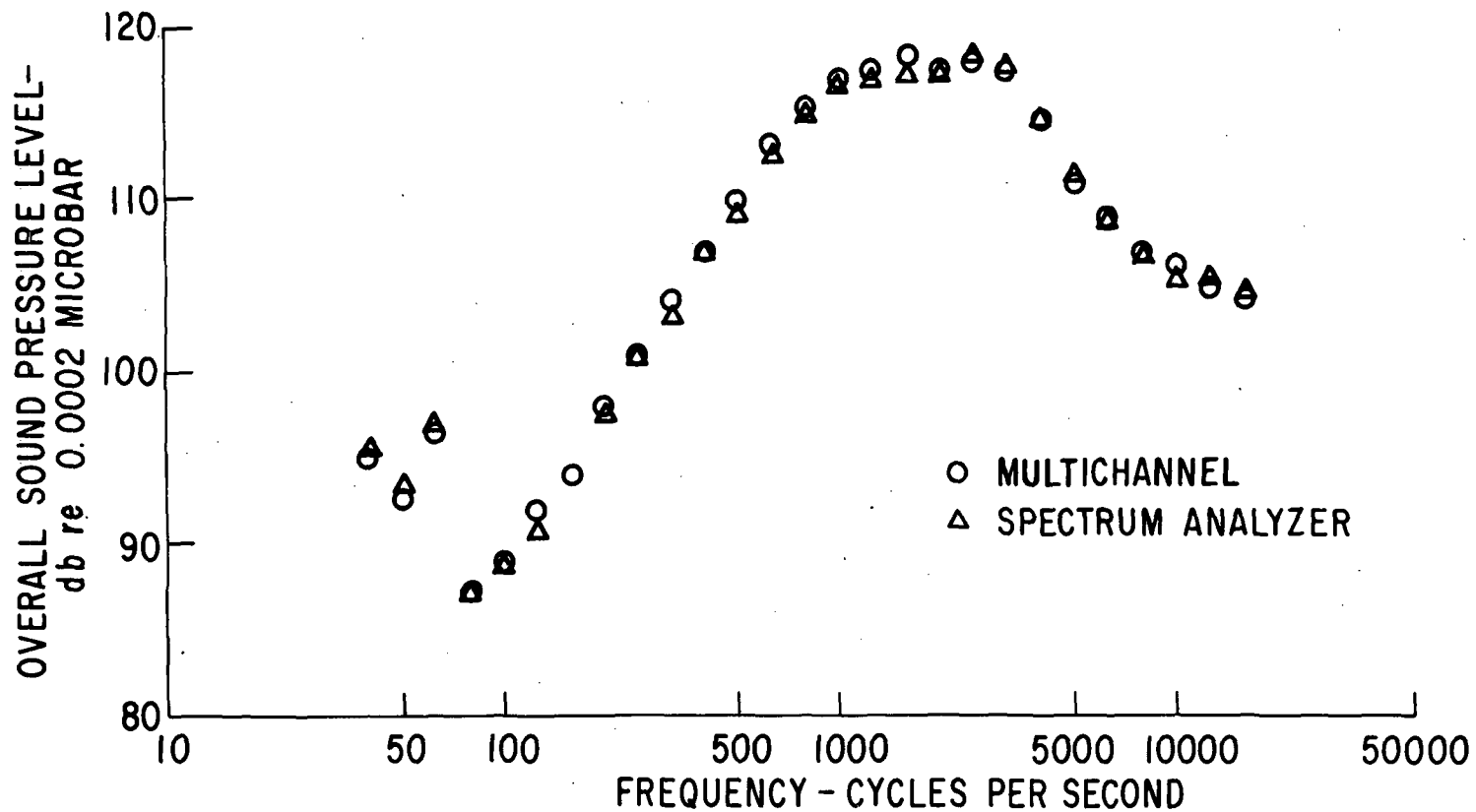
FIG. 9   COMPARISON OF SOUND PRESSURE LEVEL vs FREQUENCY OF TWO ANALYZER SYSTEMS AT 19.1° FROM JET AXIS FOR 2 INCH DIAMETER CONVERGENT NOZZLE, Mj=1.4
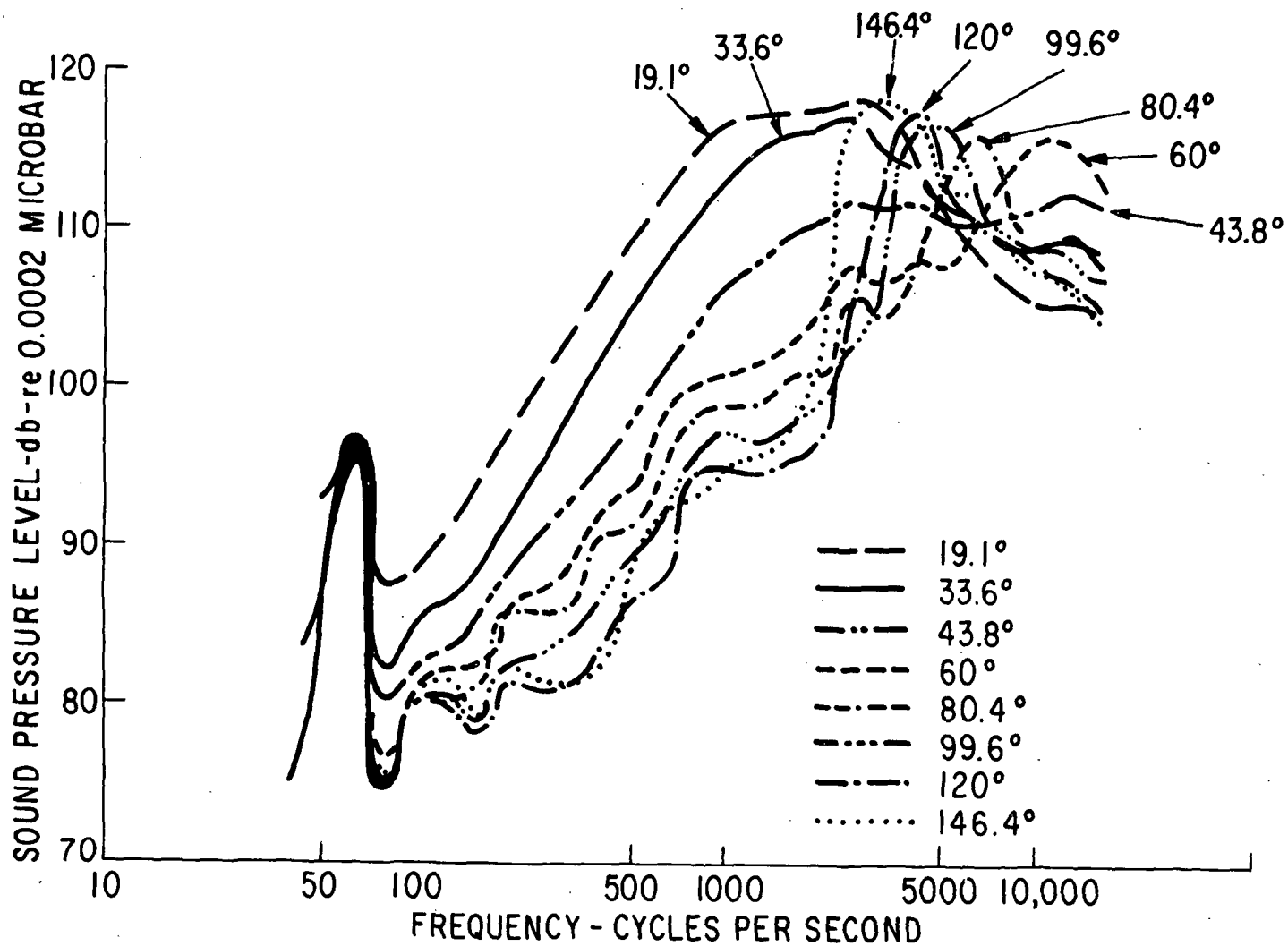
FIG. 10 SOUND PRESSURE LEVEL VS FREQUENCY AT 8 ANGULAR POSITIONS FROM JET AXIS FOR 2 INCH DIAMETER CONVERGENT NOZZLE, M_j=1.4
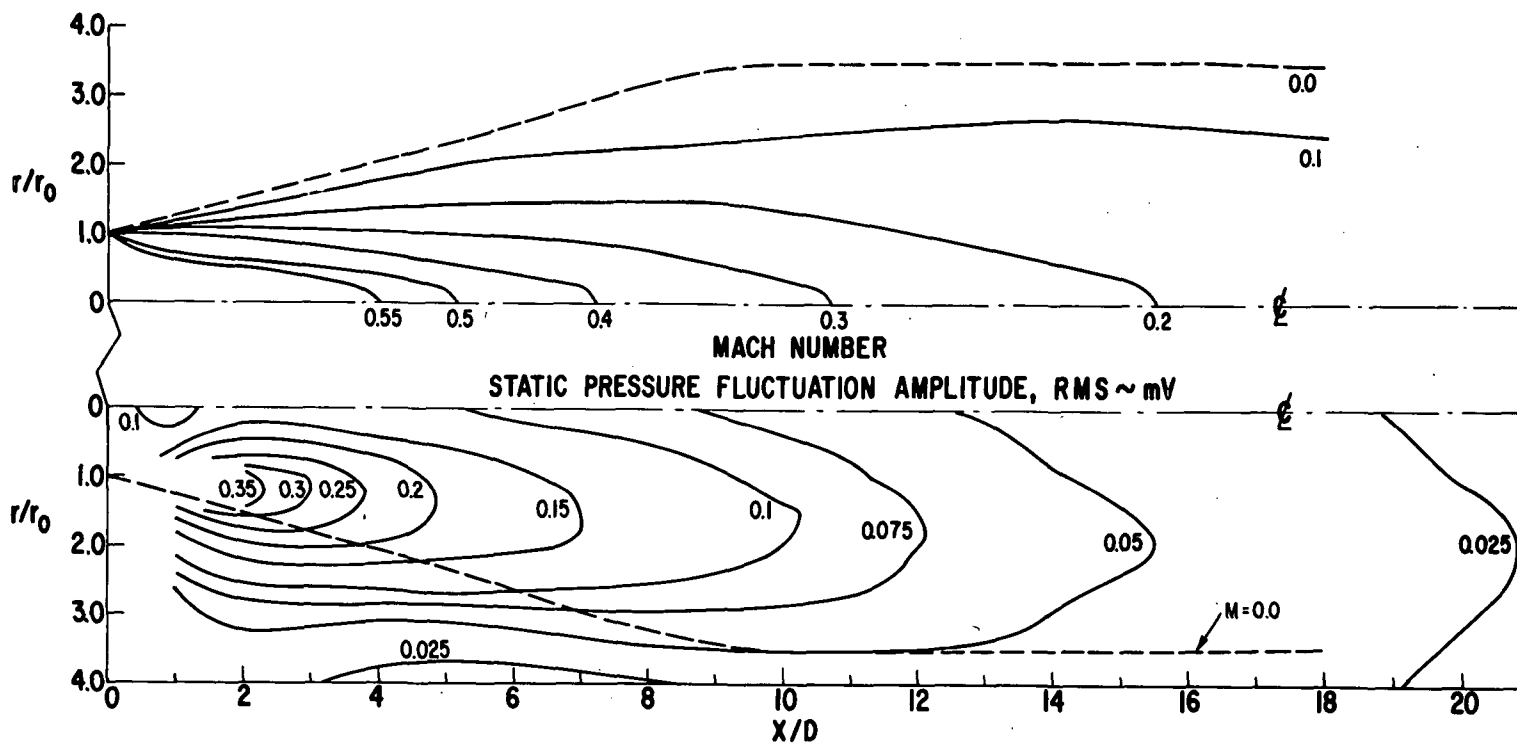
FIG. IIa CONSTANT MACH NUMBER AND PIEZOELECTRIC STATIC PRESSURE FLUCTUATION CONTOURS IN THE FLOW FIELD FROM A ONE INCH CONVERGENT NOZZLE, Mj = 0.6
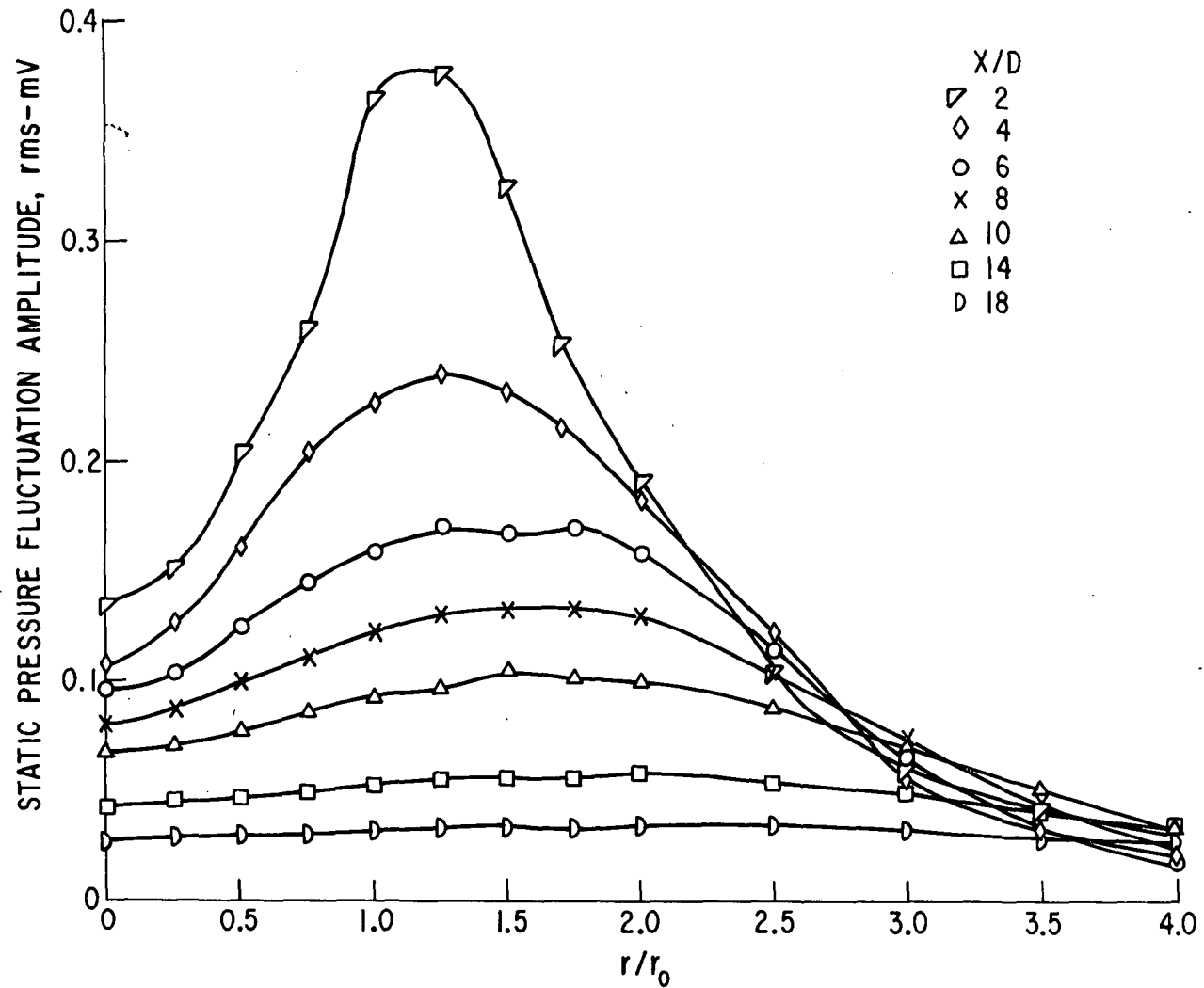
FIG.IIb PIEZOELECTRIC STATIC PRESSURE FLUCTUATION PROFILES ACROSS THE EXIT OF A ONE INCH DIAMETER CONVERGENT NOZZLE AT DIFFERENT DISTANCES FROM THE NOZZLE EXIT, $M_j = 0.6$
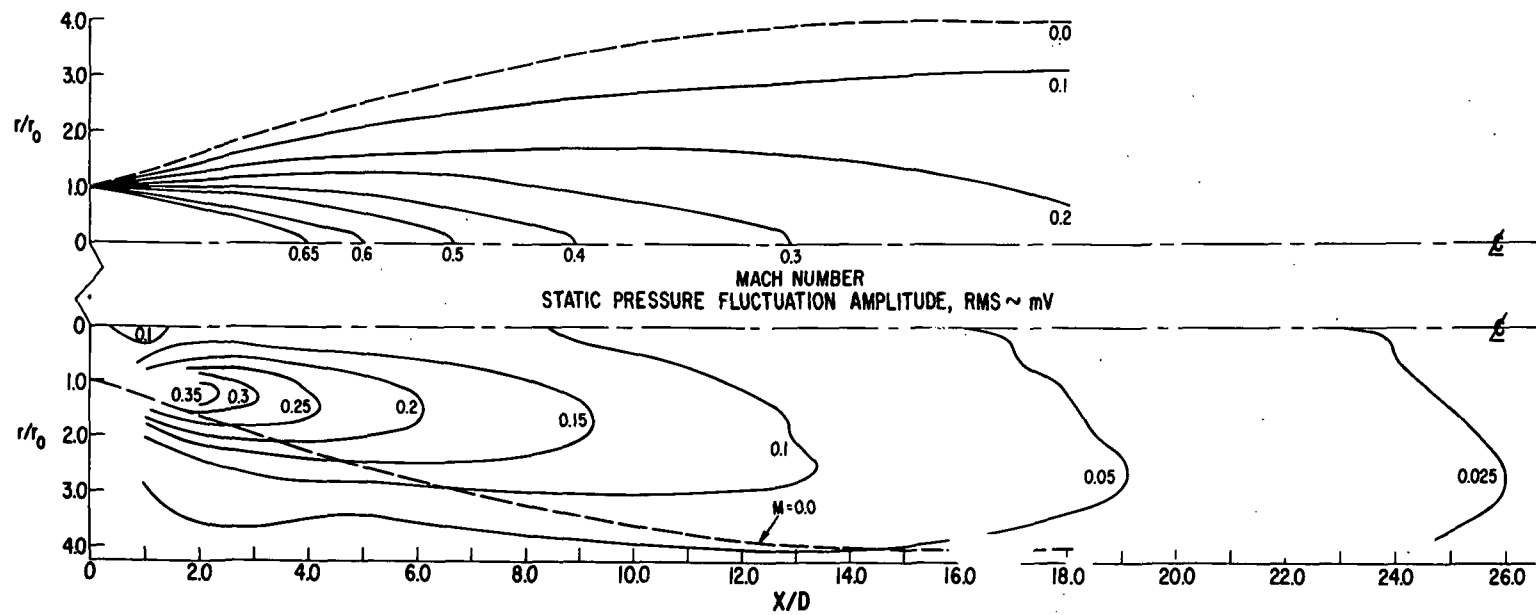
FIG. I2a CONSTANT MACH NUMBER AND PIEZOELECTRIC STATIC PRESSURE FLUCTUATION CONTOURS IN THE FLOW FIELD FROM A ONE INCH CONVERGENT NOZZLE, Mj=0.7
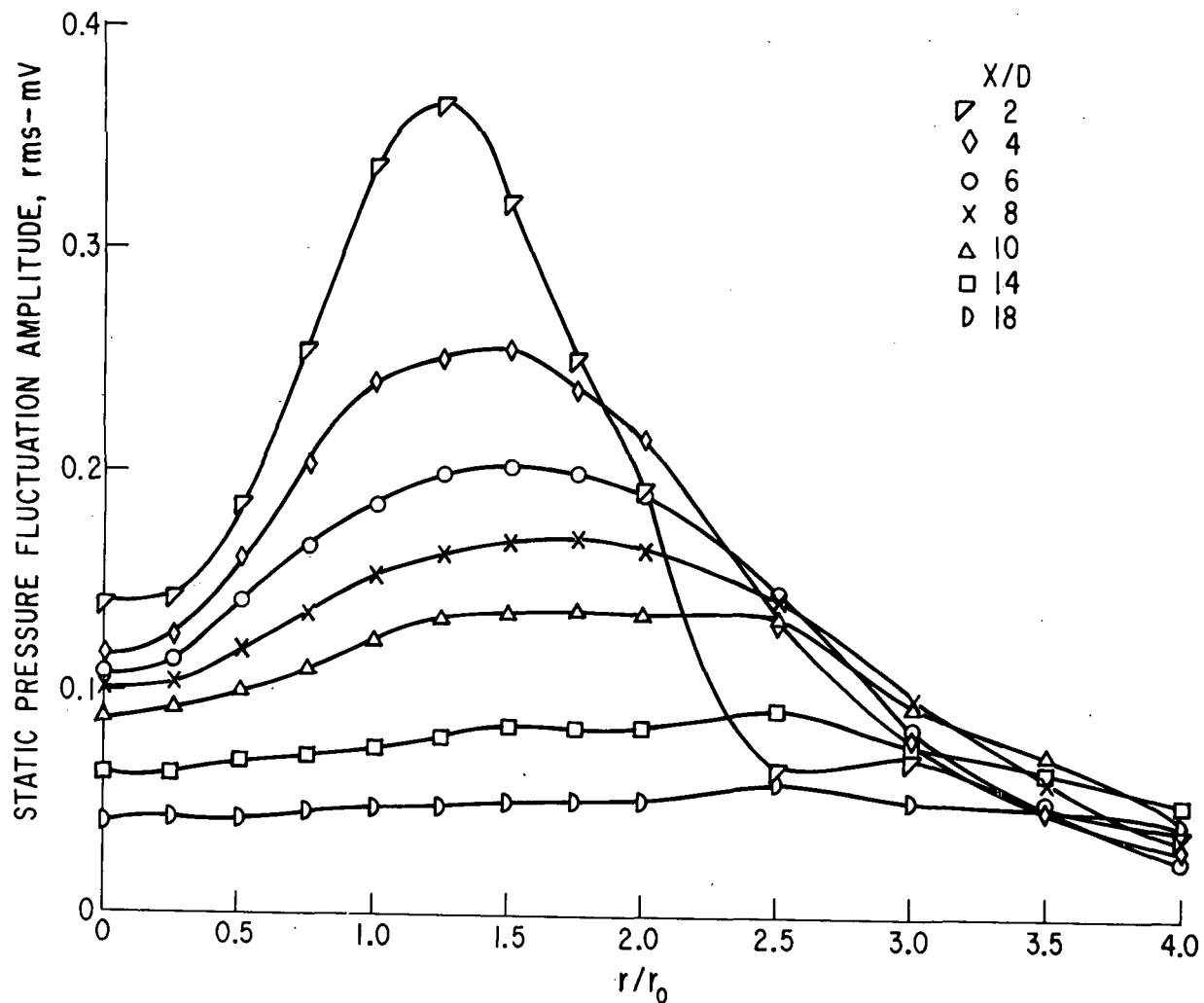
FIG. 12b-PIEZOELECTRIC STATIC PRESSURE FLUCTUATION PROFILES ACROSS THE EXIT OF A ONE INCH DIAMETER CONVERGENT NOZZLE AT DIFFERENT DISTANCES FROM THE NOZZLE EXIT, $M_j = 0.7$
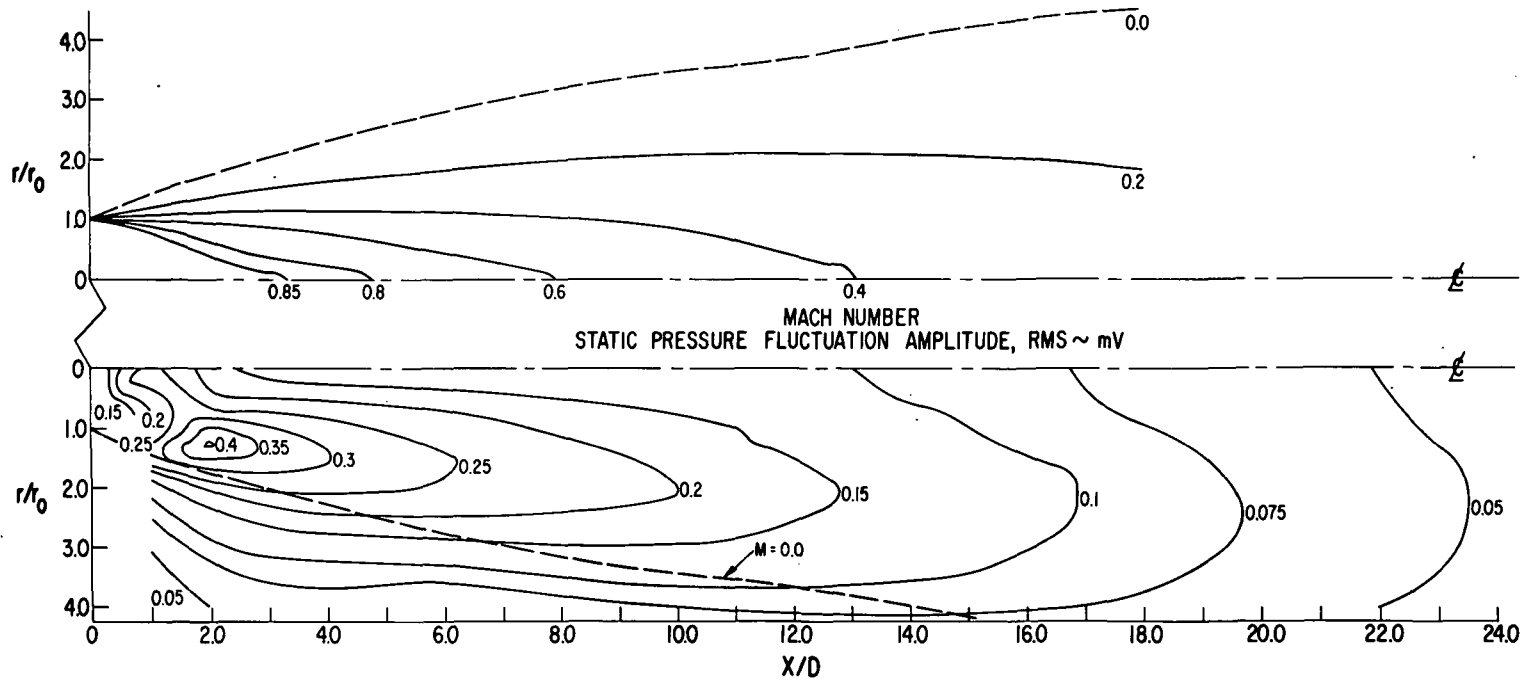
FIG. 13a CONSTANT MACH NUMBER AND PIEZOELECTRIC STATIC PRESSURE FLUCTUATION CONTOURS IN THE FLOW FIELD FROM A
ONE INCH CONVERGENT NOZZLE, Mj ~ 0.85
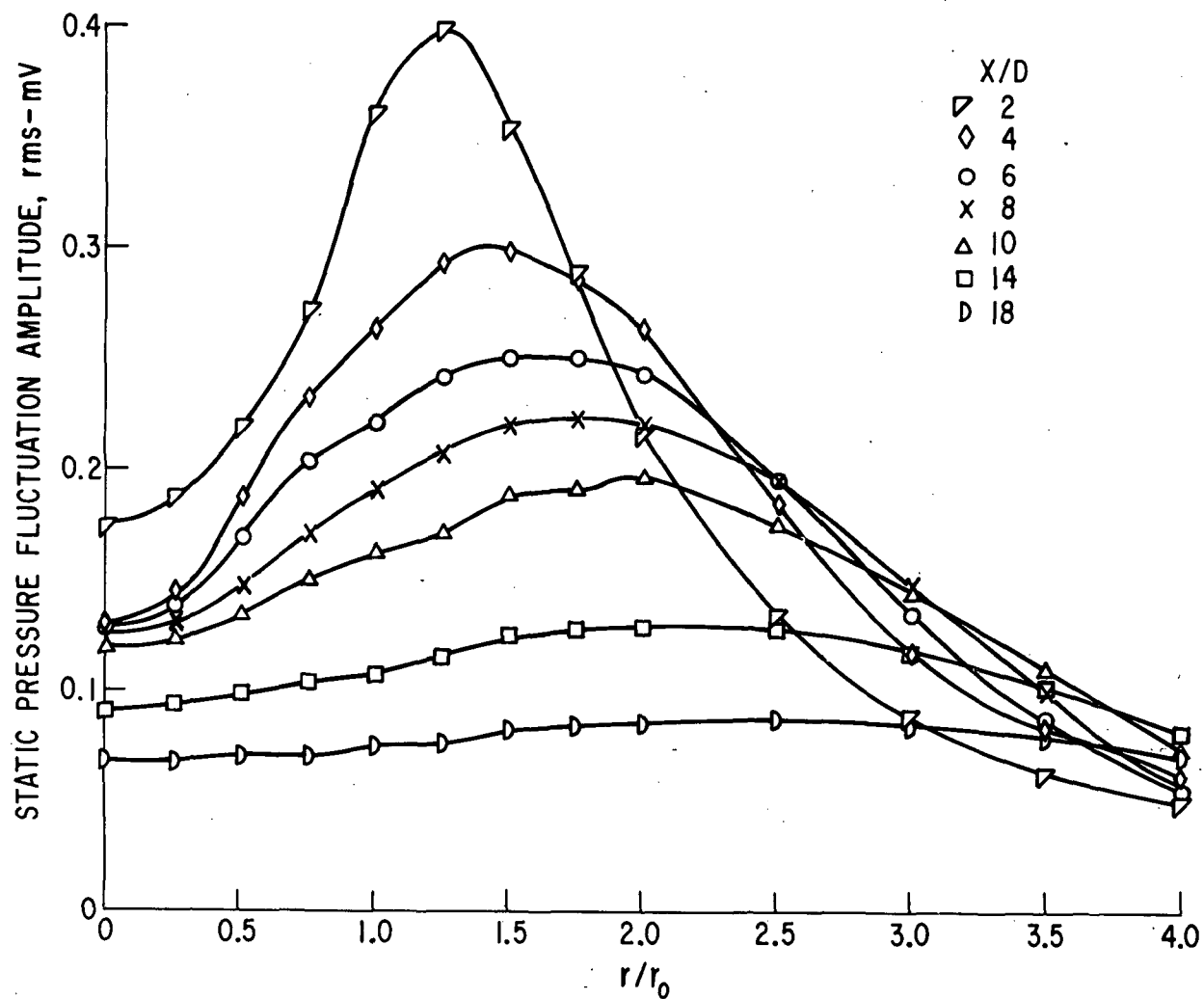
FIG.13b PIEZOELECTRIC STATIC PRESSURE FLUCTUATION PROFILES ACROSS THE EXIT OF A ONE INCH DIAMETER CONVERGENT NOZZLE AT DIFFERENT DISTANCES FROM THE NOZZLE EXIT, $M_j = 0.85$
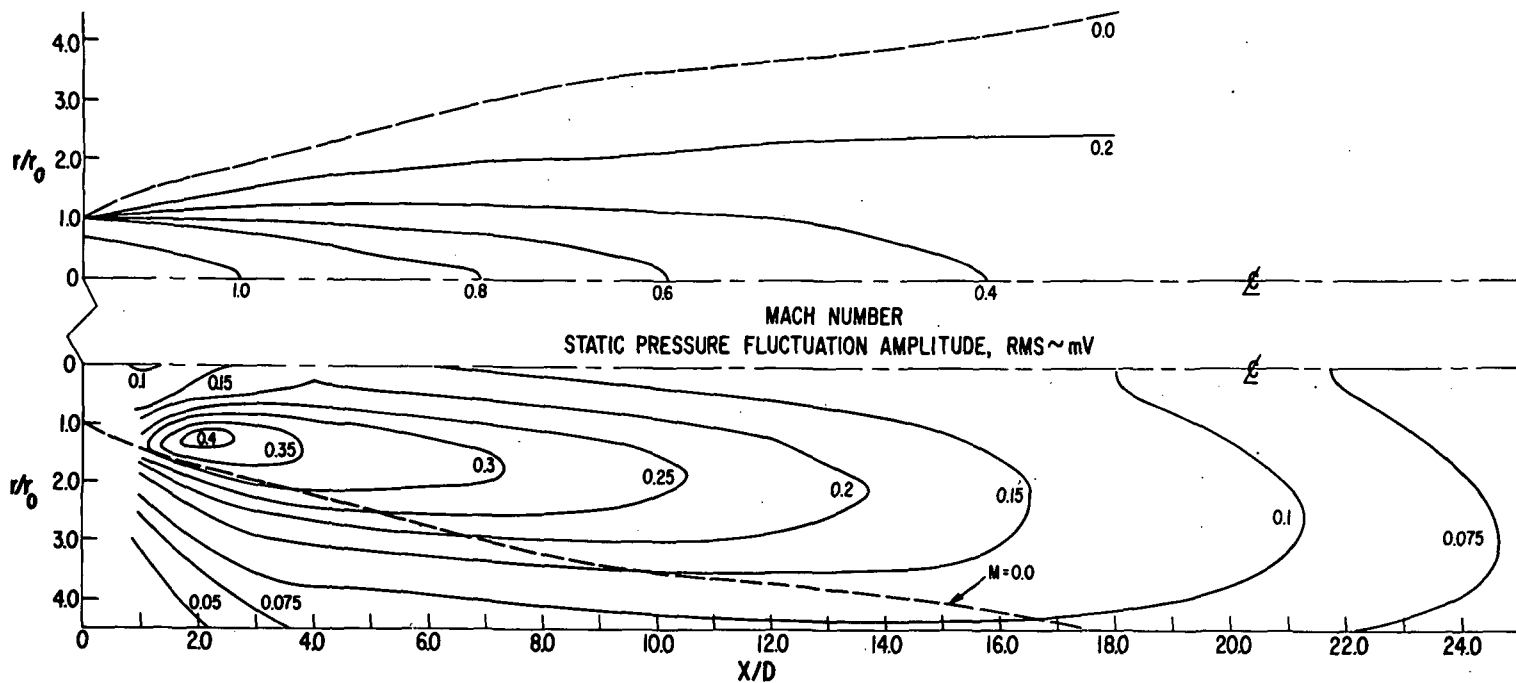
FIG. 14a CONSTANT MACH NUMBER AND PIEZOELECTRIC STATIC PRESSURE FLUCTUATION CONTOURS IN THE FLOW FIELD FROM A ONE INCH CONVERGENT NOZZLE, Mj = 1.0
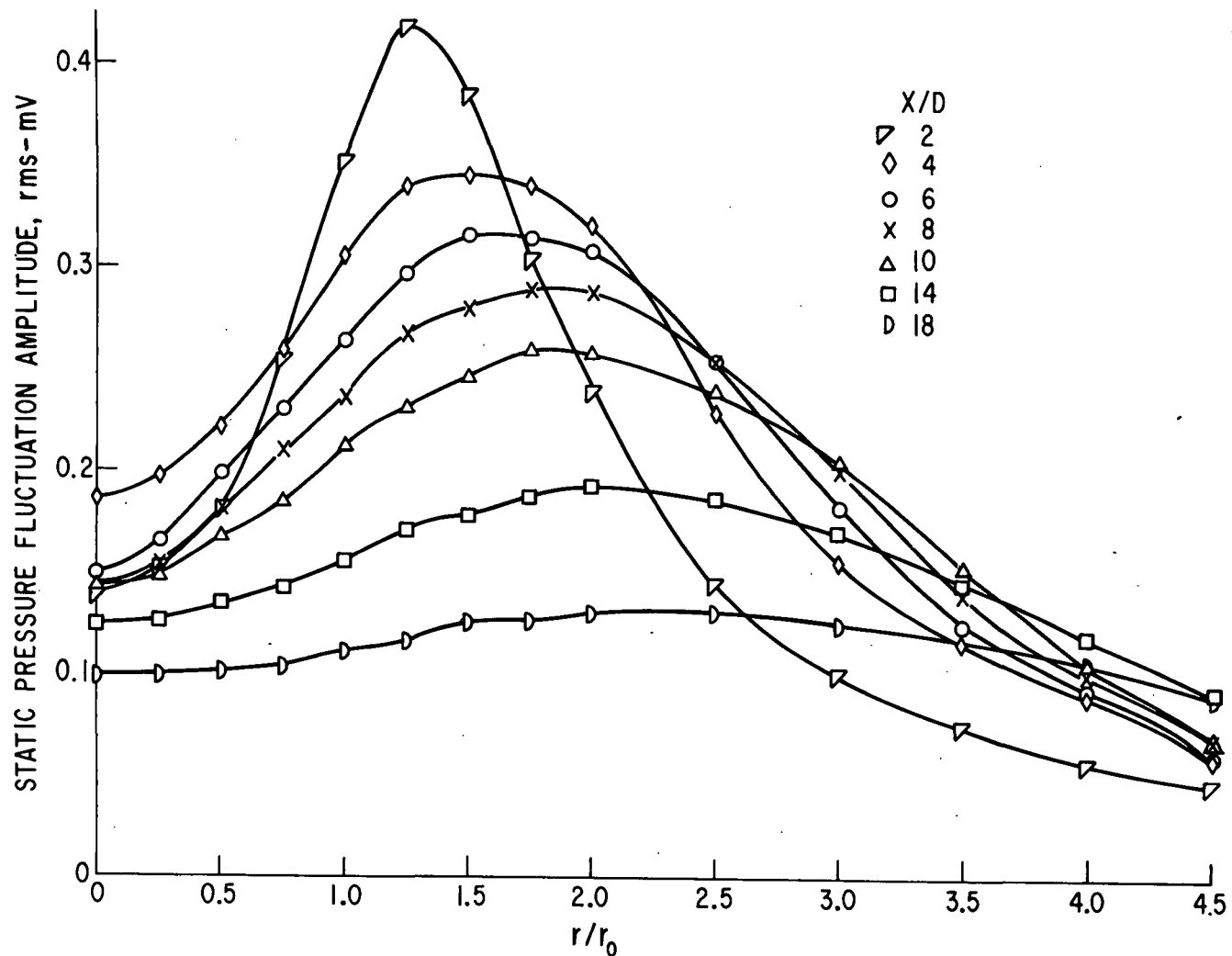
FIG. 14b-PIEZOELECTRIC STATIC PRESSURE FLUCTUATION PROFILES ACROSS THE EXIT OF A ONE INCH DIAMETER CONVERGENT NOZZLE AT DIFFERENT DISTANCES FROM THE NOZZLE EXIT, $M_j = 1.0$
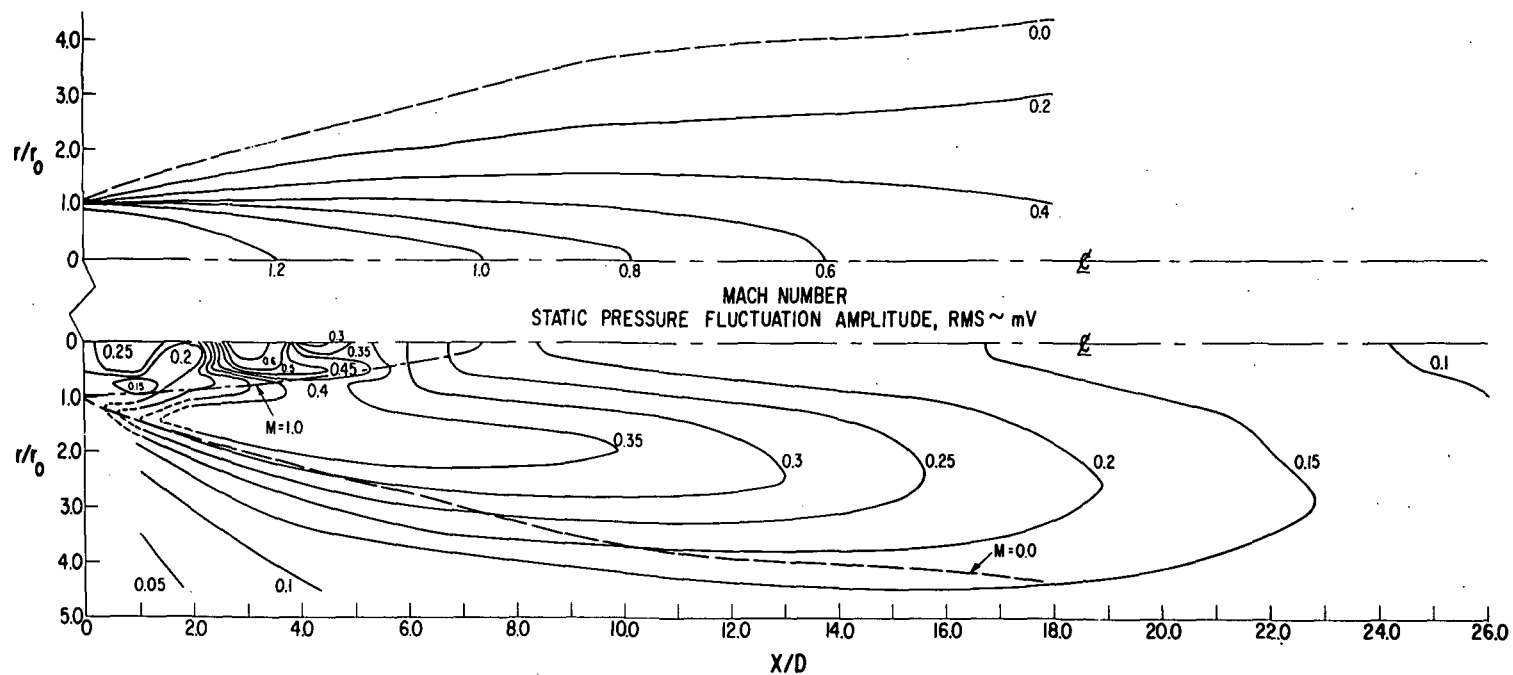
FIG. 15a CONSTANT MACH NUMBER AND PIEZOELECTRIC STATIC PRESSURE FLUCTUATION CONTOURS IN THE FLOW FIELD FROM A ONE INCH CONVERGENT NOZZLE, Mj=1.2
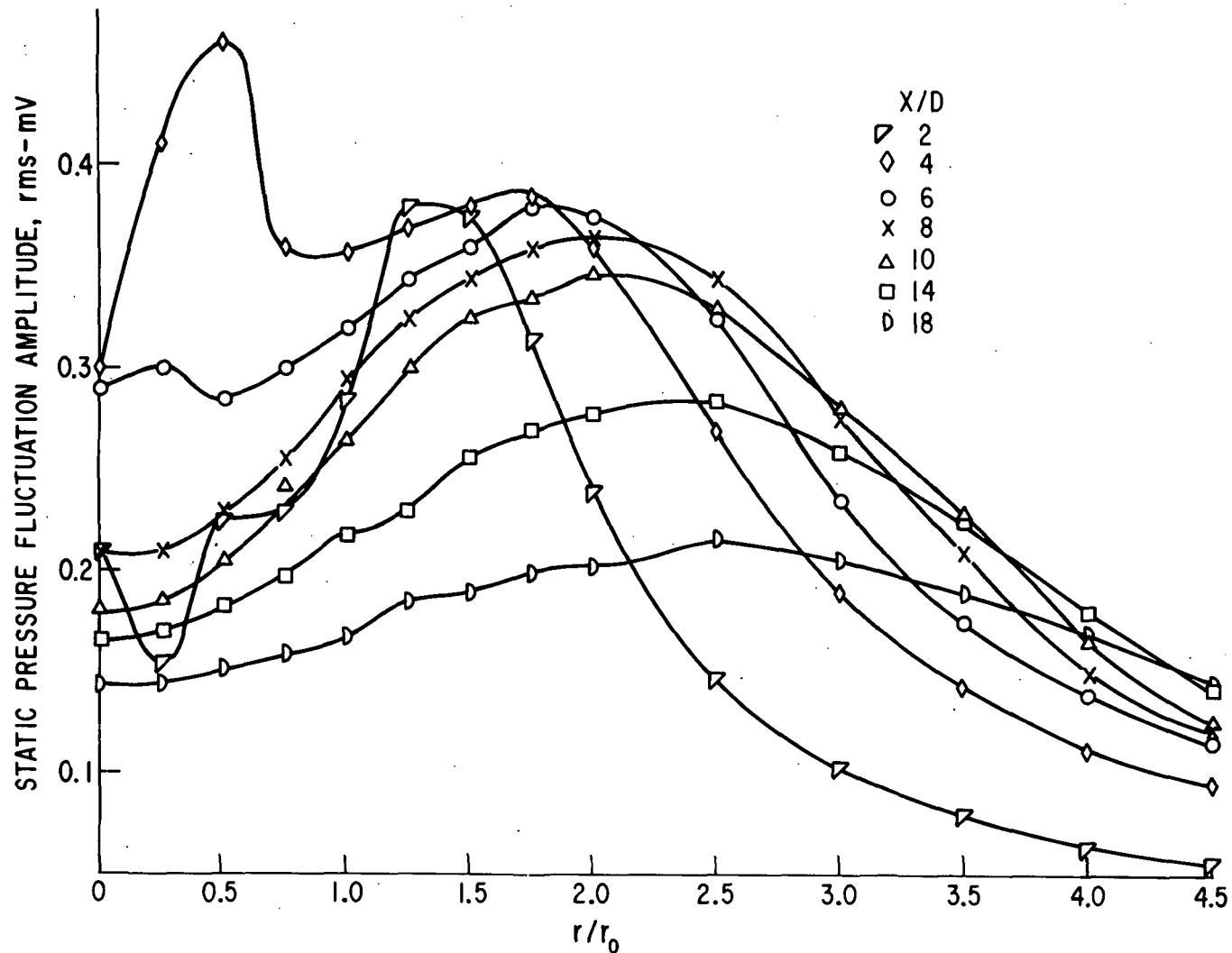
FIG. 15b—PIEZOELECTRIC STATIC PRESSURE FLUCTUATION PROFILES ACROSS THE EXIT OF A ONE INCH DIAMETER CONVERGENT NOZZLE AT DIFFERENT DISTANCES FROM THE NOZZLE EXIT, $M_j = 1.2$
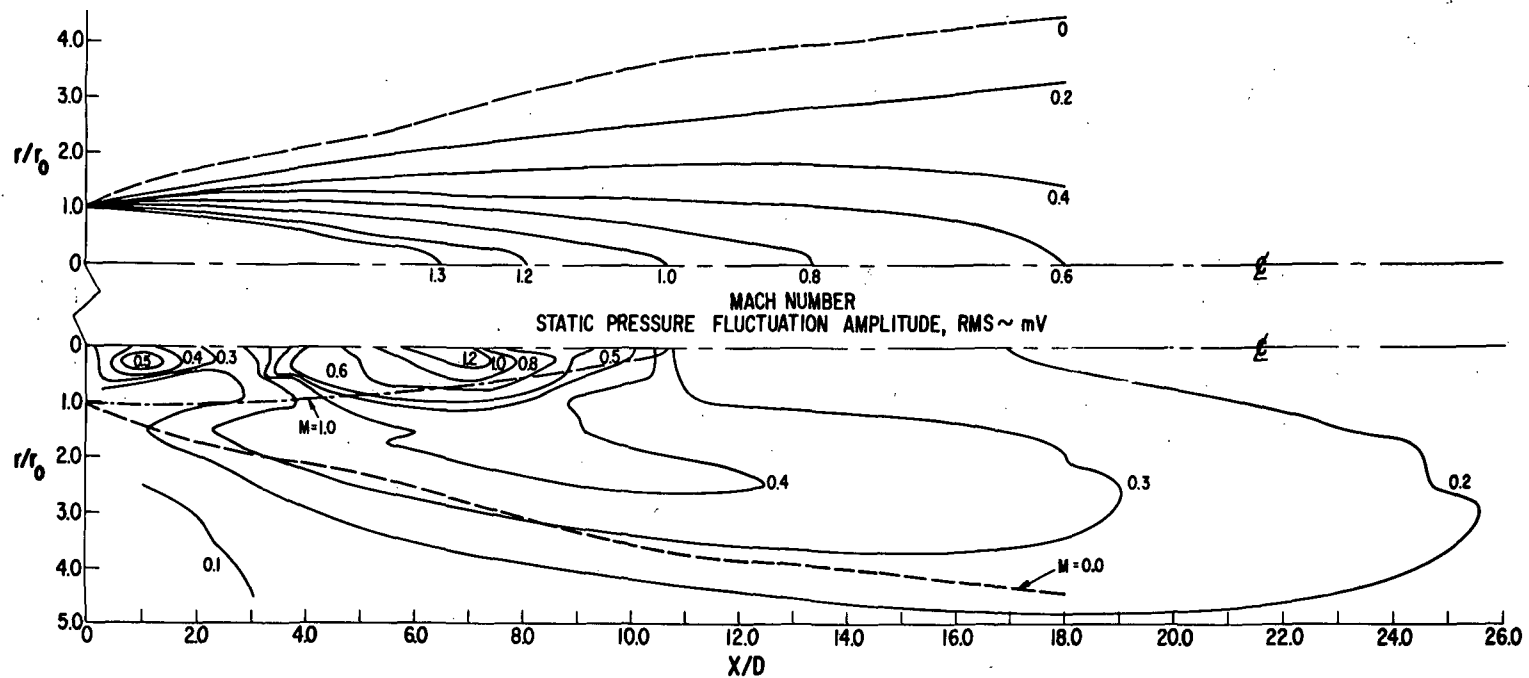
FIG. 16a CONSTANT MACH NUMBER AND PIEZOELECTRIC STATIC PRESSURE FLUCTUATION CONTOURS IN THE FLOW FIELD FROM A ONE INCH CONVERGENT NOZZLE, Mj =1.4
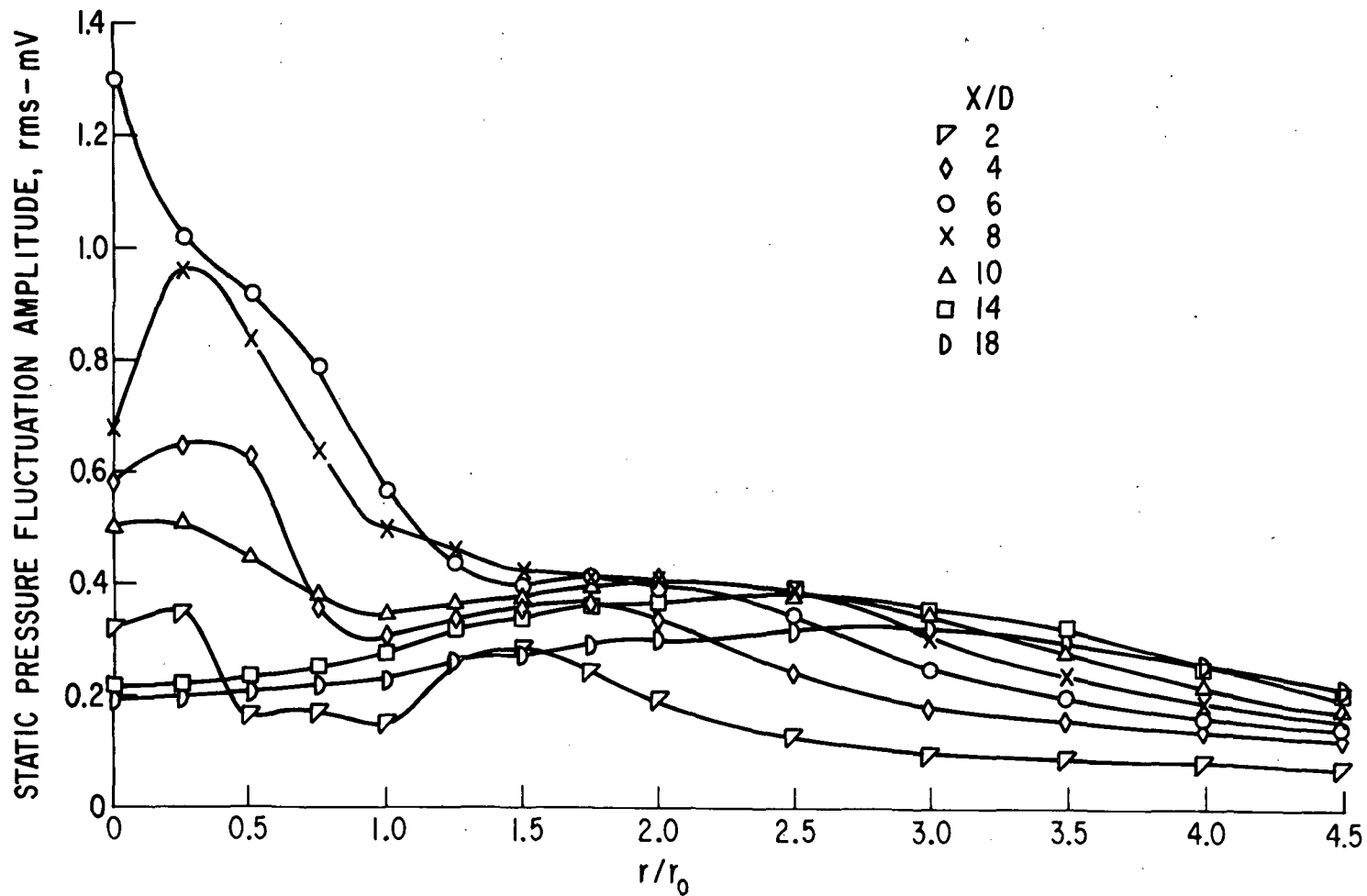
FIG.16b PIEZOELECTRIC STATIC PRESSURE FLUCTUATION PROFILES ACROSS THE EXIT OF A ONE INCH DIAMETER CONVERGENT NOZZLE AT DIFFERENT DISTANCES FROM THE NOZZLE EXIT, $M_j = 1.4$
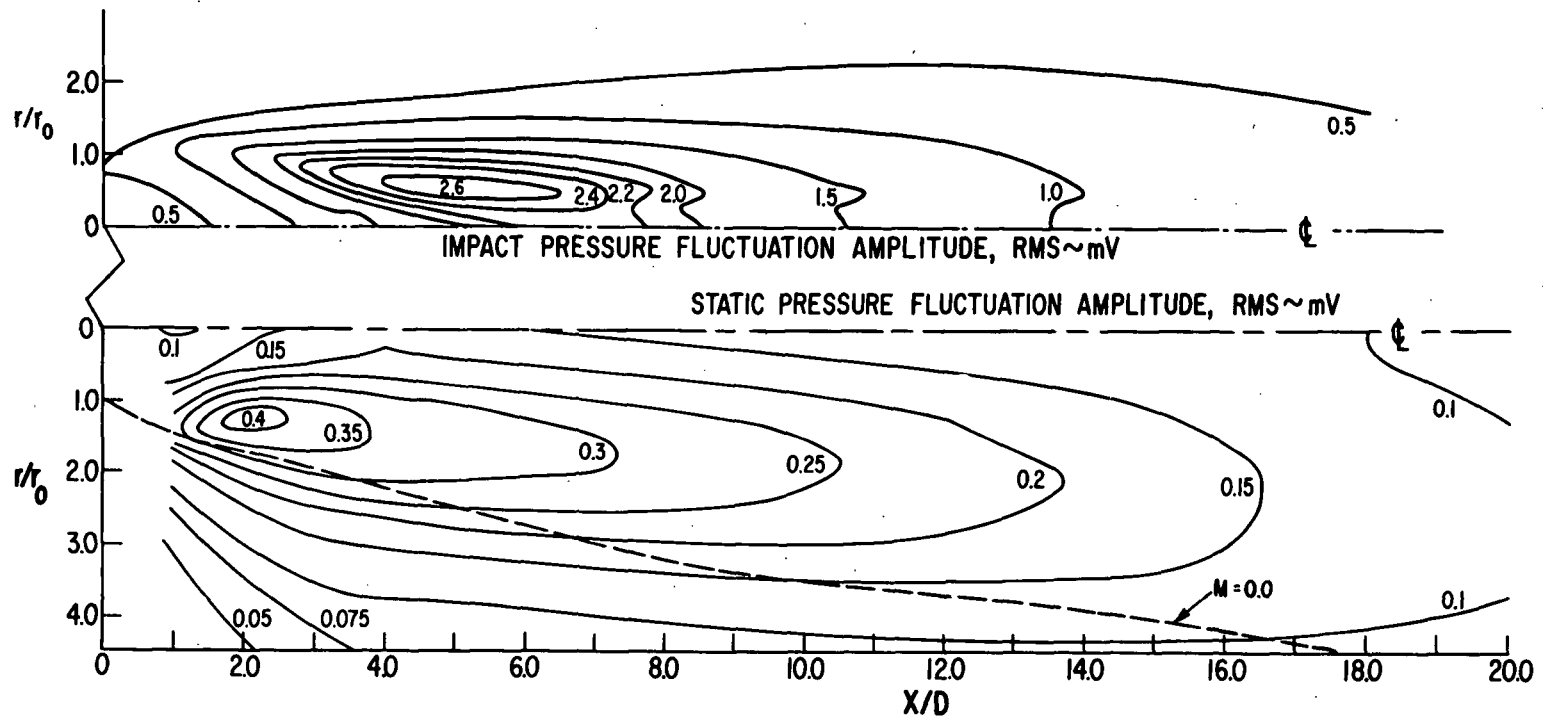
FIG. 17a CONSTANT PIEZOELECTRIC IMPACT AND STATIC PRESSURE FLUCTUATION CONTOURS IN THE FLOW FIELD FROM A ONE INCH CONVERGENT NOZZLE, $M_j = 1.0$
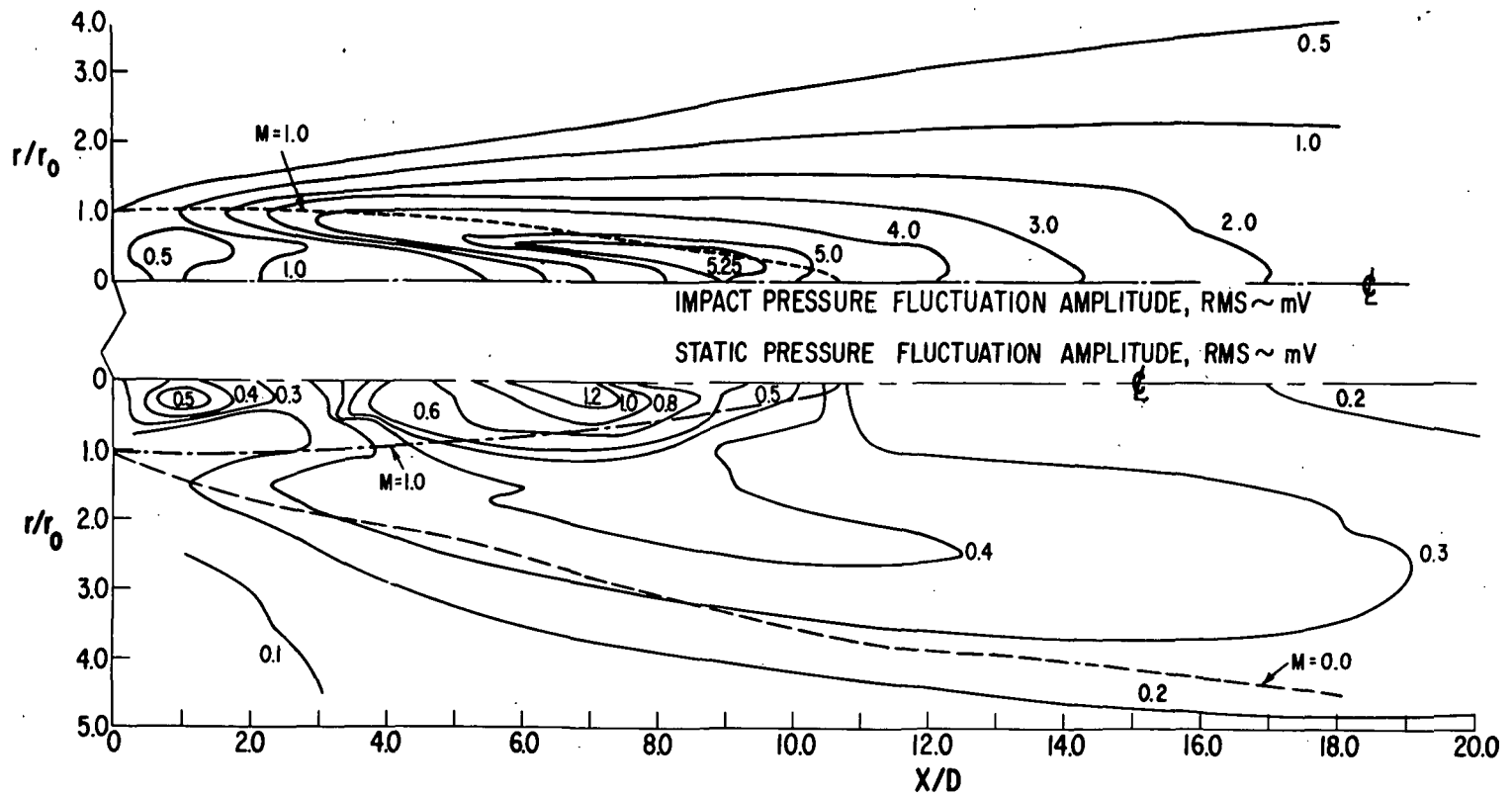
FIG.17b CONSTANT PIEZOELECTRIC IMPACT AND STATIC PRESSURE FLUCTUATION CONTOURS IN THE FLOW FIELD FROM A ONE INCH CONVERGENT NOZZLE, $M_j = 1.4$
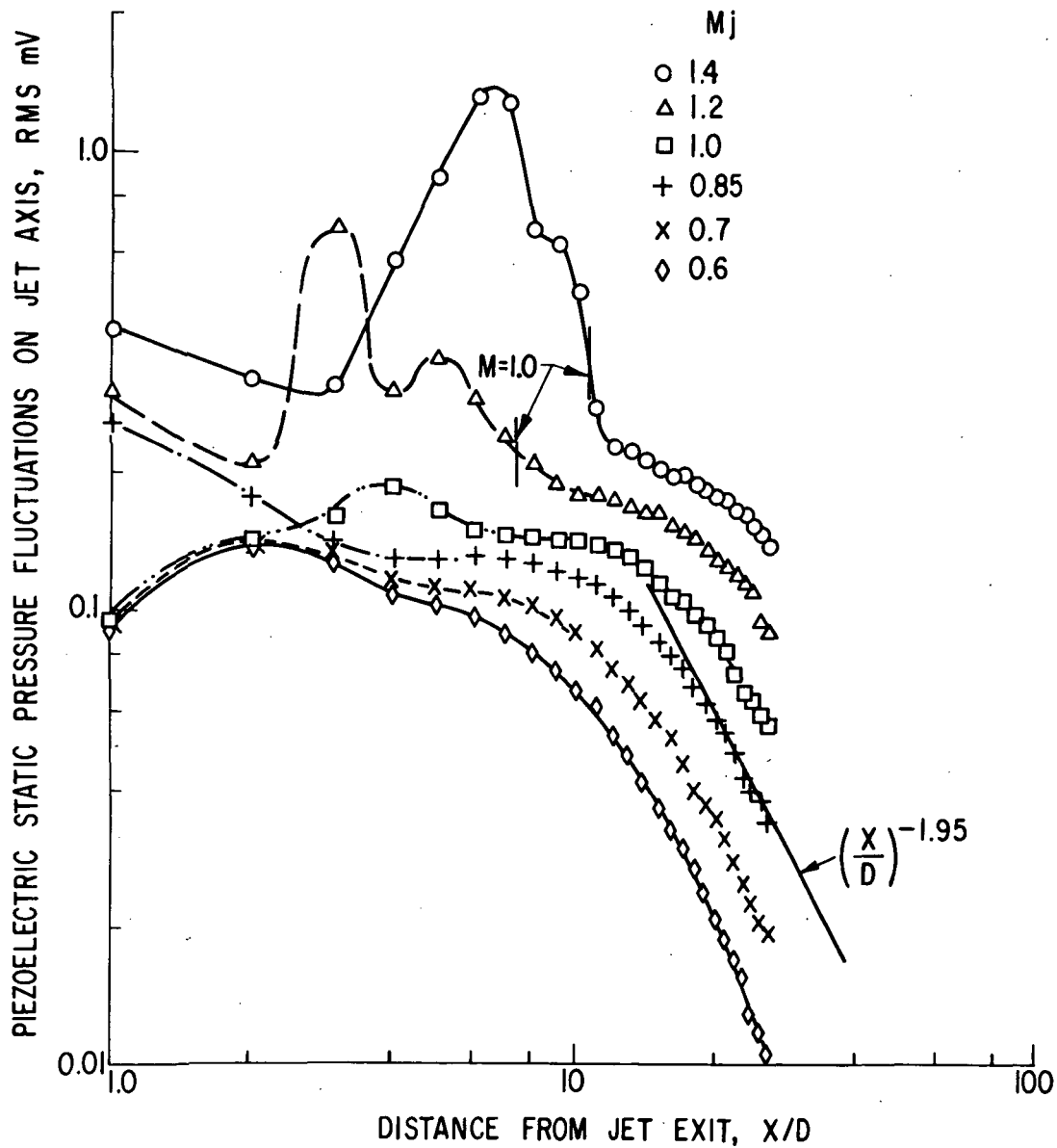
FIG. 18 VARIATION OF PIEZOELECTRIC STATIC PRESSURE FLUCTUATIONS ON JET AXIS WITH DISTANCE FROM JET EXIT FOR ONE INCH DIAMETER CONVERGENT NOZZLE
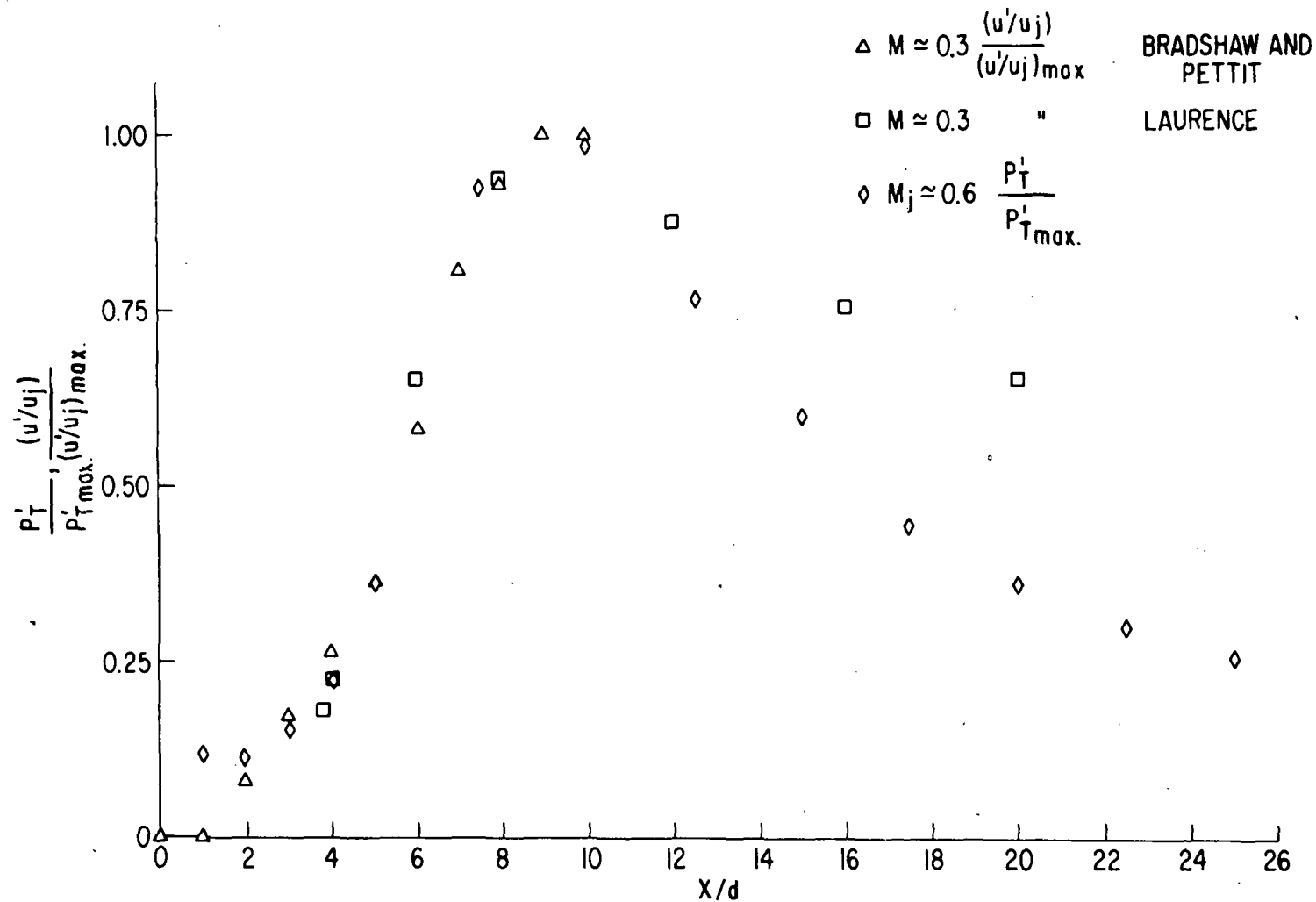
FIG. 19 VARIATION OF NORMALIZED HOT-WIRE AND PIEZOELECTRIC PRESSURE FLUCTUATIONS ALONG THE JET AXIS FOR SUBSONIC JET.

PARTIAL SECTION "A-A"

VARIABLE

A

A

191 TUBES
0.125" O.D.
0.005" WALL

FLOW

FIG. 20 SKETCH OF MULTI-TUBE MULTI-SHROUD SUPPRESSOR
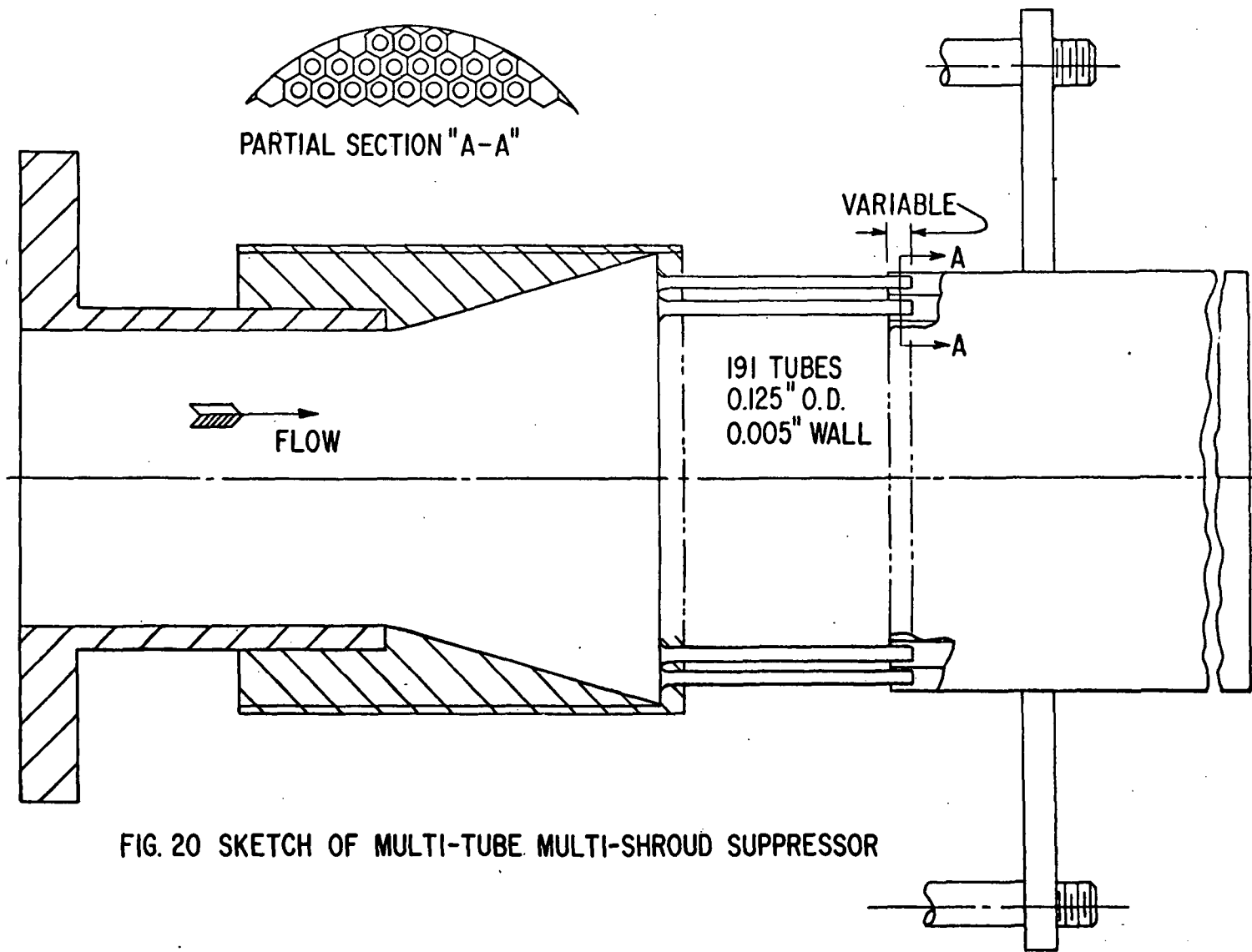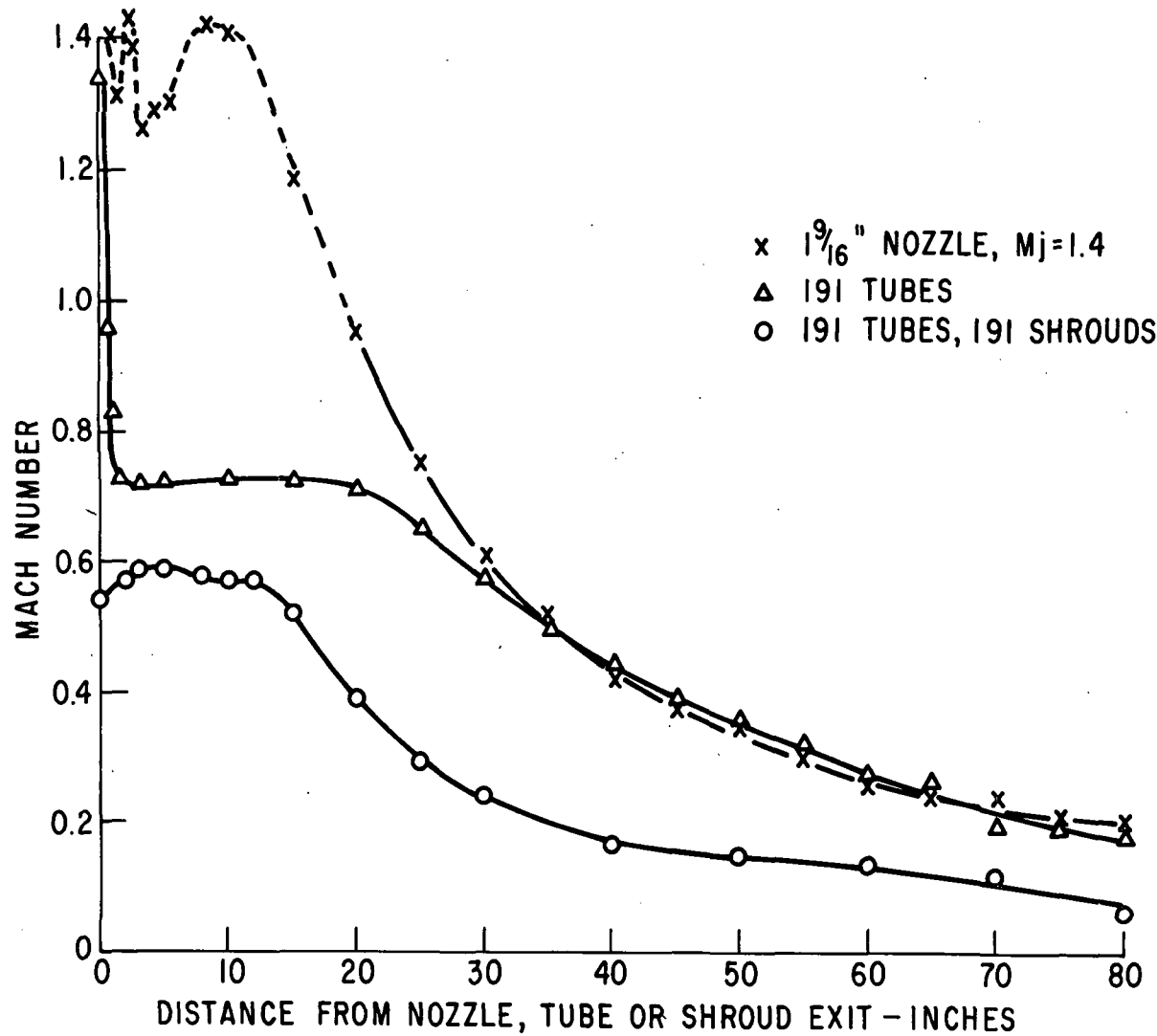
FIG.21a AXIAL MACH NUMBER DISTRIBUTION FOR MULTITUBES WITH AND WITHOUT SHROUDS, Mj=1.4
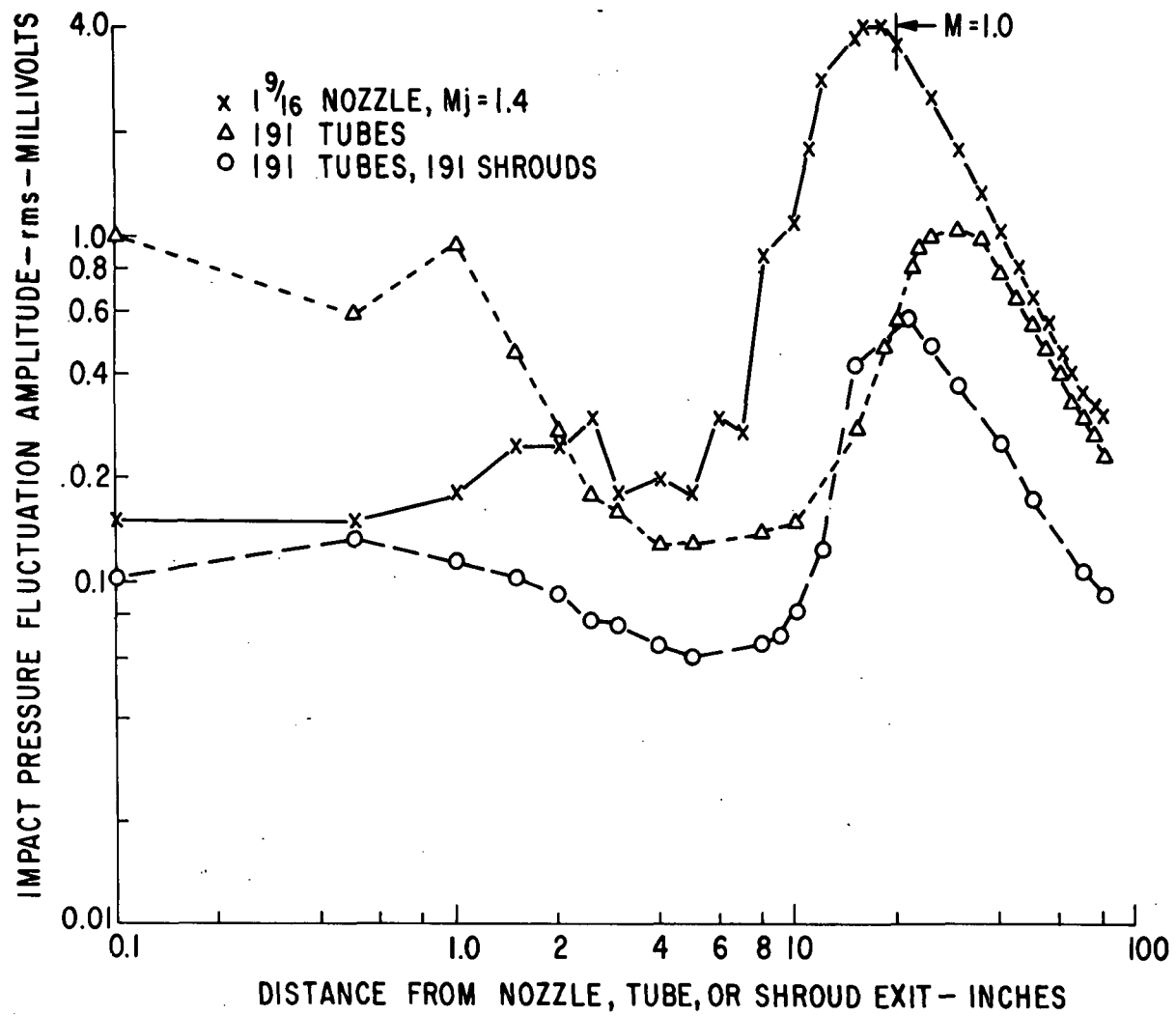
FIG. 21b-AXIAL IMPACT PRESSURE FLUCTUATIONS FOR MULTITUBES WITH AND
WITHOUT SHROUDS, Mj = 1.4
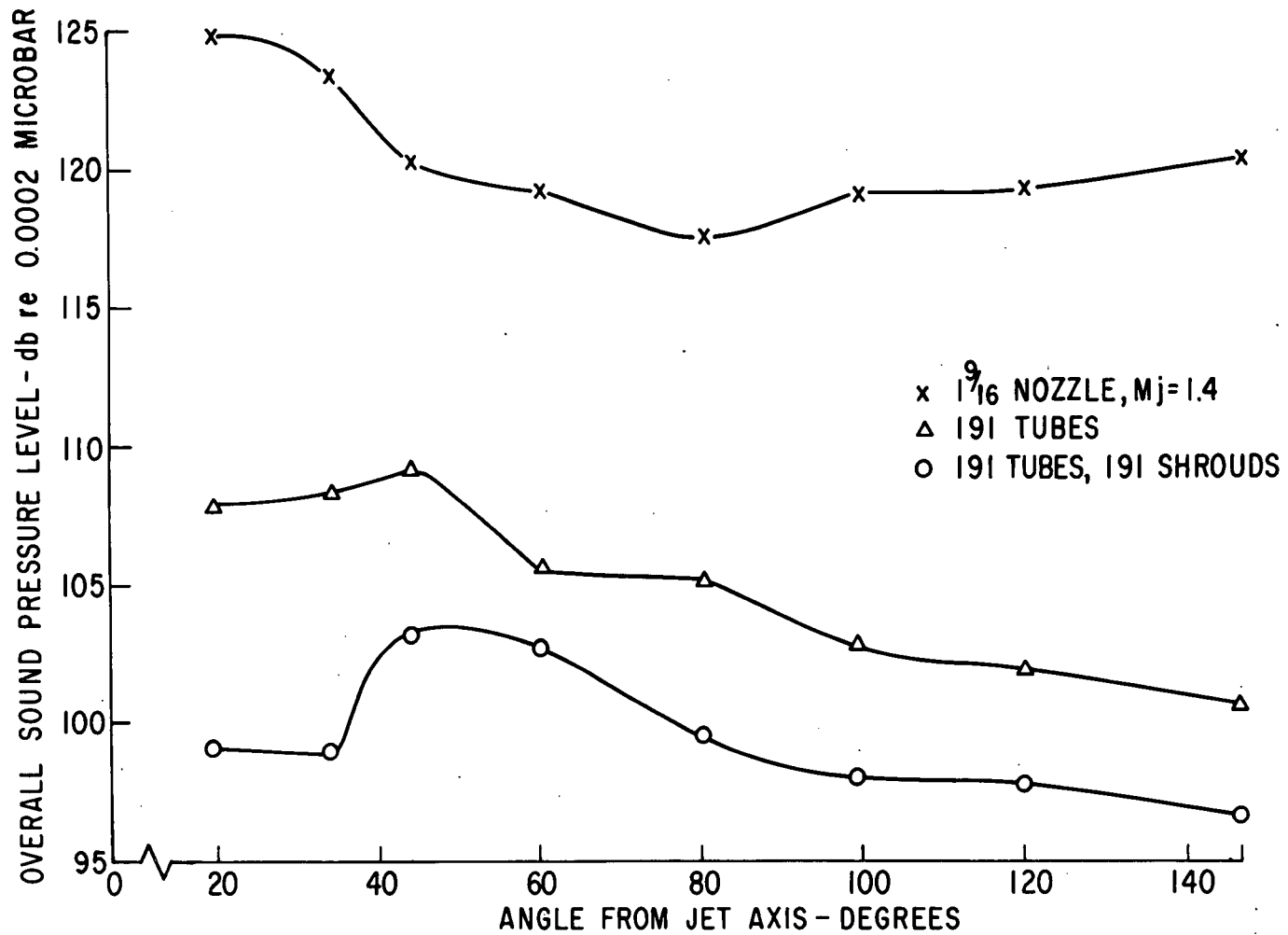
FIG. 22 OVERALL SOUND PRESSURE LEVEL AS A FUNCTION OF ANGULAR POSITION FROM JET AXIS FOR MULTITUBES WITH AND WITHOUT SHROUDS, $M_j = 1.4$
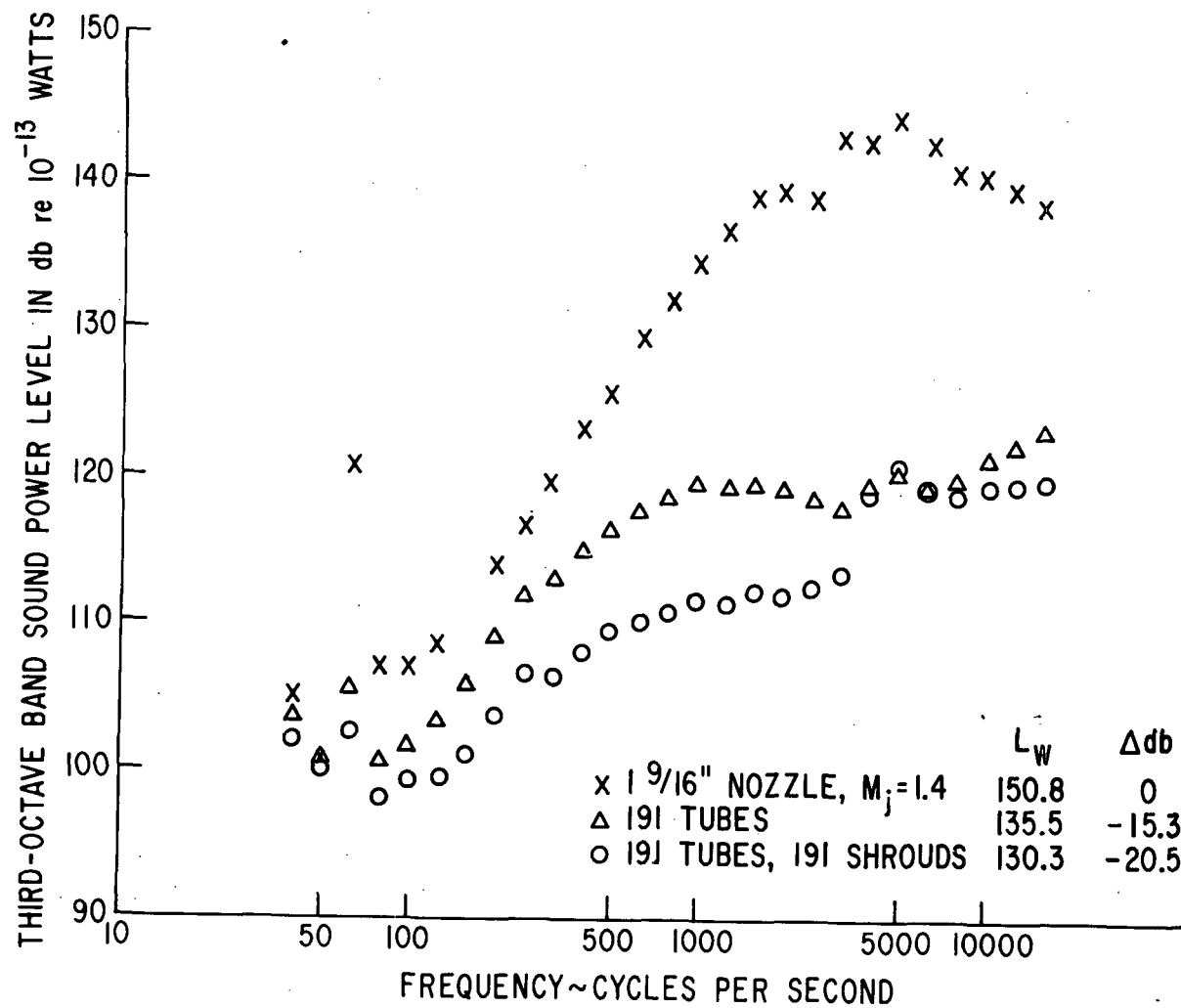
FIG. 23 SOUND POWER LEVEL SPECTRA FOR MULTITUBES WITH AND
WITHOUT SHROUDS, $M_j = 1.4$
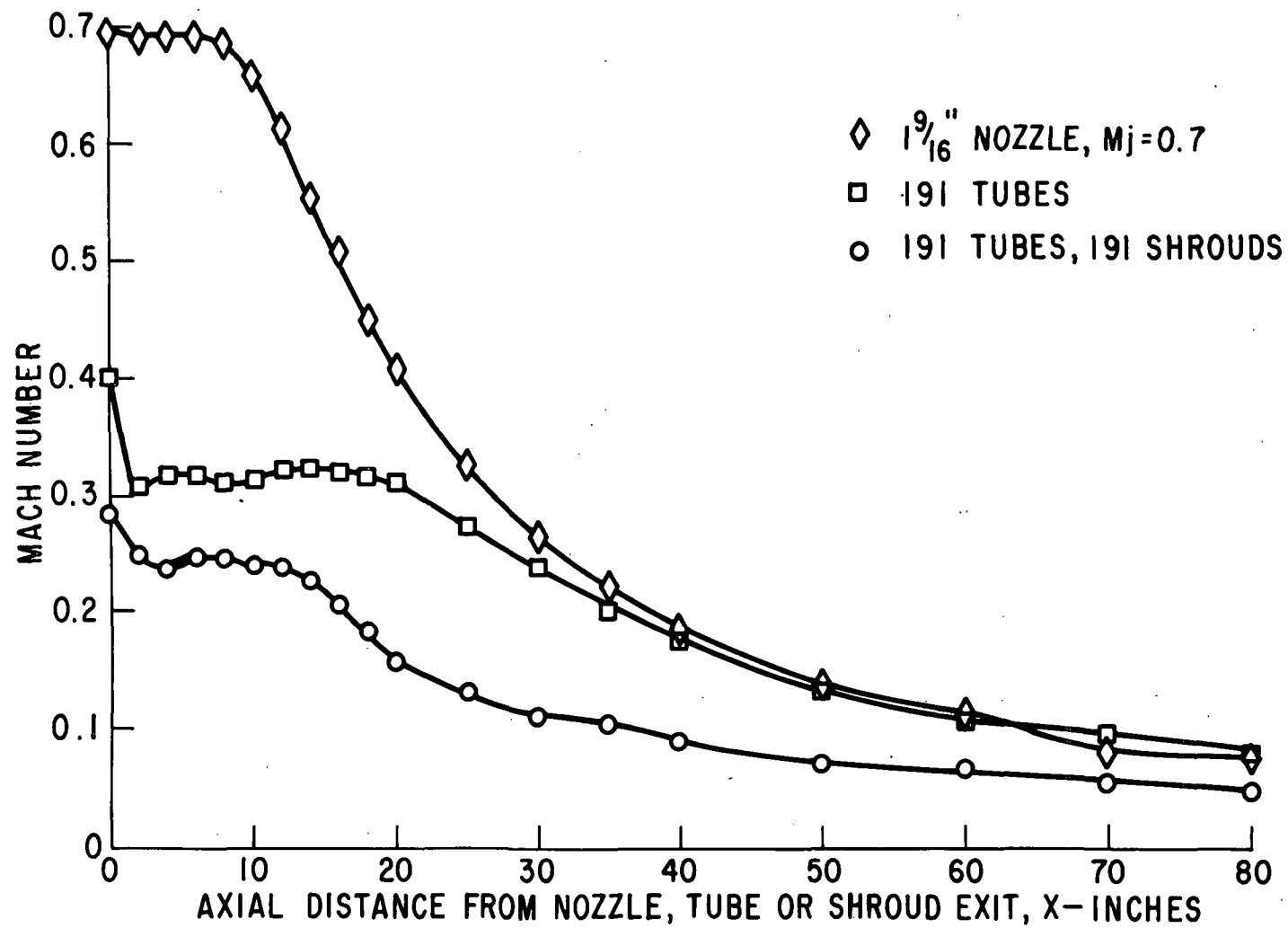
FIG. 24a AXIAL MACH NUMBER DISTRIBUTION FOR MULTITUBES WITH AND WITHOUT SHROUDS, Mj=0.7
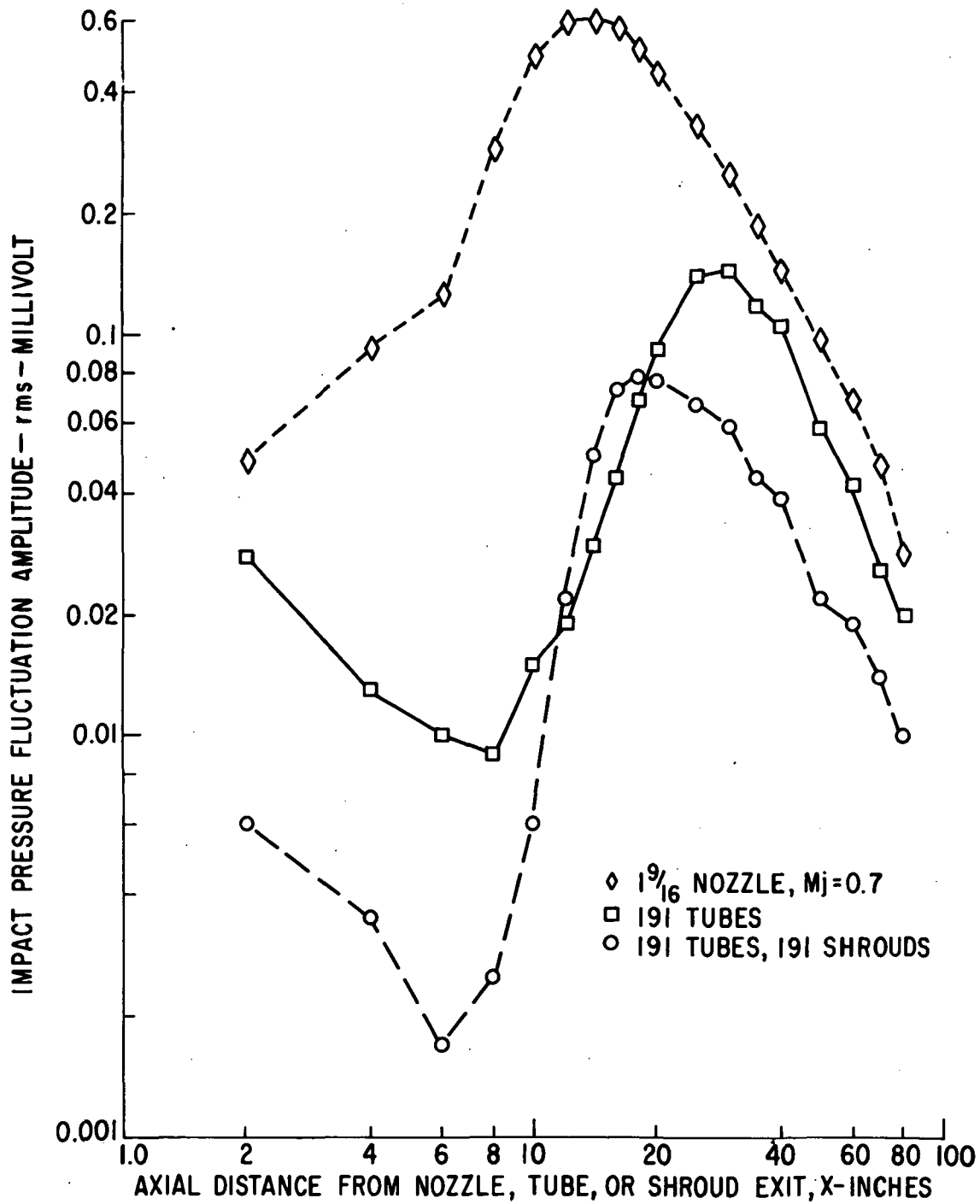
FIG. 24b AXIAL IMPACT PRESSURE FLUCTUATIONS FOR MULTITUBES
WITH AND WITHOUT SHROUDS, Mj=0.7
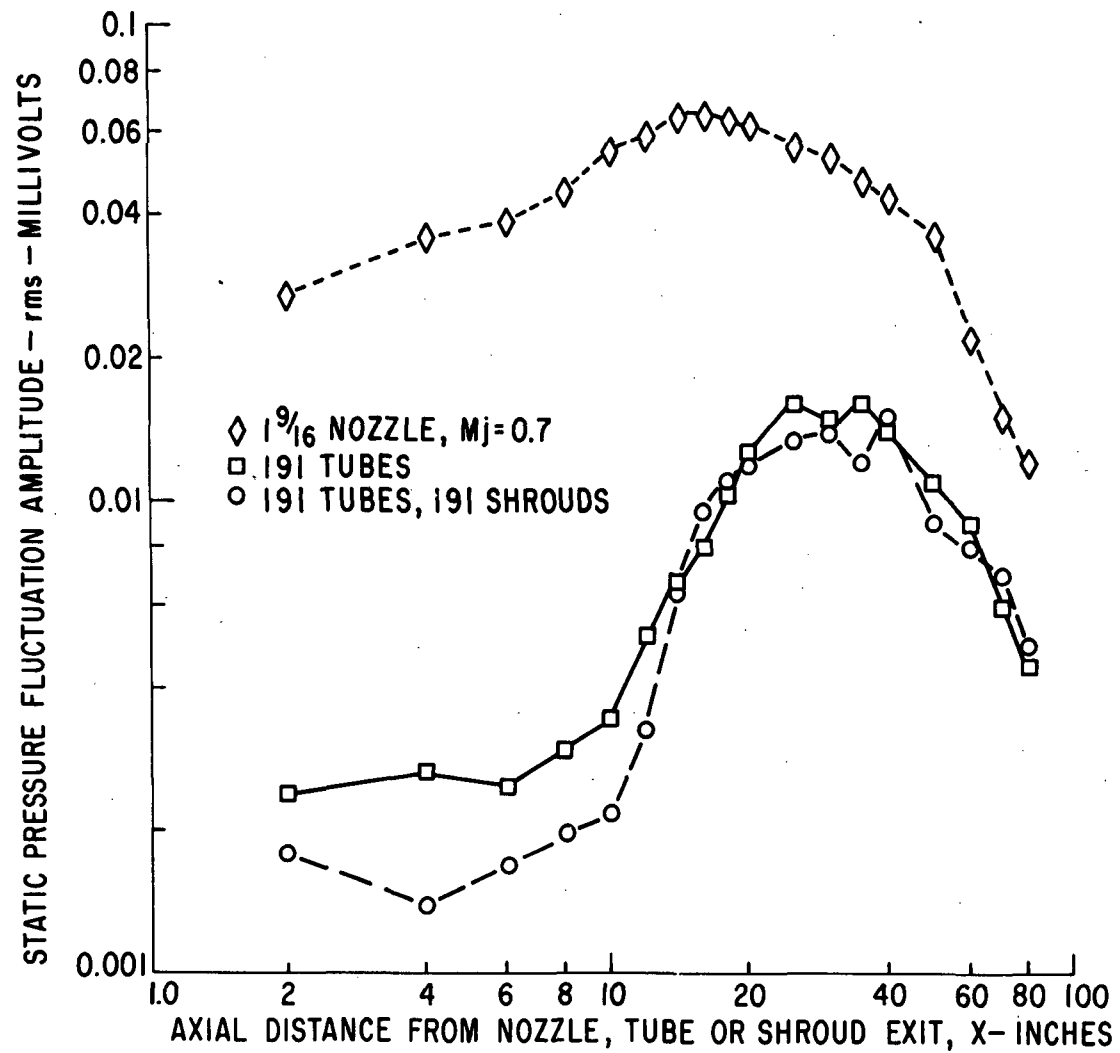
FIG. 24c AXIAL STATIC PRESSURE FLUCTUATIONS FOR MULTITUBES WITH AND WITHOUT SHROUDS, Mj = 0.7
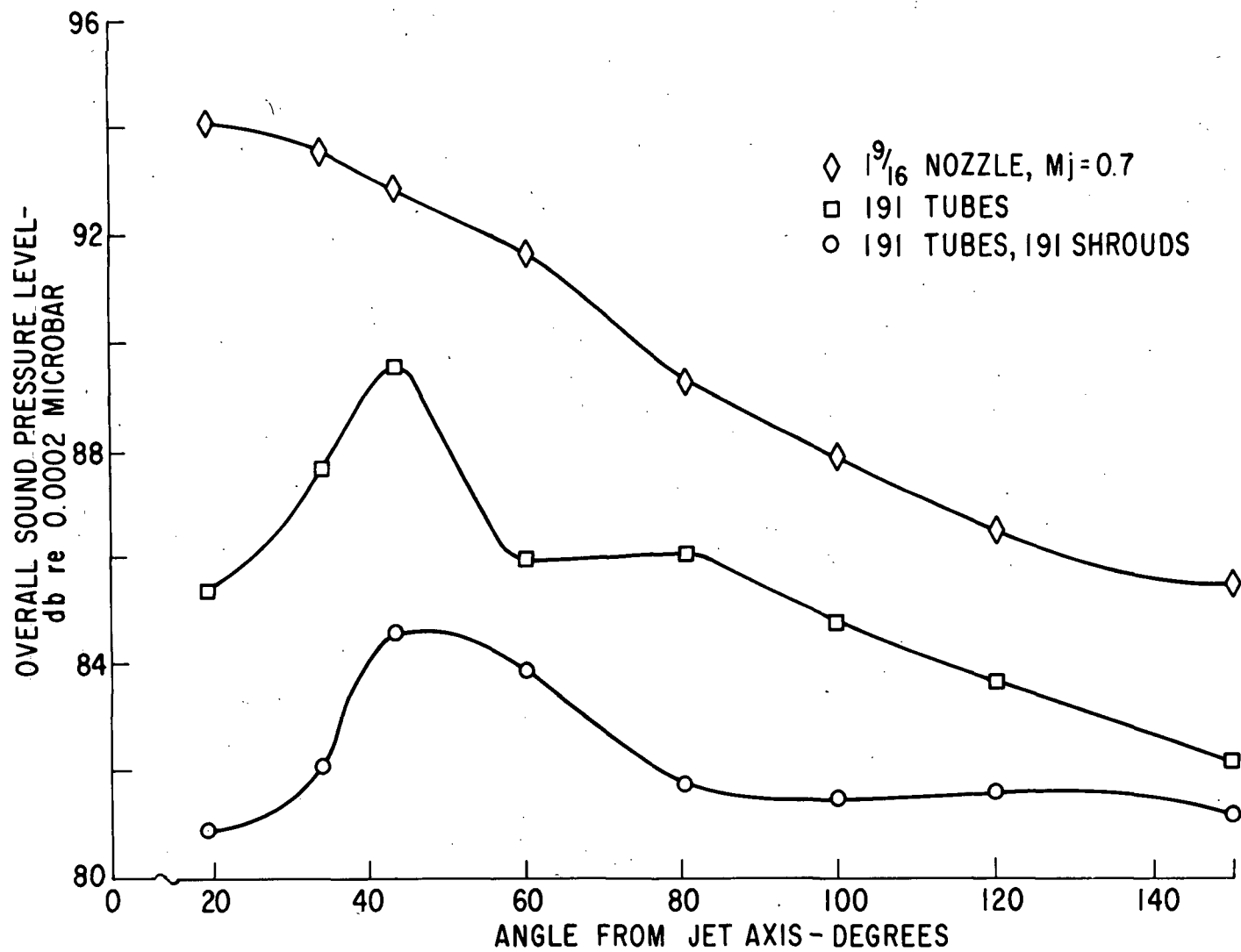
FIG. 25 OVERALL SOUND PRESSURE LEVEL AS A FUNCTION OF ANGULAR POSITION FROM
JET AXIS FOR MULTITUBES WITH AND WITHOUT SHROUDS, Mj= 0.7
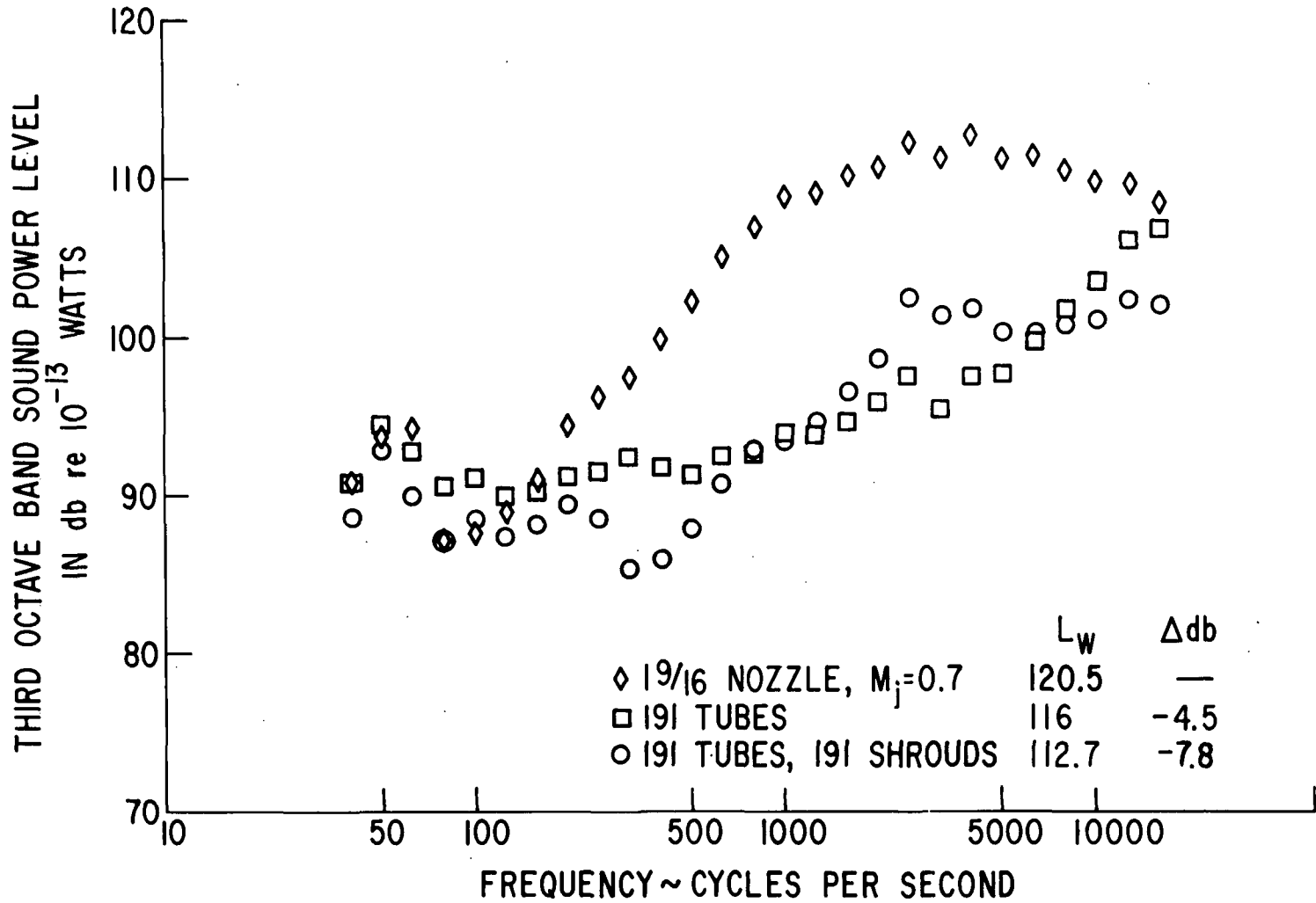
FIG.26 SOUND POWER LEVEL SPECTRA FOR MULTITUBES WITH AND WITHOUT SHROUDS, $M_j = 0.7$
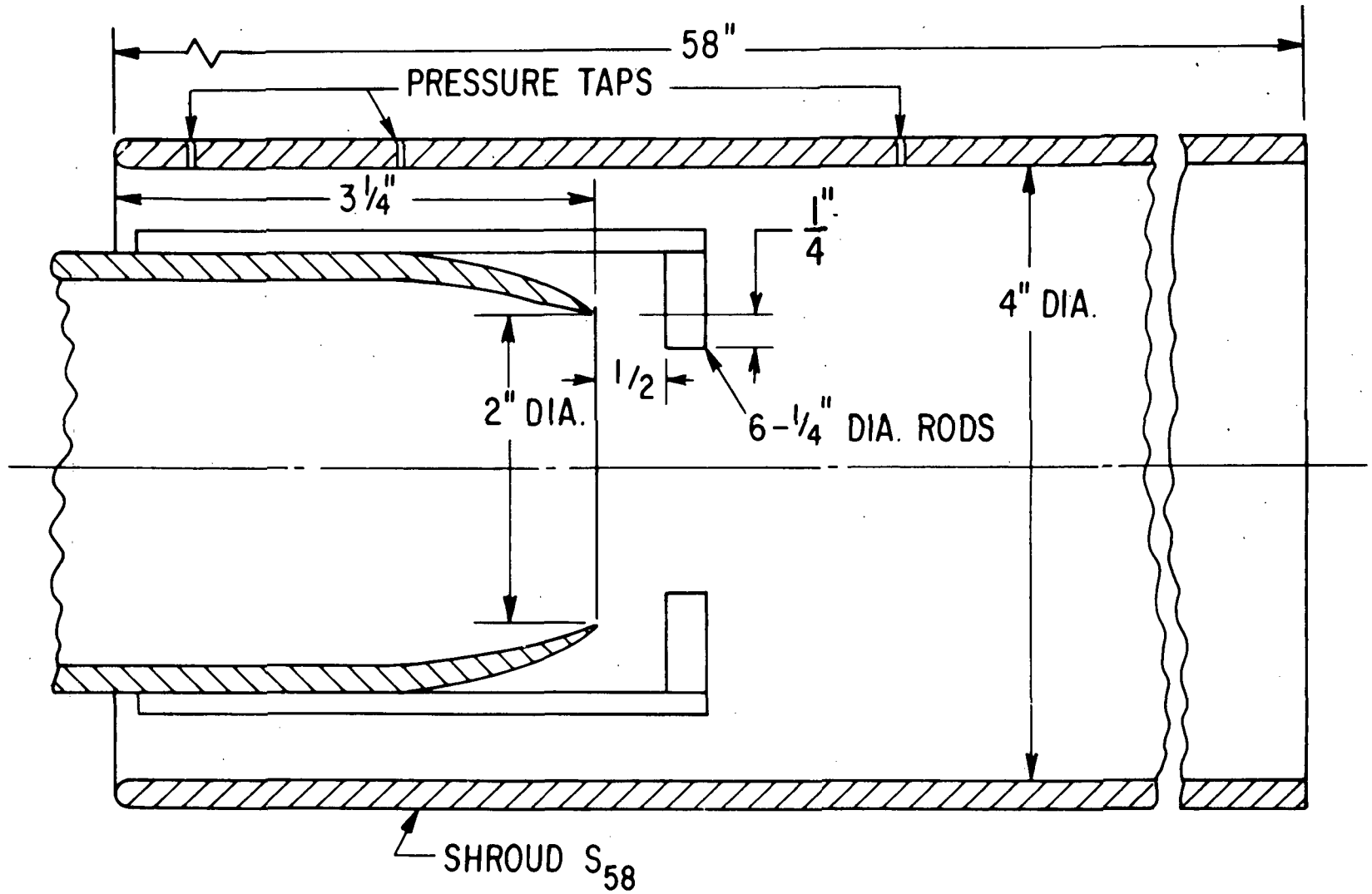
FIGURE 27 SKETCH OF NOZZLE, SHROUD, AND RODS.
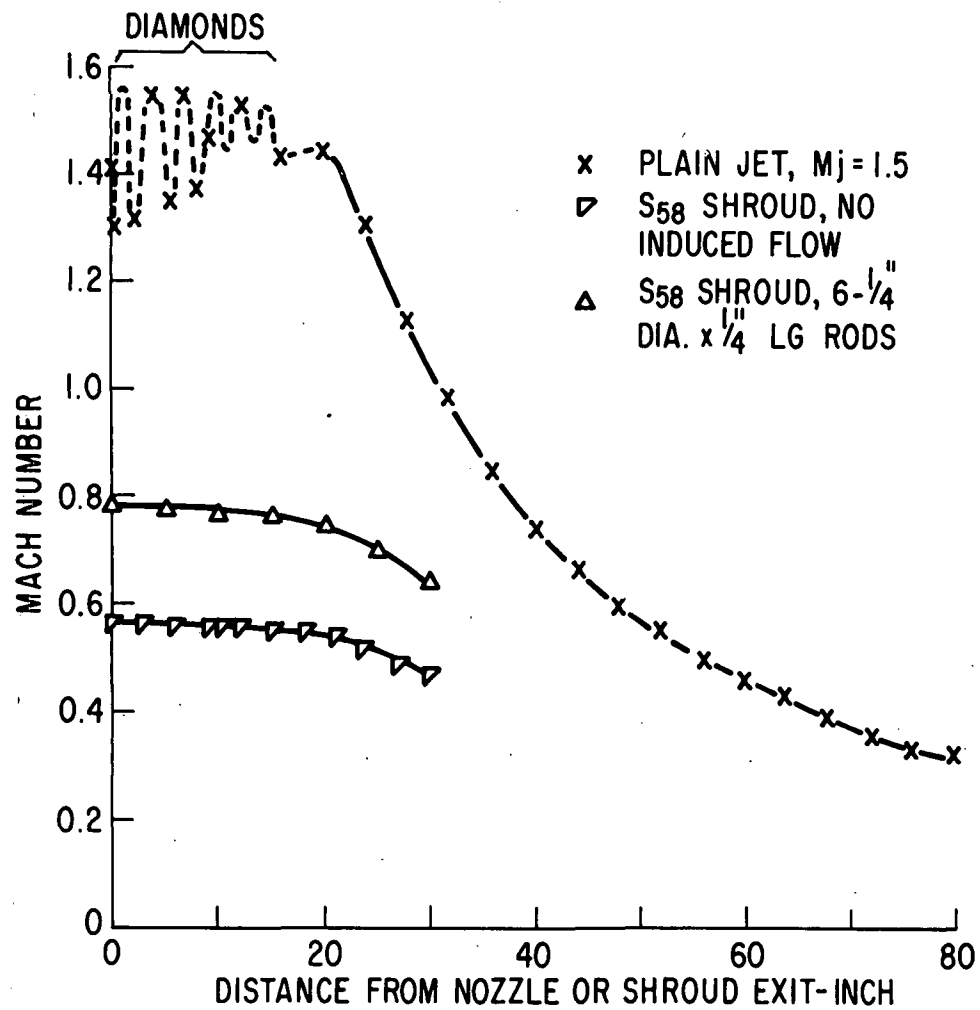
FIG. 28 AXIAL MACH NUMBER DISTRIBUTION FOR 2 INCH DIAMETER
CONVERGENT NOZZLE WITH AND WITHOUT SHROUD AND
RODS
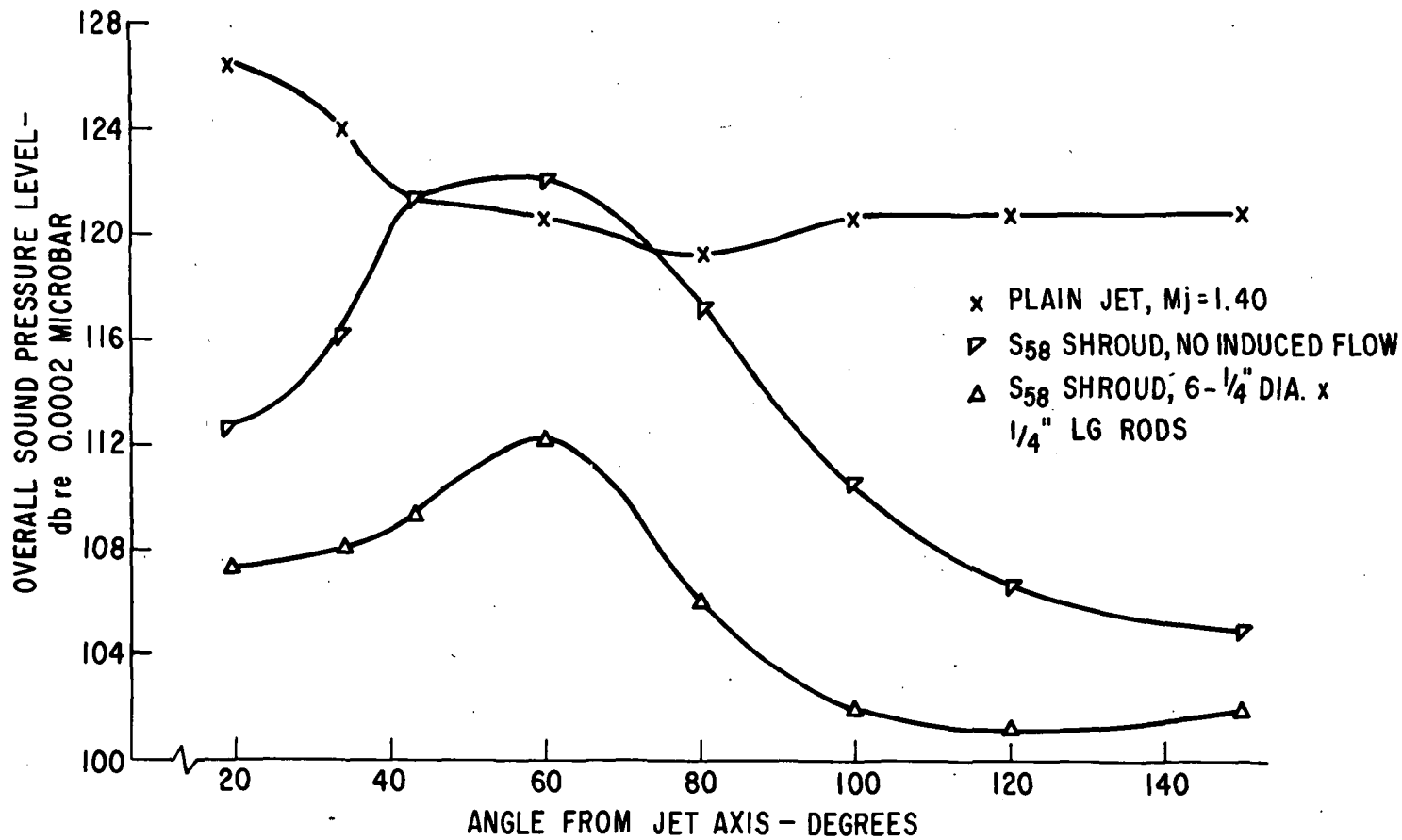
FIG.29 OVERALL SOUND PRESSURE LEVEL AS FUNCTION OF ANGULAR POSITION FROM JET AXIS FOR 2 INCH DIAMETER CONVERGENT NOZZLE WITH AND WITHOUT SHROUD AND RODS
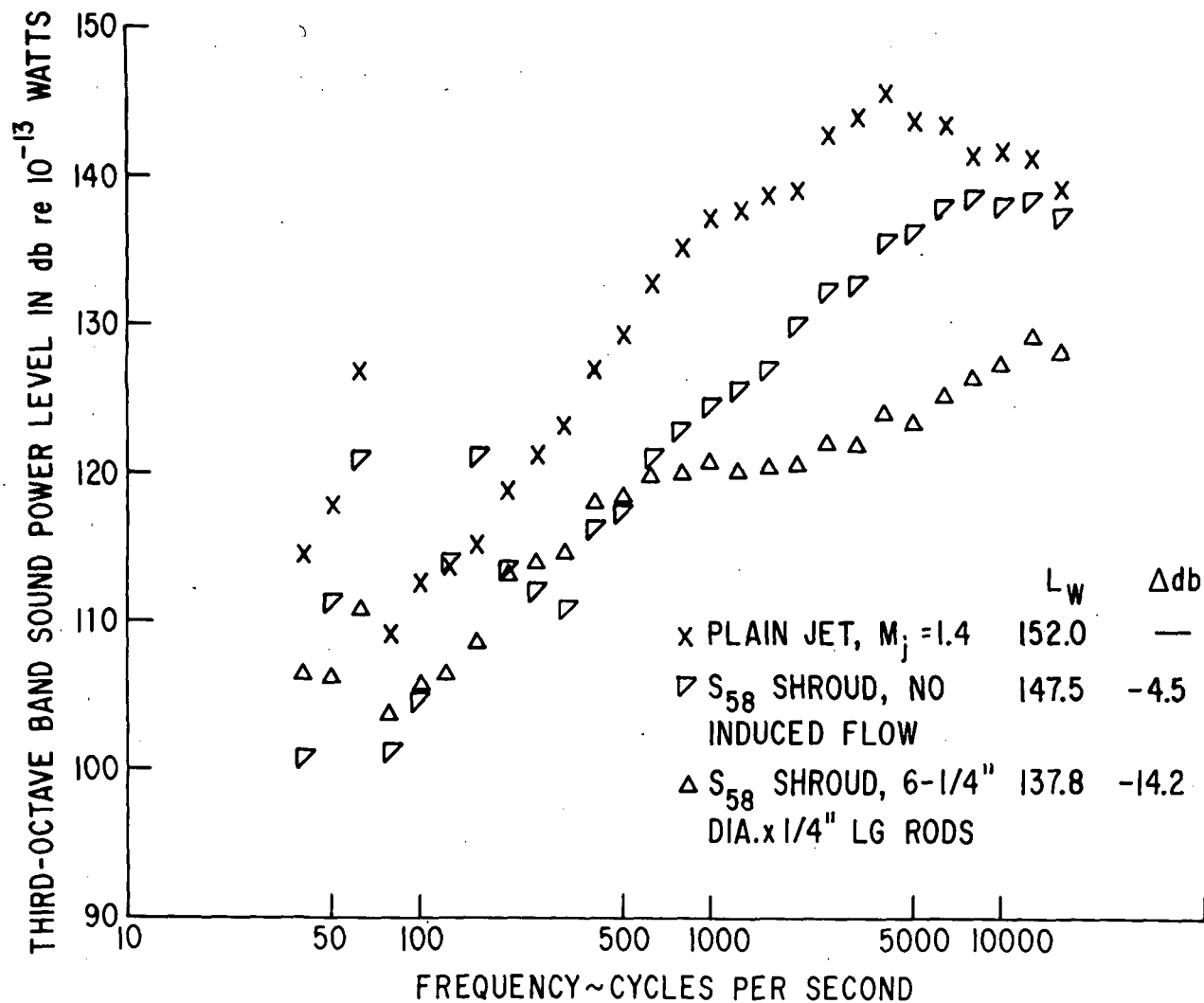
FIG. 30 SOUND POWER LEVEL SPECTRA FOR 2 INCH DIAMETER CONVERGENT
NOZZLE WITH AND WITHOUT SHROUD AND RODS
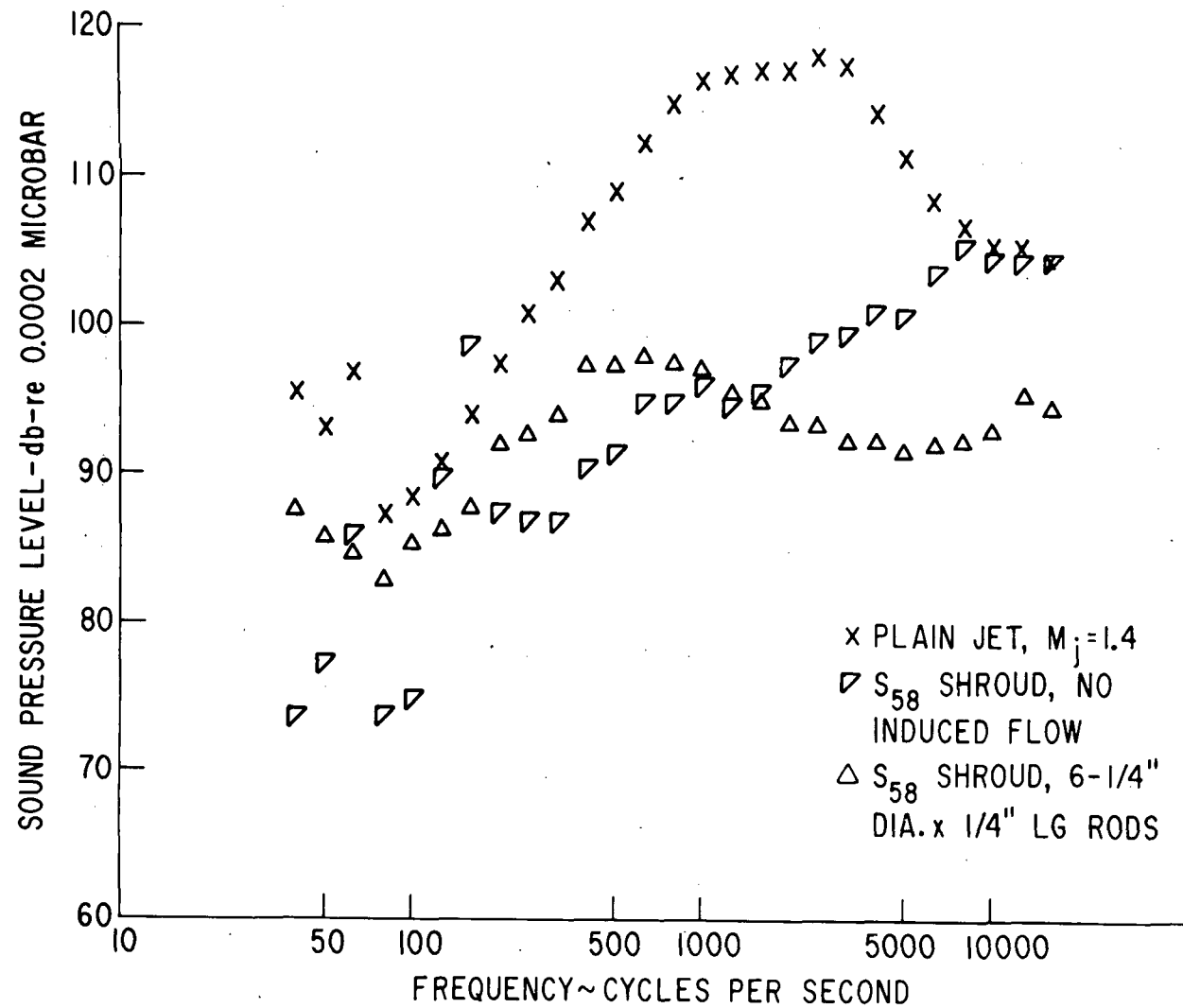
FIG.31a-SOUND PRESSURE LEVEL vs FREQUENCY AT 19.1° FROM JET AXIS
FOR 2 INCH DIAMETER CONVERGENT NOZZLE WITH AND
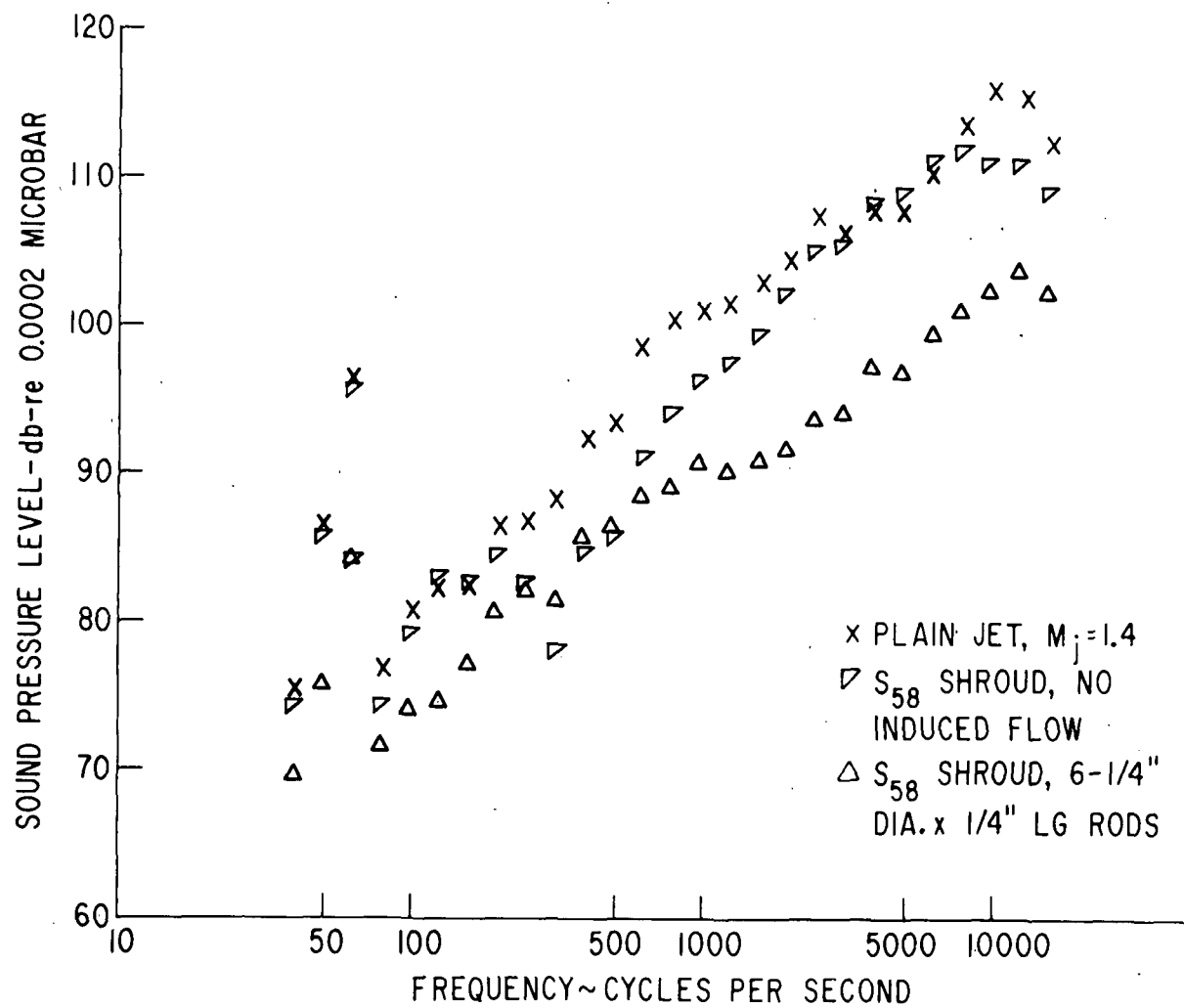WITHOUT SHROUD AND RODS
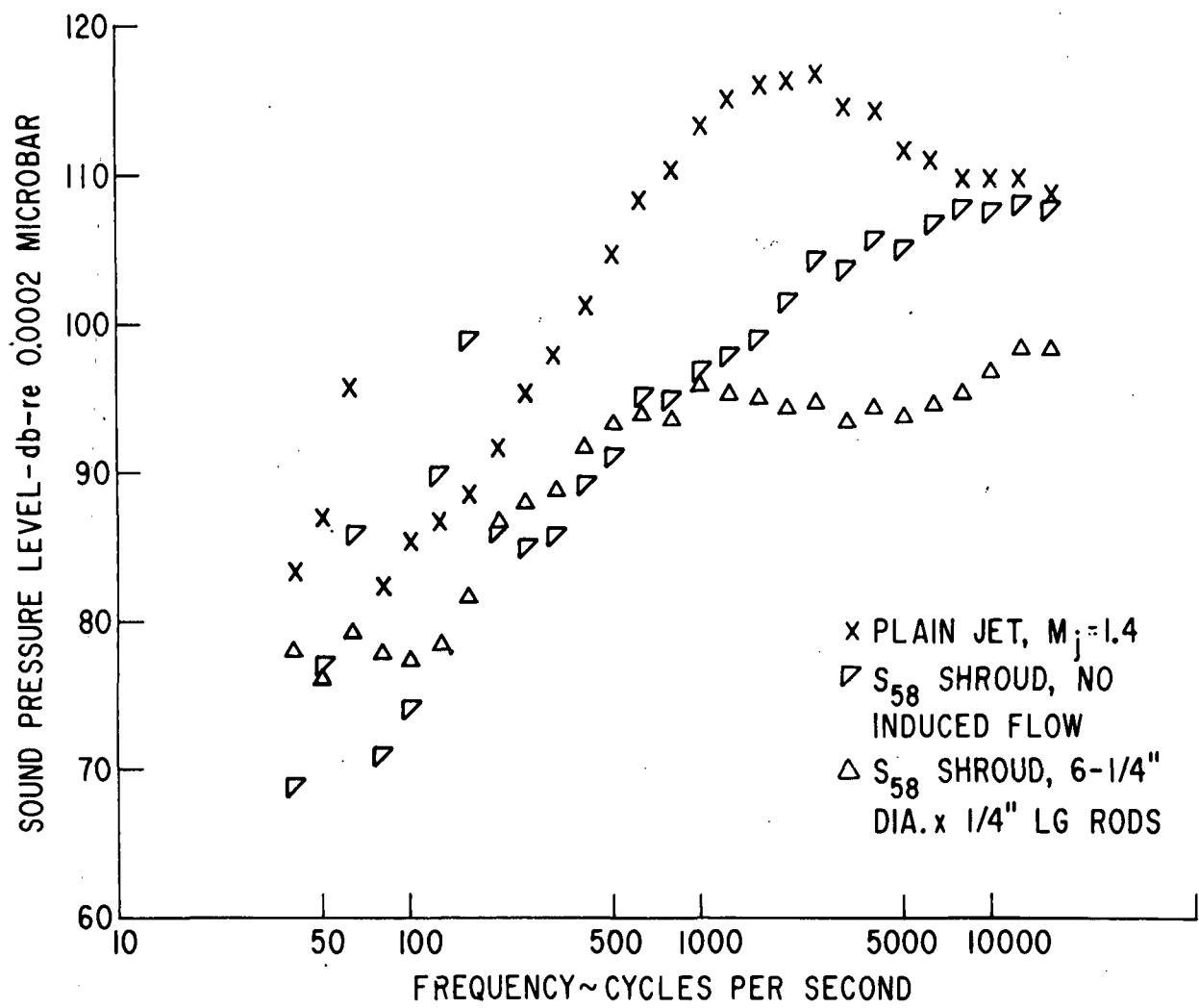
FIG.31b-SOUND PRESSURE LEVEL vs FREQUENCY AT 33.6° FROM JET AXIS FOR 2 INCH DIAMETER CONVERGENT NOZZLE WITH AND WITHOUT SHROUD AND RODS
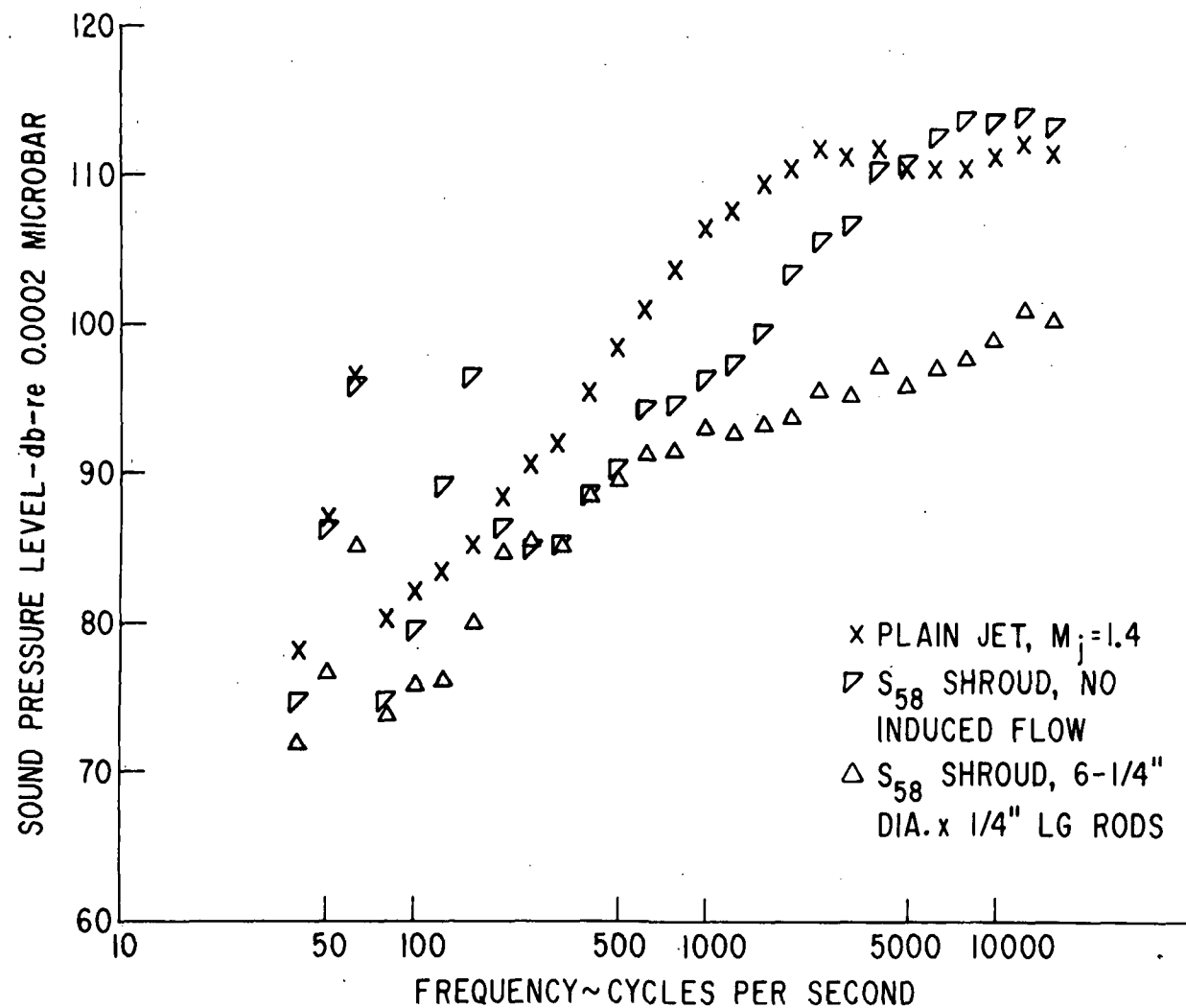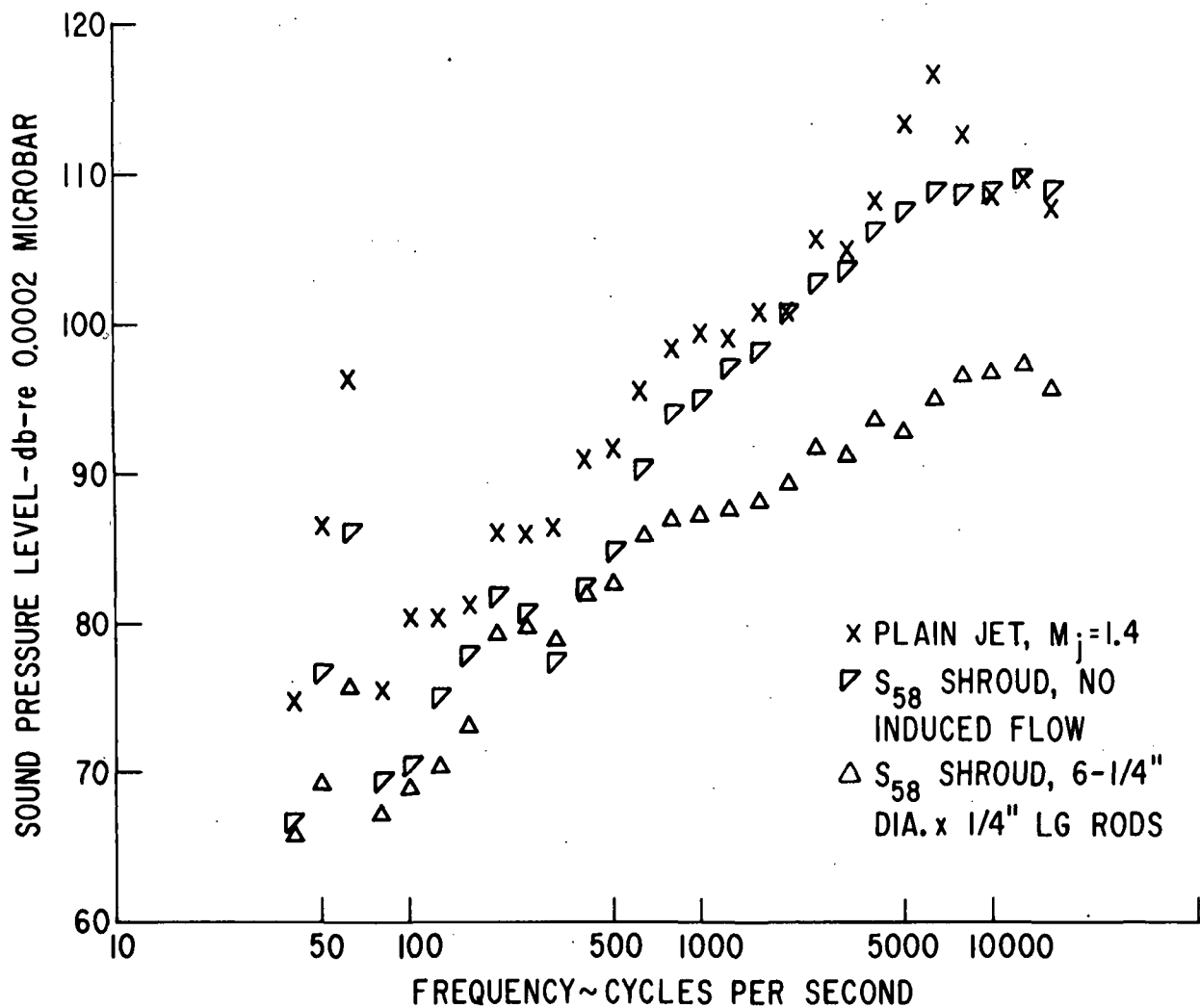
FIG.31c-SOUND PRESSURE LEVEL vs FREQUENCY AT 43.8° FROM JET AXIS
FOR 2 INCH DIAMETER CONVERGENT NOZZLE WITH AND
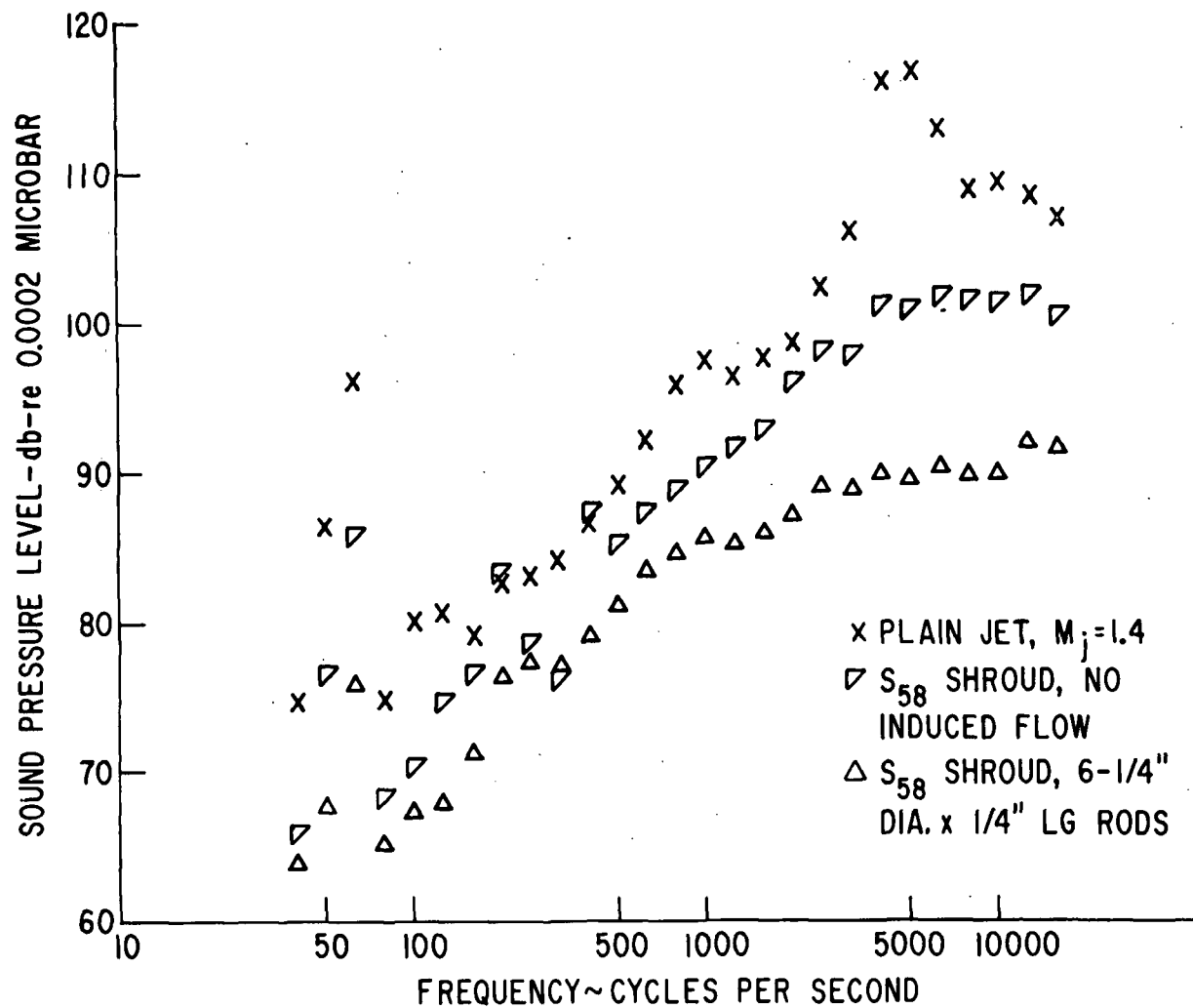WITHOUT SHROUD AND RODS

FIG. 3ld-SOUND PRESSURE LEVEL vs FREQUENCY AT 60° FROM JET AXIS
FOR 2 INCH DIAMETER CONVERGENT NOZZLE WITH AND
WITHOUT SHROUD AND RODS

FIG.31e-SOUND PRESSURE LEVEL vs FREQUENCY AT 80.4° FROM JET AXIS
FOR 2 INCH DIAMETER CONVERGENT NOZZLE WITH AND
WITHOUT SHROUD AND RODS

FIG.31f-SOUND PRESSURE LEVEL vs FREQUENCY AT 99.6° FROM JET AXIS
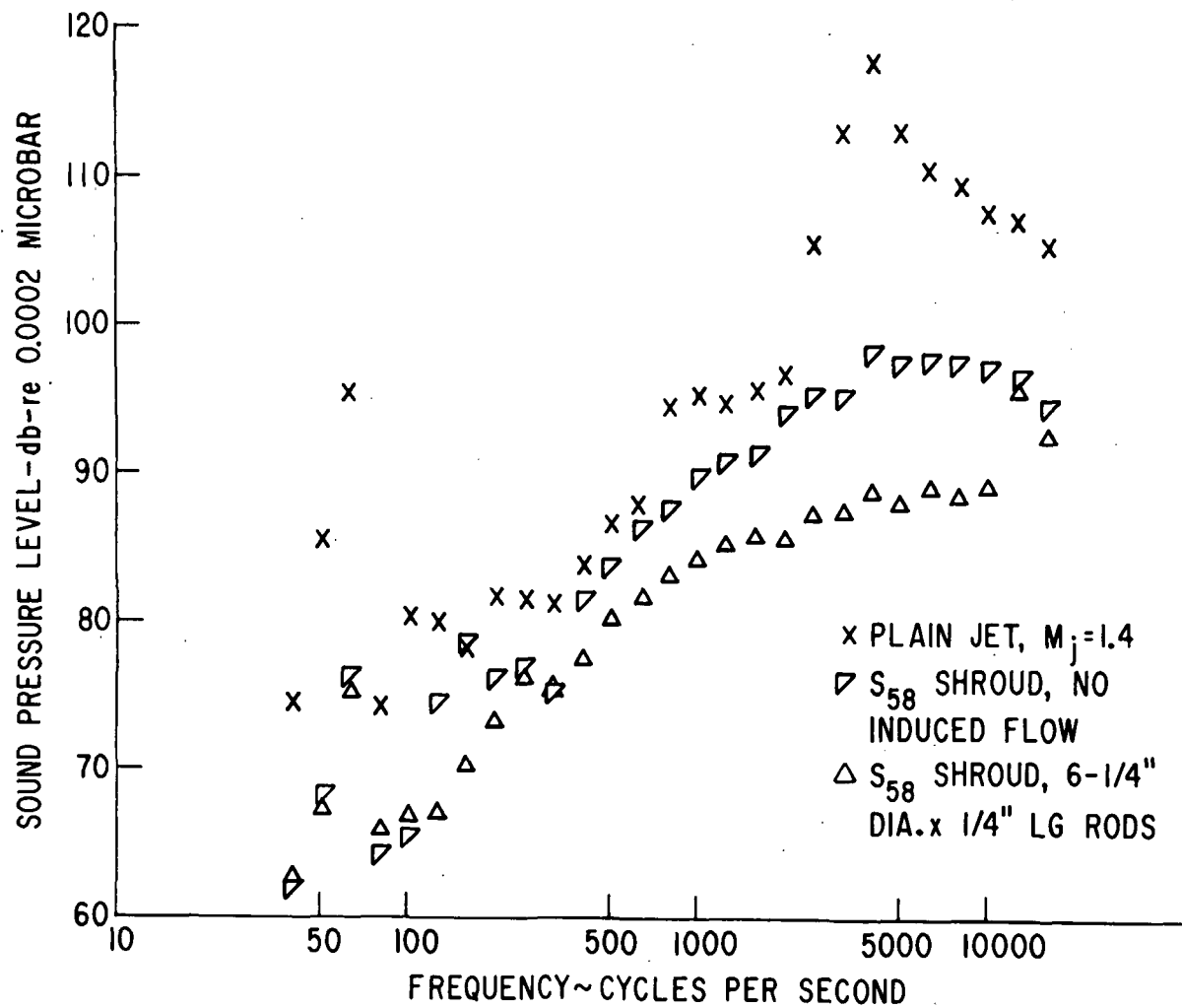FOR 2 INCH DIAMETER CONVERGENT NOZZLE WITH AND
WITHOUT SHROUD AND RODS

FIG.3Ig-SOUND PRESSURE LEVEL vs FREQUENCY AT 120° FROM JET AXIS
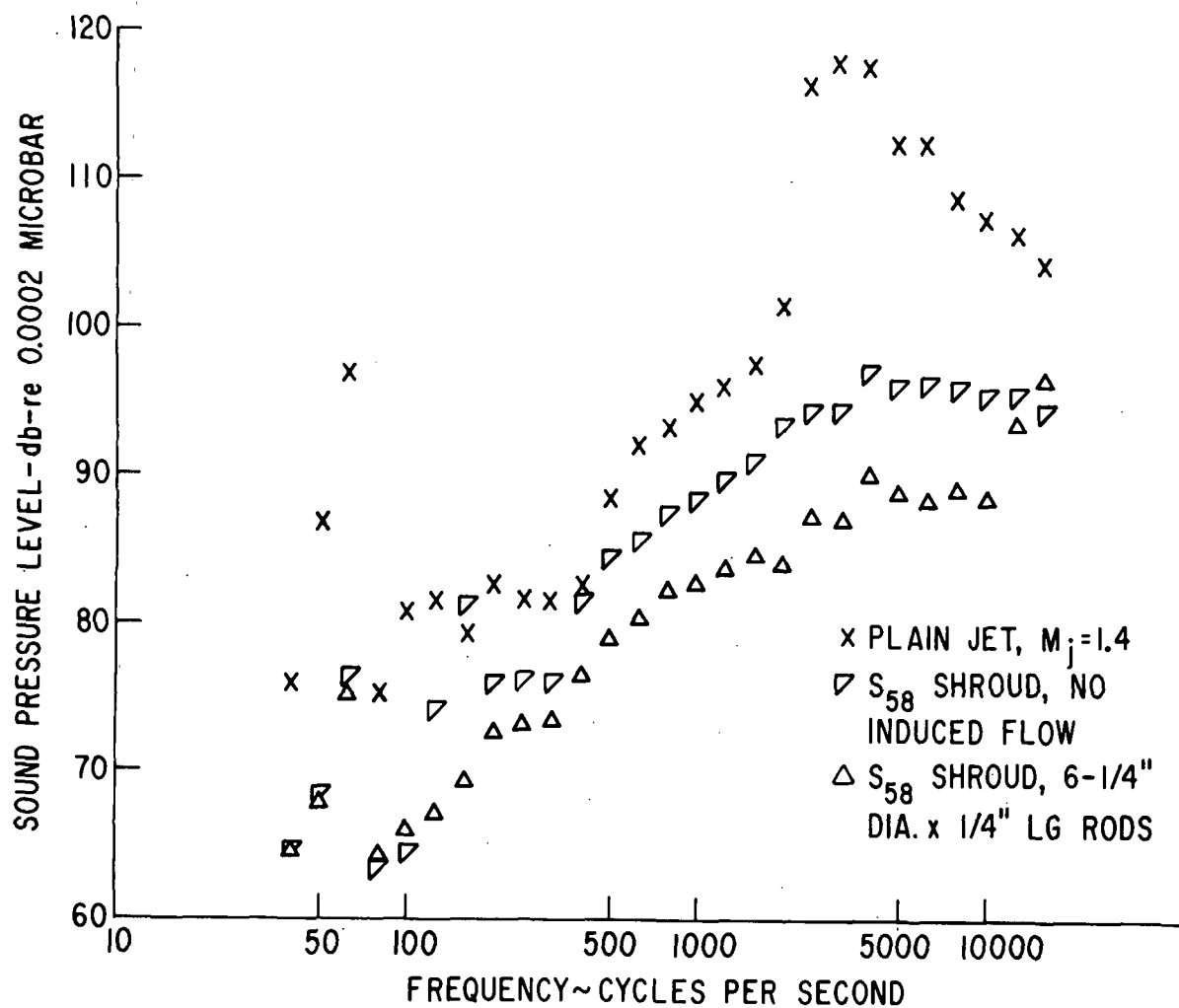FOR 2 INCH DIAMETER CONVERGENT NOZZLE WITH AND
WITHOUT SHROUD AND RODS

FIG.31h—SOUND PRESSURE LEVEL vs FREQUENCY AT 146.4° FROM JET AXIS
FOR 2 INCH DIAMETER CONVERGENT NOZZLE WITH AND
WITHOUT SHROUD AND RODS